For Reference

NOT TO BE TAKEN FROM THIS ROOM

Ex libris
universitatis
albertaensis

QUAECUMQUE VERA

The University of Albert
Printing Department
Edmonton, Alberta

THE UNIVERSITY OF ALBERTA

BROADBAND PROPERTIES OF A CLASS OF TEM-MODE HYBRIDS

by

© RONALD PETER TETARENKO

A THESIS

SUBMITTED TO THE FACULTY OF GRADUATE STUDIES

IN PARTIAL FULFILMENT OF THE REQUIREMENTS FOR THE DEGREE

OF MASTER OF SCIENCE IN

ELECTRICAL ENGINEERING

DEPARTMENT OF ELECTRICAL ENGINEERING

EDMONTON, ALBERTA

FALL, 1970

THE UNIVERSITY OF ALBERTA

BROADBAND PROPERTIES OF A CLASS OF TEM-MODE HYBRIDS

by

© RONALD PETER TETARENKO

A THESIS

SUBMITTED TO THE FACULTY OF GRADUATE STUDIES

IN PARTIAL FULFILMENT OF THE REQUIREMENTS FOR THE DEGREE

OF MASTER OF SCIENCE IN

ELECTRICAL ENGINEERING

DEPARTMENT OF ELECTRICAL ENGINEERING

EDMONTON, ALBERTA

FALL, 1970

UNIVERSITY OF ALBERTA

FACULTY OF GRADUATE STUDIES

The undersigned certify that they have read, and recommend to the Faculty of Graduate Studies for acceptance, a thesis entitled "BROADBAND PROPERTIES OF A CLASS OF TEM-MODE HYBRIDS" submitted by Ronald Peter Tetarenko in partial fulfilment of the requirements for the degree of Master of Science in Electrical Engineering.

ABSTRACT

The TEM mode hybrid studied here belongs to the class of symmetrical four-port Tee hybrids that has a three-port configuration when the series port is internally terminated. The broadband properties of this (equal power) divider/summer were found to depend upon the manner in which the series port was terminated and also upon the form of internal impedance matching utilized between the ports. For circuits employing single or multiple sections of quarter-wavelength impedance transformers, the most practical method of terminating the internal port was found to be a single discrete resistor for each quarter wavelength section used. In this case, the use of a distributed resistance did not significantly improve the VSWR or isolation characteristics of the conjugate ports. For circuits that employ tapers to provide the necessary impedance matching, the practically optimum internal termination was provided by a linear distribution of resistance that extended the entire length of the taper. This linearity of the distributed resistance enhances the practicality of the circuit by simplifying the construction. The theory developed here for the "most-practical" terminations suitable for the impedance transformation used, forms a basis for the solution of the three-port hybrid parameters when that hybrid utilizes similar impedance transformations. The experimental results substantiate the theory of this work, however, they also indicate that the use of a distributed resistance in stripline construction may be limited by a high insertion loss.

ACKNOWLEDGEMENTS

The author wishes to thank his supervising professor, Dr. P.A. Goud, for his help and encouragement throughout the course of this research.

Sincere thanks are also extended to all the members of the Microwave Electronics Group for their helpful discussions and assistance.

The financial support provided by the National Research Council of Canada and the Department of Electrical Engineering is gratefully acknowledged.

The author also wishes to express his deepest appreciation for the understanding and encouragement provided by his wife, Peggy.

TABLE OF CONTENTS

Page

CHAPTER 1 INTRODUCTION 1

CHAPTER 2 ANALYSIS OF SYMMETRICAL FOUR-PORT NETWORKS

2.1 Even and Odd Modes 7

2.2 Even and Odd Mode Analysis of a Three-Port Hybrid 11

2.3 Computer Solution of Four-Port Network Equations 16

CHAPTER 3 THREE-PORT HYBRIDS UTILIZING SINGLE-SECTION QUARTER-WAVELENGTH IMPEDANCE TRANSFORMERS

3.1 Three-Port Wilkinson Hybrid Using a Single Resistor 19

3.2 Modified Three-Port Wilkinson Hybrid Using a Distributed Resistance 22

3.3 Effects of Construction Tolerances on Three-Port Hybrid Stripline Circuits 29

3.4 Interpretation of Experimental Results for a Three-Port Wilkinson Hybrid 32

CHAPTER 4 THREE-PORT HYBRIDS USING MULTIPLE-SECTION QUARTER-WAVELENGTH IMPEDANCE TRANSFORMERS

4.1 Introduction 46

4.2 Three-Port Hybrid Using a Two-Section Chebyshev Impedance Transformer 48

4.3 Three-Port Hybrid Using a Two-Section Binomial Impedance Transformer 53

4.4 Circuit Design Considerations for Three-Port Hybrids Using Multiple Quarter-Wave Impedance Transformers 55

CHAPTER 5 THREE-PORT HYBRIDS UTILIZING TAPERED IMPEDANCE TRANSFORMERS

5.1 Introduction 60

5.2 Theory of Tapers 61

Page

5.3 Even and Odd Mode Analysis 64

5.4 Three-Port Hybrid Using a Chebyshev-Taper Impedance Transformer 66

5.5 Three-Port Hybrid Using an Exponential-Taper Impedance Transformer 70

5.6 Experimental Results and Their Interpretation 74

CHAPTER 6 CONCLUSION 84

APPENDIX A EFFECTIVE ELECTRICAL LENGTH OF CORNERS AND JUNCTIONS

A.1 Introduction 87

A.2 Corners in Stripline Circuits 87

A.3 Junction Areas in Stripline Circuits 91

APPENDIX B COMPENSATION FOR COAX-STRIPLINE CONNECTOR DISCONTINUITIES

B.1 Introduction 94

B.2 Single Section Quarter-Wave Impedance Transformer Model 97

B.3 Tapered Impedance Transformer Model 102

APPENDIX C ACCURACY OF COMPUTED CALCULATIONS 106

BIBLIOGRAPHY 110

LIST OF TABLES

Page

TABLE C.1: Characteristics of the Chebyshev taper 108

LIST OF FIGURES

Page

FIGURE 1.1 Frequency Multiplier Circuits Showing Some Possible Uses of Three-Port Hybrids 2

1.2 Schematic of Three-Port Hybrid Circuit 2

FIGURE 2.1 Symmetrical Four-Port 8

2.2 Even and Odd Mode Equivalent Circuits for a Symmetrical Four-Port 8

2.3 General Circuit of the Three-Port Hybrid 12

2.4 Three-Port Hybrid Equivalent Circuits 12

2.5 General Flow Chart for Computer Programs 17

2.6 Discretization of a Continuous Distribution of Resistance 18

FIGURE 3.1 Stripline Model of a Three-Port Wilkinson Hybrid (center conductor only) 20

3.2 Equivalent Circuits for the Three-Port Wilkinson Hybrid 20

3.3 Computed Characteristics of the Three-Port Wilkinson Hybrid (single resistor model) 23

3.4 Computed Characteristics for Three-Port Wilkinson Hybrid (Odd Mode Cancelled-Single Resistor Model) 25

3.5 Computed Characteristics of the Three-Port Wilkinson Hybrid (Distributed Resistance Model) 27

3.6 Thin Film Distributed Resistances 34

3.7 Experimental Model of Three-Port Wilkinson Hybrid (Stripline Center Conductor Only) 34

3.8 Computed Characteristics of Three-Port Wilkinson Hybrid, 23-R Model (resistance centered on reference line) 35

3.9 Computed Characteristics of Three-Port Wilkinson Hybrid, 23-R Model (2/3 Resistance on 70.7 Ohm Line) 36

Page

FIGURE 3.10 Computed Characteristics of Three-Port Wilkinson Hybrid, 27-R Model (Resistance Centered on reference line) 37

3.11 Computed Characteristics of Three-Port Wilkinson Hybrid, 27-R Model (R = 1800 ohms) 38

3.12 Computed Characteristics of Three-Port Wilkinson Hybrid, 27-R Model (R = 2000 ohms) 39

3.13 Experimentally Measured Characteristics of the Three-Port Wilkinson Hybrid (Single Resistor Model) 41

3.14 Experimentally Measured Characteristics of the Three-Port Wilkinson Hybrid (23-R Model) 42

3.15 Experimentally Measured Characteristics of the Three-Port Wilkinson Hybrid (27-R Model) 43

FIGURE 4.1 Three-Port Hybrid Using Two-Section Chebyshev Impedance Transformer (Stripline Model and Equivalent Circuits) 47

4.2 Computed Characteristics of Three-Port Hybrid Using Two-Section Chebyshev Impedance Transformer (Two-Resistor Model) 50

4.3 Computed Characteristics of Three-Port Hybrid Using Two-Section Chebyshev Impedance Transformer (Distributed Resistance Model) 52

4.4 Computed Characteristics of Three-Port Hybrid Using Two-Section Binomial Impedance Transformer (Two Resistor Model) 54

4.5 Computed Effects of Length Variations in Chebyshev Two-Section Impedance Transformer Model of Three-Port Hybrid (Two Resistor Case) 57

4.6 Computed Effects of Length Variations in Binomial Two-Section Impedance Transformer Model of Three-Port Hybrid (Two Resistor Case) 58

FIGURE 5.1 Three-Port Hybrid Using a Tapered Impedance Transformer (Stripline Model and Equivalent Circuits) 62

5.2 Approximate Model for a Taper 62

5.3 Characteristics of Chebyshev Taper 67

Page

FIGURE 5.4 Computed Characteristics of Three-Port Hybrid Using Chebyshev Taper Impedance Transformer 69

5.5 Characteristics of Exponential Taper 72

5.6 Computed Characteristics of Three-Port Hybrid Using Exponential Taper Impedance Transformer 73

5.7 Computed Characteristics of Three-Port Hybrid Using Chebyshev Taper Impedance Transformer (Various Distributed Resistances) 77

5.8 Computed Characteristics of Three-Port Hybrid Using Chebyshev Tapered Impedance Transformer (Various Distributed Resistances) 78

5.9 Experimentally measured Characteristics of Chebyshev Taper Impedance Transformer 79

5.10 Experimentally Measured Characteristics of Three-Port Hybrid Using Chebyshev Taper Impedance Transformer 80

FIGURE A.1 Stripline Material 88

A.2 Corners in Stripline Circuits (Center Conductor Only) 88

A.3 Variations of Right Angle Corners in Stripline Center Conductors 92

A.4 Methods of Forming Junction Areas 92

FIGURE B.1 Stripline Connectors and Circuit Construction 95

B.2 Thin Film Resistor Construction and Equivalent Circuits 98

B.3 Effect of Resistor Construction on the Characteristics of the Three-Port Wilkinson Hybrid 101

CHAPTER I

INTRODUCTION

An important characteristic of semiconductor microwave devices is their small physical size. This small size limits the R.F. power that a single device can handle(1). If R.F. power levels are required that are larger than those achievable in a single device, several devices must be employed, creating a need for power division/summation circuits. The rapid advances that have been made in solid state devices and in metallization techniques in recent years, have permitted a large reduction in the size of microwave circuits. This size reduction lends itself well to the use of power division/summation methods, as several stages of amplification or of frequency generation can be placed in one small package. At present, power divider/summer techniques are being used extensively in the design and manufacture of power amplifiers(2,3,4,5) and high frequency power sources(6).

Power division/summation techniques are also useful when high-power frequency multipliers are required(7,8). One application of such multipliers occurs when a microwave signal with high frequency-stability is required. Such a signal can be generated by a crystal controlled source, whose output is subsequently amplified and multiplied in frequency. Some variations of a possible configuration are shown in figure 1.1. A significant property of frequency multipliers is that the phase, as well as the frequency of the input signal are

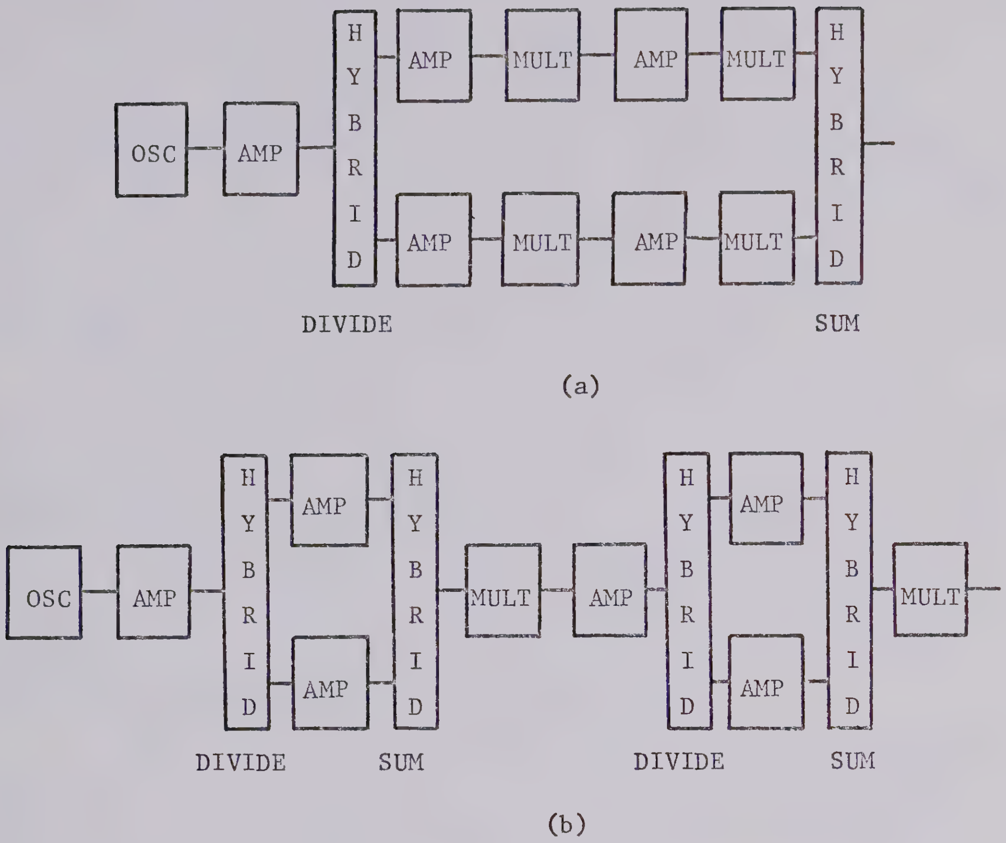

FIGURE 1.1 FREQUENCY MULTIPLIER CIRCUITS SHOWING SOME POSSIBLE USES OF THREE-PORT HYBRIDS

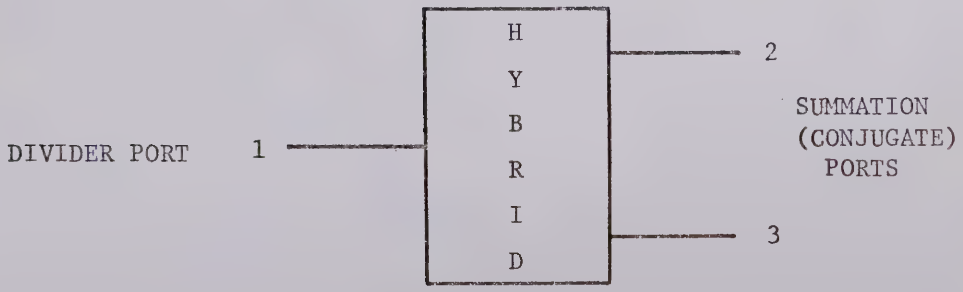

FIGURE 1.2 SCHEMATIC OF THREE-PORT HYBRID CIRCUIT

multiplied. Therefore, the use of parallel chains of multipliers (to achieve higher power output) as shown in Figure 1.1(a), can result in the signals of each chain being largely out-of-phase. Hence, when the outputs of the chains are combined, a significant loss of power could occur. This source of power loss can be avoided by rearranging the circuit into the configuration of Figure 1.1(b), where there are no phase differences to be multiplied.

Another important area when power division/summation techniques are useful is the phase-locking of oscillators. Here, the phase-locking of several oscillators can be accomplished by the use of only one locking signal source(6), along with a suitable signal divider network. The outputs of the several locked devices may be combined by an appropriate power summing network.

There are many ways in which power division/summation can be achieved. Generally, these divider/summers can be classified into three main groups, such as:

(a) Reactive dividers/summers - These have the capability of having many branches but there is no isolation between the summer ports (Figure 1.2). Hence, for most purposes, some form of additional circuitry is necessary to provide the required isolation. This additional circuitry adds to the cost and increases the size and weight of the total divider/summer circuit(7). An example of a reactive divider/summer would be an N-Way coaxial junction.

(b) Hybrid divider/summers - This type of circuit has a built-in isolation between the conjugate ports and when properly terminated, can be an N-Way(9) device. The most

commonly used class of hybrids is the symmetrical four-port, such as the T-network(10), hybrid ring(11,12) and directional coupler(13,14).

(c) Asymmetric-nonlinear circuits - such as the ferrite or YIG circulators(15,6). These devices can offer good isolation and low loss properties.

The device considered in this thesis is a three-port hybrid(16) that is equivalent to the four-port T hybrid, with the series port internally terminated in a reflectionless load. This device is sometimes referred to as a split-T power divider/summer(17). Many papers have been written on various forms of these hybrids(18,19,20). In most cases, some combination of quarter-wave impedance transformers, along with suitable values of discrete resistors, were used to provide the desired VSWR and isolation characteristics for the hybrid. The purpose of the work reported in the following chapters is to extend the analysis of the symmetrical three-port hybrid to investigate the possibilities of increasing the usable frequency band width of this device. This investigation was primarily concerned with the manner in which the series port was internally terminated and also with the method of impedance transformation used.

It should be possible to extend the impedance transformation methods used, to included the use of tapered-transmission-line impedance transformers. When operating in the TEM mode, satisfactory impedance matching over a frequency bandwidth of several octaves can be obtained with the use of either a tapered transmission line or multiple sections of quarter-wavelength transmission line. An advantage of the taper is that it is physically much shorter in length than the

multi-section quarter-wavelength transformer for the same bandwidth. Therefore, it should be possible to design a power divider/summer with several octaves of frequency bandwidth, while still maintaining a relatively small physical size. It will probably be desirable to use some form of distributed resistance to internally terminate the series port formed by the tapered transmission line. Generally, the use of a distributed resistance, in lieu of some combination of single discrete resistors, should provide better internal termination of the series port for any method of impedance transformation used. An improvement in the internal termination of the series port should provide acceptable VSWR and isolation characteristics over a broader frequency range. The use of a distributed resistance should not present any serious construction problems.

Three-port hybrids, operating as matched, in-phase, power combiners or power splitters can be realized by the use of stepped quarter-wave or tapered impedance transformers. Hence, these hybrids can be classified as to the type of impedance transformation used. Accordingly, the work discussed in the following chapters has been divided into three main categories:

(a) Hybrids using single-section, quarter-wave, impedance transformers

(b) Hybrids utilizing multiple-section, quarter-wave impedance transformers

(c) Hybrids using tapered impedance transformers.

In the past, these hybrids would likely have been constructed in waveguide or coaxial line form. However, the recent trend (for most applications) has been away from these circuit forms and towards strip

transmission line construction. These newer circuit forms, mainly stripline and microstrip, have enabled the physical size of the device to be greatly reduced and also have the advantage of being relatively less expensive than their counterparts in waveguide or coaxial line. All the experimental work reported in the following chapters was carried out using stripline construction techniques.

CHAPTER II

ANALYSIS OF SYMMETRICAL FOUR-PORT NETWORKS

2.1 Even and Odd Modes

The symmetrical four-port network under study here is one that has a plane of symmetry as shown in Figure 2.1. A convenient method of analysis for this type of network is the use of even and odd modes(21). For the purposes of this analysis it is assumed that the network is lossless and that the reactive effects of the circuit junctions and step discontinuities can be ignored.

For the even mode, coherent signals (V_e) of equal amplitude ($\frac{1}{2}$) and equal phase, are fed into ports 1 and 4. Here there is no difference of potential between the two divisions of the four-port. Hence, the line of symmetry can be regarded as a plane of voltage maxima and can be replaced by an open circuit (Figure 2.2(a)).

For the odd mode, coherent signals (V_o) of equal amplitude ($\frac{1}{2}$) but of opposite phase are applied to ports 1 and 4 respectively. Now there will be a maximum difference of potential between the two divisions of the four-port and the line of symmetry can be regarded to lie in a plane of voltage minimum. On either side of the line of symmetry the magnitude of the potential increases but, it is of opposing phase, hence, the plane of symmetry can be regarded as being at ground potential (Figure 2.2(b)).

Associated with each port there is a voltage reflection coefficient (Γ), a voltage transmission coefficient (T) and the

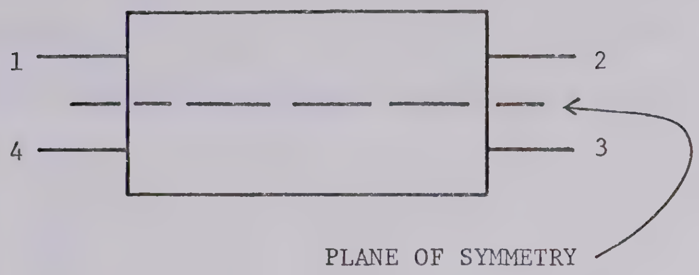

FIGURE 2.1 SYMMETRICAL FOUR-PORT

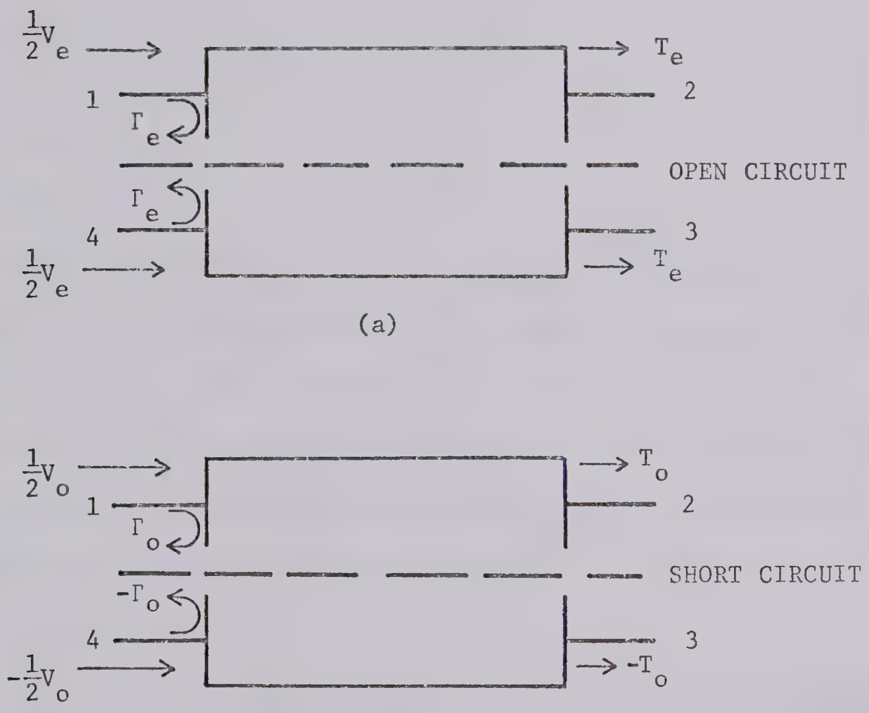

(b)

FIGURE 2.2 EVEN AND ODD MODE EQUIVALENT CIRCUITS FOR A SYMMETRICAL FOUR-PORT
(a) EVEN MODE
(b) ODD MODE

vector amplitude (A) of the signals emerging from each port. When signals of equal amplitude ($\frac{1}{2}$) and equal phase are supplied to ports 1 and 4, the resultant signals emerging from each port are:

$$\begin{aligned} A_1 &= \frac{1}{2}\Gamma_e \\ A_2 &= \frac{1}{2}T_e \\ A_3 &= \frac{1}{2}T_e \\ A_4 &= \frac{1}{2}\Gamma_e \end{aligned} \tag{2.1}$$

Similarily for the odd mode, with ports 1 and 4 excited

$$\begin{aligned} A_1 &= \frac{1}{2}\Gamma_o \\ A_2 &= \frac{1}{2}T_o \\ A_3 &= -\frac{1}{2}T_o \\ A_4 &= -\frac{1}{2}\Gamma_o \end{aligned} \tag{2.2}$$

By the principle of superposition the sum of the even and odd modes is a signal of unit amplitude incident upon port 1. The signals at the other ports, as a result of this unit input at port 1, are the superposition of the results obtained for both the even and odd modes. Therefore, the total signals emerging from all the ports as a result of a unit input signal at port 1 are:

$$\begin{aligned} A_1 &= \frac{1}{2}(\Gamma_e + \Gamma_o) \\ A_2 &= \frac{1}{2}(T_e + T_o) \\ A_3 &= \frac{1}{2}(T_e - T_o) \\ A_4 &= \frac{1}{2}(\Gamma_e - \Gamma_o) \end{aligned} \tag{2.3}$$

when ports 1 and 4 are joined into one port the result is a symmetrical three-port network, where the amplitude of the emerging signal (A_J), at this newly formed port, is

$$A_J = \frac{1}{2}(\Gamma_e + \Gamma_o) + \frac{1}{2}(\Gamma_e - \Gamma_o) = \Gamma_e \tag{2.4}$$

The power reflected (emerging) from the joined port is $|\Gamma_e|^2$ and hence the power transmitted into the circuit from this combination port is $1 - |\Gamma_e|^2$. For the situation where this power is transmitted equally to ports 2 and 3 the power to each of these ports is $\frac{1}{2}(1 - |\Gamma_e|^2)$ and hence the voltage transmission coefficient ($T_{2,J}$ or $T_{3,J}$) from the port J to either ports 2 or 3 is, for a lossless network,

$$|T_{2,J}| = |T_{3,J}| = \frac{1}{\sqrt{2}} \sqrt{1 - |\Gamma_e|^2} \qquad (2.5)$$

Similarly, when ports 2 and 3 have a signal applied to them whose amplitude is $\frac{1}{2}$ but whose phase is first equal and then opposite, the resultant amplitudes (A) of the signals emerging from all the ports are

$$\begin{aligned} A_J &= \frac{1}{2}(T_e + T_o) + \frac{1}{2}(T_e - T_o) = T_e \\ A_2 &= \frac{1}{2}(\Gamma_e + \Gamma_o) \qquad (2.6) \\ A_3 &= \frac{1}{2}(\Gamma_e - \Gamma_o) \end{aligned}$$

As stated previously this superposition of the even and the odd modes represents a unit signal incident upon port 2. The isolation (I) between two ports is defined as

$$\text{Isolation} = \frac{\text{power emerging from one port}}{\text{power incident upon the other port}} \qquad (2.7)$$

with all other ports match terminated. Therefore the isolation of port 3 with respect to port 2 is

$$I_{3,2} = \left(\frac{1}{2}|\Gamma_e - \Gamma_o|\right)^2 \qquad (2.8)$$

as both ports have the same characteristic impedance. Using the conventional units of decibels

$$I_{3,2} = 20 \log_{10} (\tfrac{1}{2} |\Gamma_e - \Gamma_o|) \qquad (2.9)$$

Since there is a line of symmetry separating ports 2 and 3, the same results (Equations (2.6) and (2.9)) will be obtained when port 3 is taken as the reference for the unit input signal (i.e. interchange the indices 2 and 3 in Equations (2.6) and (2.9)).

The main advantage of this even and odd mode type of analysis is that it permits the four-port (or three-port) network to be divided into two, two-port networks which are much simpler to analyse. However, it may lead to some conceptual difficulties when one tries to visualize the conversion of a four-port T hybrid into a three-port configuration by internally terminating the series port. The previous development of the even and odd mode analysis was mainly to show that this particular type of analysis, which is usually restricted to four-port devices, can be successfully applied to three port devices. The following work will be concerned with the application of the even and odd mode analysis as it applies to the three-port configuration of the four-port T hybrid.

2.2 Even and Odd Mode Analysis of a Three Port Hybrid

The type of circuit with which this thesis is concerned is illustrated in Figure 2.3. In this configuration, the same characteristic impedance (Z_o), from the external circuit, is connected to all three ports. Internally, the network is characterized by the circuit characteristic impedances (Z's), the values of the shunt resistances (R's) and the separation between the resistances (ℓ's). These characteristic variables can, in theory, assume a wide range of values, however, as will be seen later, practical circuit constraints place

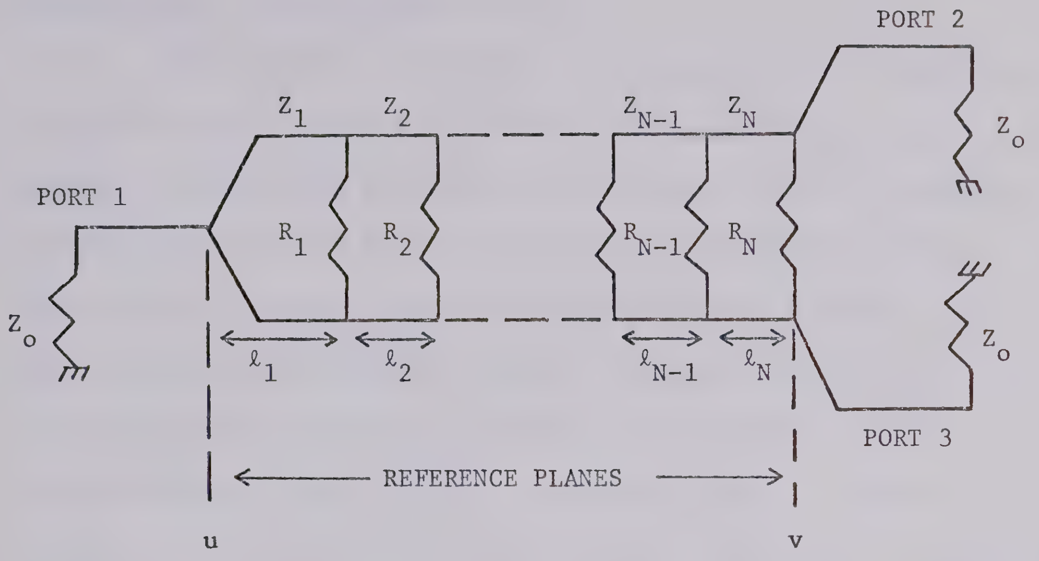

FIGURE 2.3 GENERAL CIRCUIT OF THE THREE-PORT HYBRID

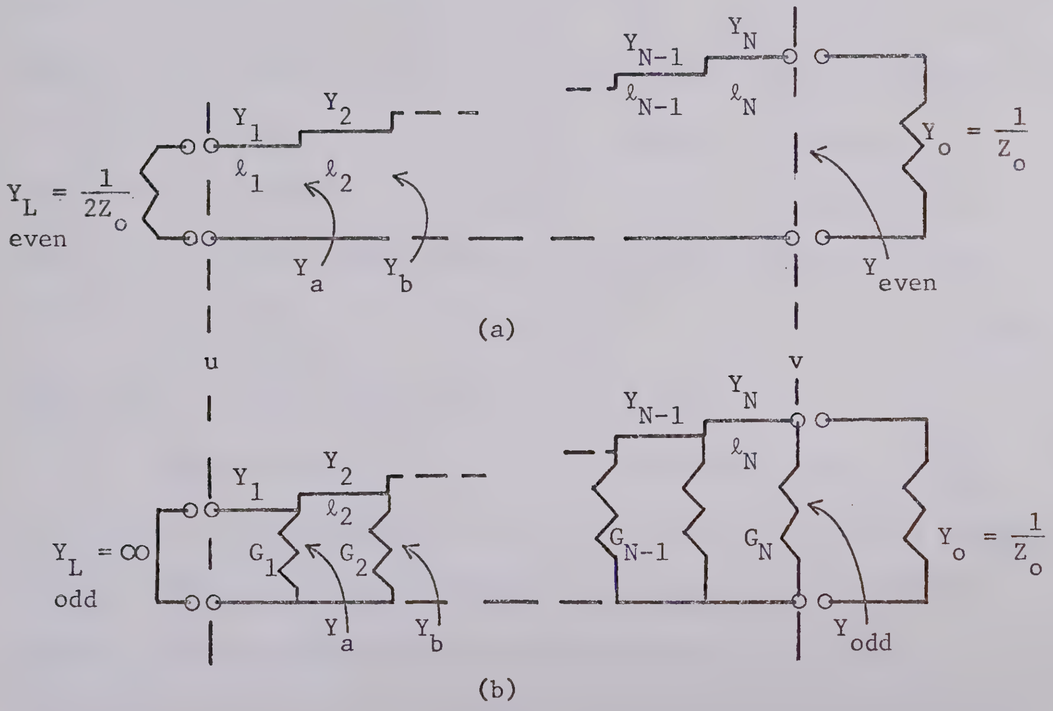

FIGURE 2.4 THREE-PORT HYBRID EQUIVALENT CIRCUITS
(a) EVEN MODE
(b) ODD MODE

definite restrictions on these values.

The behaviour of the line of symmetry in the junction area is illustrated in Figure 2.4. For the even mode the junction is divided into two equal ports by an open circuit, thus the impedance of each port must be 2 Z_o to satisfy the superposition principle. Also the open circuit division by the line of symmetry means that there is no current flowing through the resistors and therefore the resistors can be omitted from the even mode equivalent circuit, as shown in Figure 2.4(a). For the odd mode the line of symmetry is at ground potential and the junction area is divided into two equal parts, both at ground potential, therefore the equivalent circuit (Figure 2.4(b)) shows an admittance ($Y_{L\ odd}$) of infinity, at the plane of the junction (reference plane "u"). Since the line of symmetry is at ground potential and divides the circuit into two equal parts, the maximum currents flow through the resistors and they must be included in the equivalent circuit, but at $\frac{1}{2}$ of their value. For the admittance representation of the odd mode we have,

$$G_n = \frac{2}{R_n} \qquad n = 1,2,3, \ . \ . \ . \ N \tag{2.10}$$

where N is the total number of resistors used.

These hybrid circuits will be constructed using stipline techniques with the internal circuitry separated a sufficient distance so that there is no electro-magnetic coupling between the various sections. Hence, the characteristic admittances (Y_1, Y_2 ... Y_N, Figure 2.4(a),(b)) will be the same for both the even and odd modes. By keeping the physical dimensions of the stripline sufficiently small, with respect to the operating wavelength, propagation is restricted to the transverse electromagnetic mode and hence the

characteristic admittances are frequency independent.

The analysis of the three-port hybrid was carried out assuming that all ports were match terminated. Utilizing the standard transmission line equations and starting at the reference plane "u" (Figure 2.4), the characteristic admittance at the reference plane "v" was calculated for both the even and odd modes. For the even mode the calculations are as follows

$$Y_a = Y_1 \frac{Y_{L\,\text{even}} + j\,Y_1 \tan\theta_1}{Y_1 + j\,Y_{L\,\text{even}} \tan\theta_1} \tag{2.11a}$$

$$Y_b = Y_2 \frac{Y_a + j\,Y_2 \tan\theta_2}{Y_2 + j\,Y_a \tan\theta_2} \tag{2.11b}$$

$$Y_s = Y_n \frac{Y_{s-1} + j\,Y_n \tan\theta_n}{Y_n + j\,Y_{s-1} \tan\theta_n} \tag{2.11c}$$

$n = 1,2,\ldots N$

$s = 1,2,\ldots N$

$\theta_n = (\frac{2\pi}{\lambda})\ell_n$

where N is the total number of increments, the electrical distance between reference planes "u" and "v" is divided into. Once Y_{even} is found (i.e. s = N, n = N) then the voltage reflection coefficient for the even mode (Γ_e) is

$$\Gamma_e = \frac{Y_o - Y_{\text{even}}}{Y_o + Y_{\text{even}}} \tag{2.12}$$

The odd mode calculations are similar except that the effects of the shunt conductances have to be taken into account, hence,

$$Y_a = Y_1 \frac{Y_{L\,\text{odd}} + j\,Y_1 \tan\theta_1}{Y_1 + j\,Y_{L\,\text{odd}} \tan\theta_1} + G_1 \tag{2.13a}$$

$$Y_b = Y_2 \frac{Y_a + j\,Y_2 \tan\theta_2}{Y_2 + j\,Y_a \tan\theta_2} + G_2 \tag{2.13b}$$

$$Y_s = Y_n \frac{Y_{s-1} + j\, Y_n \tan \theta_n}{Y_n + j\, Y_{s-1} \tan \theta_n} + G_n \tag{2.13c}$$

where θ, n, s, N are as defined for the even mode. The voltage reflection coefficient at the reference plane v for the odd mode (Γ_o) is

$$\Gamma_o = \frac{Y_o - Y_{odd}}{Y_o + Y_{odd}} \tag{2.14}$$

The reflection coefficient at ports 2 or 3 (Γ_2, Γ_3) has a magnitude (ρ_2, ρ_3) such that (from Equation 2.6)

$$\rho_2 = \rho_3 = \frac{1}{2} |\Gamma_e + \Gamma_o| \tag{2.15}$$

The isolation (I) between ports 2 and 3 is (from Equation (2.9))

$$I = 20 \log_{10} [\frac{1}{2} |\Gamma_e - \Gamma_o|] \tag{2.16}$$

For port 1 the voltage reflection coefficient (from Equation (2.4)) is

$$\rho_1 = |\Gamma_1| = |\Gamma_e| \tag{2.17}$$

Since the admittance(s) and the length(s) of the transmission line(s) between the reference planes u and v (Figure 2.4) serve to match the admittances of the junction area to those of ports 2 and 3 (and vice-versa), Γ_e is essentially the reflection coefficient of the impedance matching method employed. The usable frequency bandwidth of port 1 is governed by the maximum permissible reflection coefficient and hence, by the impedance matchings method used. Therefore once this is selected, the circuit admittances, Y_1 to Y_N, in Equations (2.11) and (2.13), are specified and the only real variables in the analysis are the shunt resistances (R's) and their separation (ℓ's).

2.3 Computer Solution of Four-Port Network Equations

The Equations (2.11) to (2.17) were solved on the IBM 360/67 digital computer, using both APL and Fortran IV languages. All the programs run had the same general format and could be written in any available language. A flow chart for this general format is shown in Figure 2.5.

The theoretical simulation of the circuit using a continuous distribution of resistances between the circuitry of ports 2 and 3 was accomplished by a discretization process. Discretization of a continuous function is a process quite common in numerical analysis and normally the resultant errors can be reduced to an acceptable level. This discretization process, when applied to a thin film, continuous resistance, consists of dividing the resistive shape into a large number of sections, then taking the resistance of each section and applying it as a discrete resistor separated from its neighbors by a short length of transmission line. Figure 2.6 illustrates this process, with the resistor separation (ℓ) being the length of the short piece of transmission line (which is also the width of the resistive section selected). The above procedure assumes that the current flow through each resistive section is restricted to a path that is parallel to the height of the section. In Figure 2.6, the current path would be in a vertical direction. This assumption is standard to most work involving thin film resistors. The magnitude of the possible errors involved in the use of this discretization process, as it was applied to the work in this thesis, are discussed in Appendix C and are shown to be minimal.

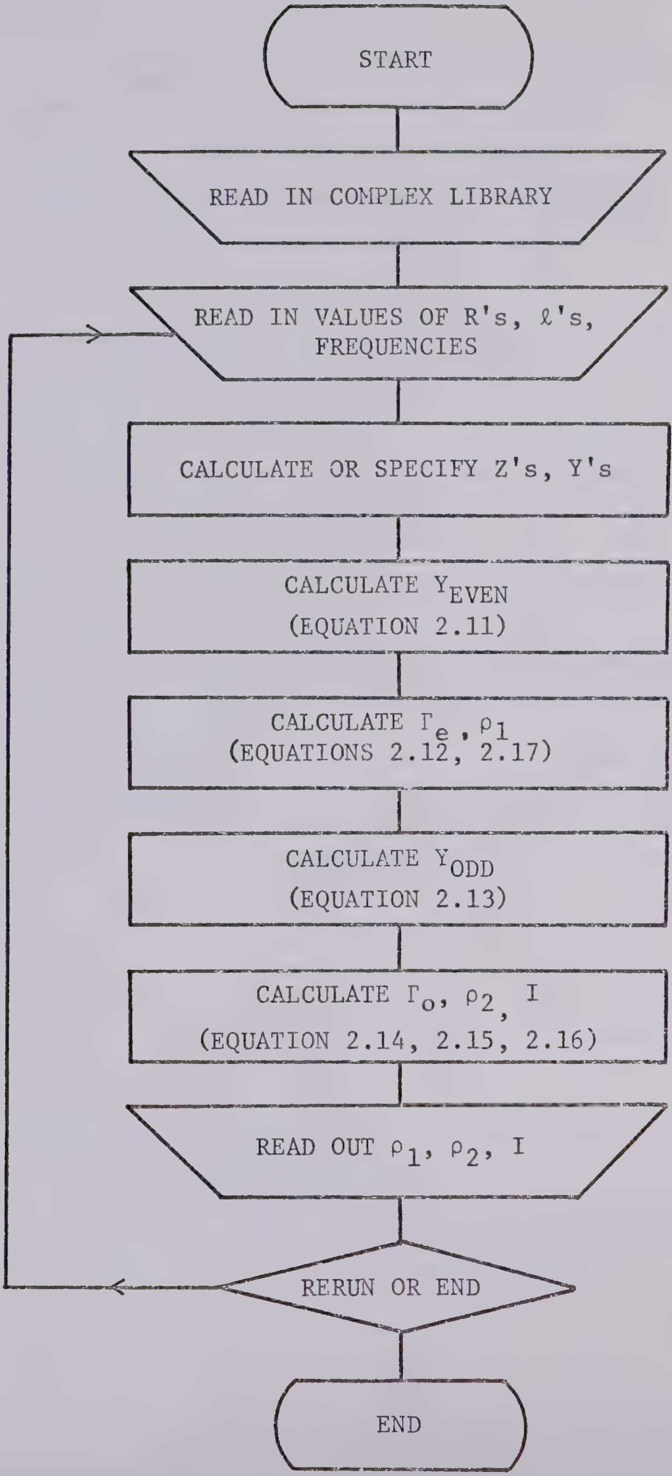
START
READ IN COMPLEX LIBRARY
READ IN VALUES OF R's, ℓ's, FREQUENCIES
CALCULATE OR SPECIFY Z's, Y's
CALCULATE Y_{EVEN} (EQUATION 2.11)
CALCULATE Γ_e, ρ_1 (EQUATIONS 2.12, 2.17)
CALCULATE Y_{ODD} (EQUATION 2.13)
CALCULATE Γ_o, ρ_2, I (EQUATION 2.14, 2.15, 2.16)
READ OUT ρ_1, ρ_2, I
RERUN OR END
END

FIGURE 2.5 GENERAL FLOW CHART FOR COMPUTER PROGRAMS

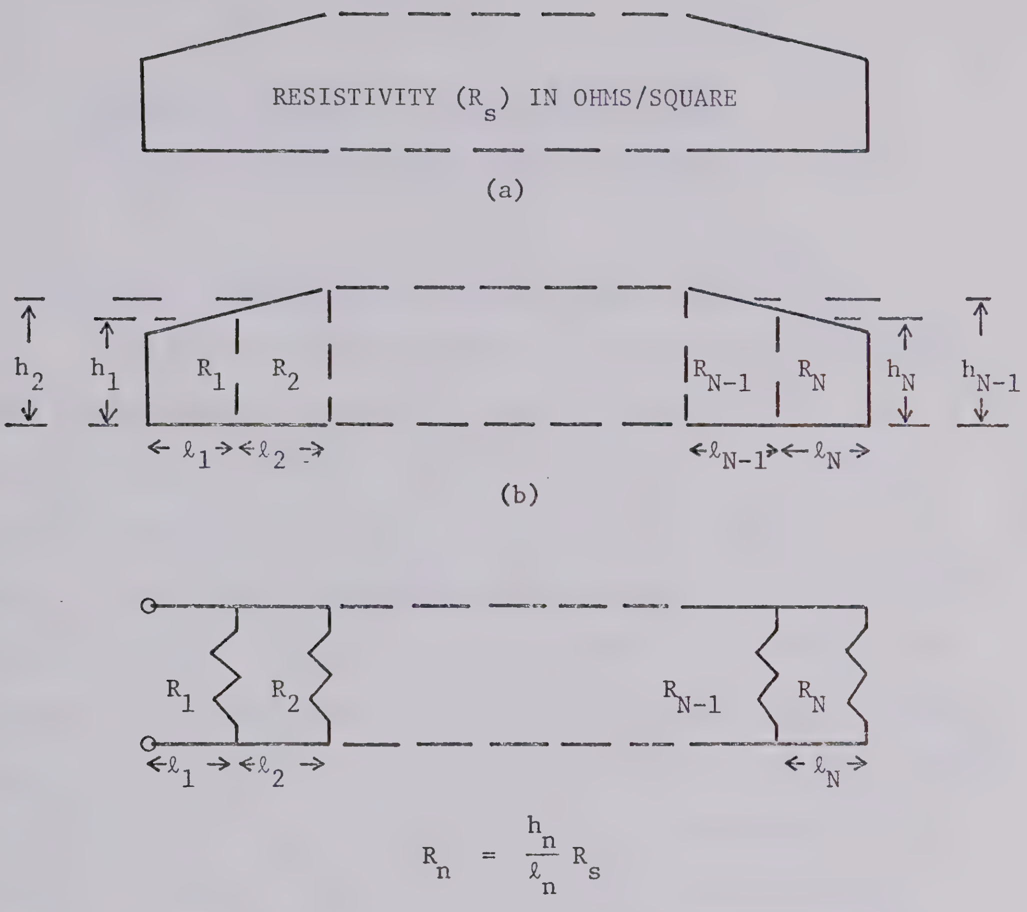

$$R_n = \frac{h_n}{\ell_n} R_s$$

$$n = 1, 2, \ldots N$$

(c)

FIGURE 2.6 DISCRETIZATION OF A CONTINUOUS DISTRIBUTION OF RESISTANCE
(a) COMPLETE AREA OF THIN FILM RESISTOR
(b) DISCRETE SECTIONS
(c) EQUIVALENT CIRCUIT

CHAPTER III

THREE-PORT HYBRIDS UTILIZING SINGLE-SECTION QUARTER-WAVELENGTH IMPEDANCE TRANSFORMERS

3.1 Three-Port Wilkinson Hybrid Using a Single Resistor

The configuration of the center conductor for a stripline model of this device is shown in Figure 3.1. This circuit uses a single-section, quarter-wave impedance transformer, for impedance matching purposes, in each of the port 1-to-port 3 and port 1-to-port 2 circuits. The $\frac{\lambda}{4}$ transformer theoretically provides a perfect impedance match at only one frequency; however, the impedance matching may be acceptable over a narrow bandwidth centered on the design frequency. It is generally accepted that the first person to discuss this hybrid circuit was E.J. Wilkinson(9) and, consequently, this particular circuit is often referred to as the Wilkinson hybrid. Although this three-port network has been analysed previously(9,16), the analysis is carried out again here, but this time using the even-and odd mode approach. This analysis is carried out to illustrate the use of the even-and odd mode approach, as well as to clarify design constraints inherent in this circuit.

The design of this hybrid follows the procedures outlined in Section 2.2; starting from the plane of the junction (reference plane u Figure 2.3) the even and odd mode equivalent circuits are shown in Figure 3.2. Using the values for the circuit components given in Figure 3.1, the even mode admittance at the reference plane v (Y_{even}) is, with reference to Equation (2.11),

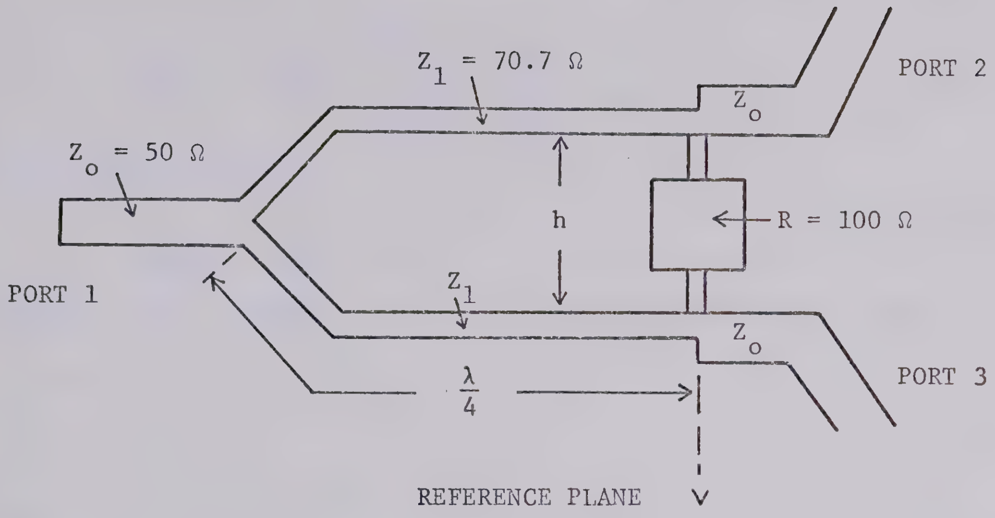

FIGURE 3.1 STRIPLINE MODEL OF A THREE-PORT WILKINSON HYBRID (CENTER CONDUCTOR ONLY)

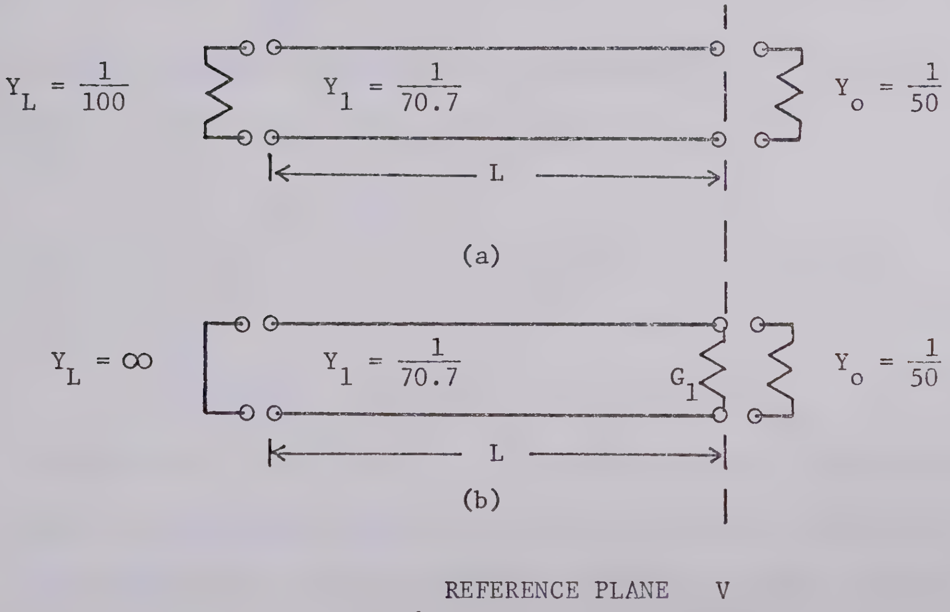

$L = \frac{\lambda}{4}$ AT THE DESIGN FREQUENCY

FIGURE 3.2 EQUIVALENT CIRCUITS FOR A THREE-PORT WILKINSON HYBRID
(a) EVEN MODE
(b) ODD MODE

$$Y_{even} = \frac{1}{70.7} \frac{\frac{1}{100} + j\frac{1}{70.7}\tan\theta}{\frac{1}{70.7} + j\frac{1}{100}\tan\theta} \tag{3.1}$$

At the design frequency $\theta = \frac{\pi}{2}$ and

$$Y_{even} = \frac{1}{50} \tag{3.2}$$

therefore, from Equation (2.12), the even mode reflection coefficient (Γ_e) is

$$\Gamma_e = 0.0 \tag{3.3}$$

Similarly for the odd mode, using Equation (2.13), the admittance Y_{odd}, is equal to G_1, as the load admittance is infinite (Figure 3.2). Therefore, from Equation (2.14), the odd mode reflection coefficient (Γ_o) at the design frequency is

$$\Gamma_o = \frac{\frac{1}{50} - G_1}{\frac{1}{50} + G_1} \tag{3.4}$$

To obtain a perfect impedance match at the design frequency, Γ_o should be set to zero; therefore, from (3.4)

$$G_1 = \frac{1}{50} \quad \text{mhos} \tag{3.5}$$

and from Equation (2.10), the value of the resistance (R) in Figure 3.1 is

$$R = \frac{2}{G_1} = 100 \text{ ohms} \tag{3.6}$$

From the above calculations, at the design frequency, the magnitudes of the reflection coefficients (ρ) at all three ports and the isolation between ports 2 and 3 are, from Equations (2.15), (2.16) and (2.17):

$$\begin{aligned} \rho_1 &= \rho_2 = \rho_3 = 0.0 \\ I &= \infty \text{ db} \end{aligned} \tag{3.7}$$

Using Equations (2.11) to (2.17) inclusive, in a manner similar to Equation (3.1), the frequency dependent characteristics of the single-resistor model were computed and are illustrated in Figure 3.3. Here, the voltage standing wave ratio (VSWR) is plotted instead of ρ, because the commonly measured parameter is VSWR. Since

$$\mathrm{VSWR} = \frac{1 + \rho}{1 - \rho} \tag{3.8}$$

the variation of VSWR with frequency has the same general form (for ρ small) as the variation of ρ with frequency.

3.2 Modified Three-Port Wilkinson Hybrid Using a Distributed Resistance

From Equation (2.13) it is apparent that the odd mode depends on the value of G, hence this mode can be controlled by the magnitude, location and number of resistive components used. In this fashion, the values of the reflection coefficients of, and the isolation between, ports 2 and 3 can be controlled (Equations (2.15) and (2.16)). However, the reflection coefficient associated with port 1 (Equation 2.17) cannot be altered in this way, as it depends on the even mode alone, and the even mode is independent of the resistive components used. This independence of the even mode places a limit on the effectiveness of varying the resistive components, for even if the odd mode were completely cancelled, the port 2 and 3 characteristics would be

$$\begin{aligned} \rho_2 \Big|_{\text{odd mode zero}} &= \rho_3 = \frac{1}{2} |\Gamma_e| \\ I \Big|_{\text{odd mode zero}} &= 20 \log_{10} [\tfrac{1}{2} |\Gamma_e|] \end{aligned} \tag{3.9}$$

Therefore, unless $|\Gamma_e|$ is small, the value of ρ_2 and ρ_3 will be too large and the isolation (I) will be too small for most practical applications. Typically, it is desirable to have $\rho \leq 0.05$

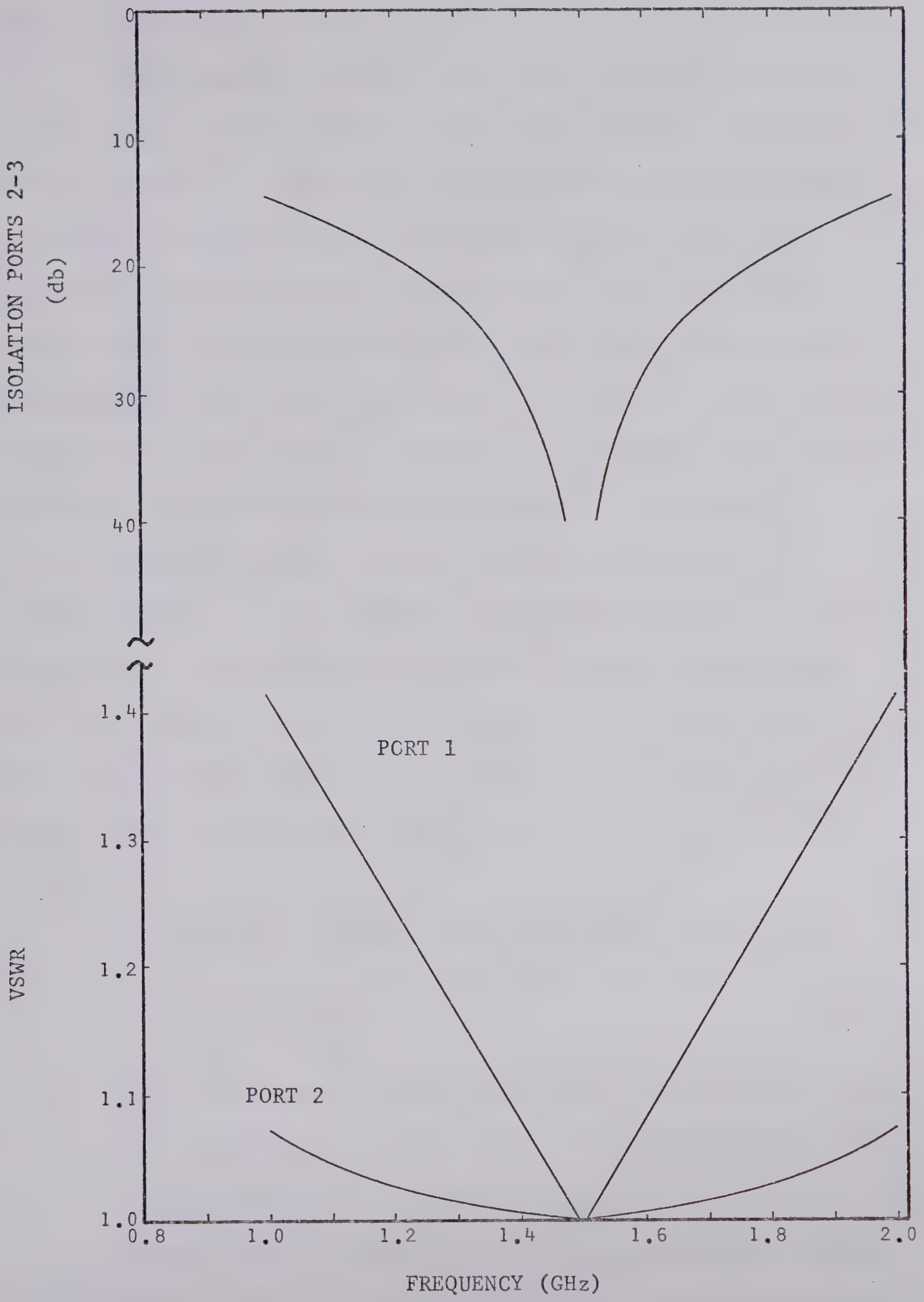

FIGURE 3.3 COMPUTED CHARACTERISTICS OF THE THREE-PORT WILKINSON HYBRID (SINGLE RESISTOR MODEL)

(VSWR ≤ 1.1) and $|I| \geq 30$ db.

The limitations placed, by the even mode, upon the frequency characteristics of the circuit studied here are shown in Figure 3.4. From this figure it is seen that a theoretical optimum design having the odd mode completely cancelled has about double the frequency bandwidth (with respect to the characteristics of the basic one-resistor model) over which the isolation is ≥ 30 db, while maintaining the VSWR of ports 2 and 3 ≤ 1.065. It was felt that this increase in VSWR was acceptable and that the increased bandwidth, with respect to isolation, justified further investigation of this circuit.

Using the method of analysis outlined in Chapter II (Equations (2.11) to (2.17) inclusive, along with Figures 2.4 and 2.6) the three-port hybrid using a distributed resistance was analysed. The various resistive distributions studied can be grouped according to the region of the hybrid circuit (Figure 3.1) in which they were located. These regions were between the circuits of ports 2 and 3 and either

(a) along only the impedance transformers (that part of the circuits whose characteristic impedance is z_1 in Figure 3.1) or

(b) on both sides of, but close to the reference plane v or

(c) continuously from the junction of ports 2 and 3 circuits up to and past the reference plane v.

It was found, for case (b) above, that this method resulted in characteristics that were less desirable than those of the single-resistor model. However, closely equivalent characteristics could be

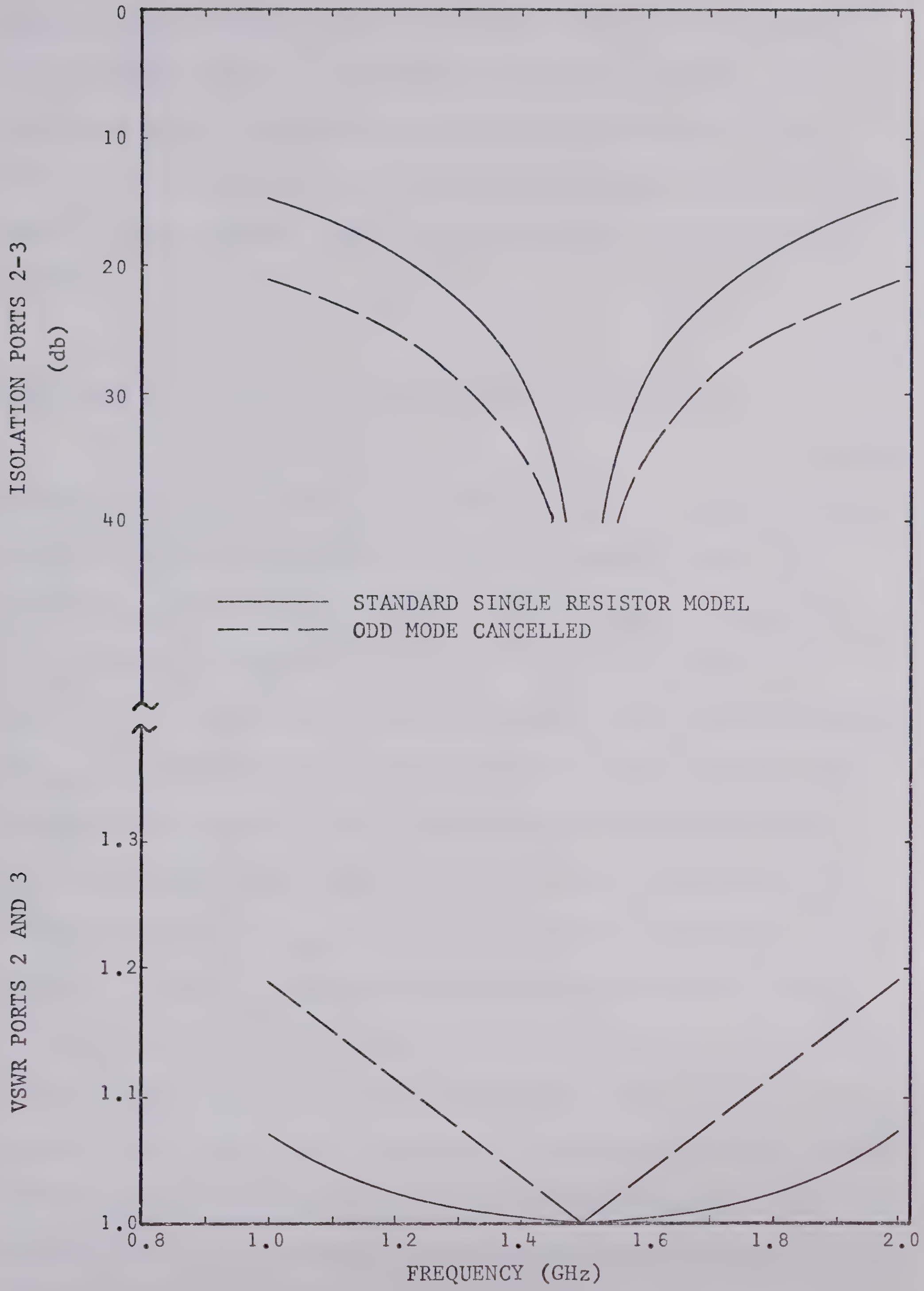

FIGURE 3.4 COMPUTED CHARACTERISTICS FOR THREE-PORT WILKINSON HYBRID [ODD MODE CANCELLED — SINGLE RESISTOR MODEL]

obtained if the values of the theoretical discrete resistors were such that their parallel combination resulted in 100 ohms. The theoretical models for resistive distributions (a) and (c) above indicated that the odd mode could not be completely cancelled using resistive distributions alone. For the odd mode to be cancelled, we need

$$\Gamma_o = 0.0 \tag{3.10}$$

so from Equation (2.14) this would further require that

$$Y_{odd} = Y_o = \frac{1}{50} \tag{3.11}$$

However, since Y_{odd} is normally a complex number, its real part has to equal Y_o, while its imaginary part has to be cancelled. By computing Y_{odd} for various resistive distributions, the real part of Y_{odd} could be controlled such that it closely approached the value of Y_o but this condition produced a significant imaginary part of Y_{odd} that was inductive. This inductance can be compensated for by adding capacitance but since the capacitive susceptance has an inverse frequency characteristic to that of inductive susceptance, the imaginary part of Y_{odd} can only be completely cancelled at one frequency. Figure 3.5 illustrates the characteristics of a design in which the odd mode is "minimized" as far as the use of resistances and capacitances will allow, within the bounds of this study. It is seen from this figure that there is some improvement over the single-resistor model; however, the inability to completely cancel the imaginary part of Y_{odd} has made the improvement rather small. The design of Figure 3.5 used a continuous distribution of resistance (R_n) along the entire length of the impedance transformers, plus an additional resistor (R_a) and capacitor (C_a) located on the reference

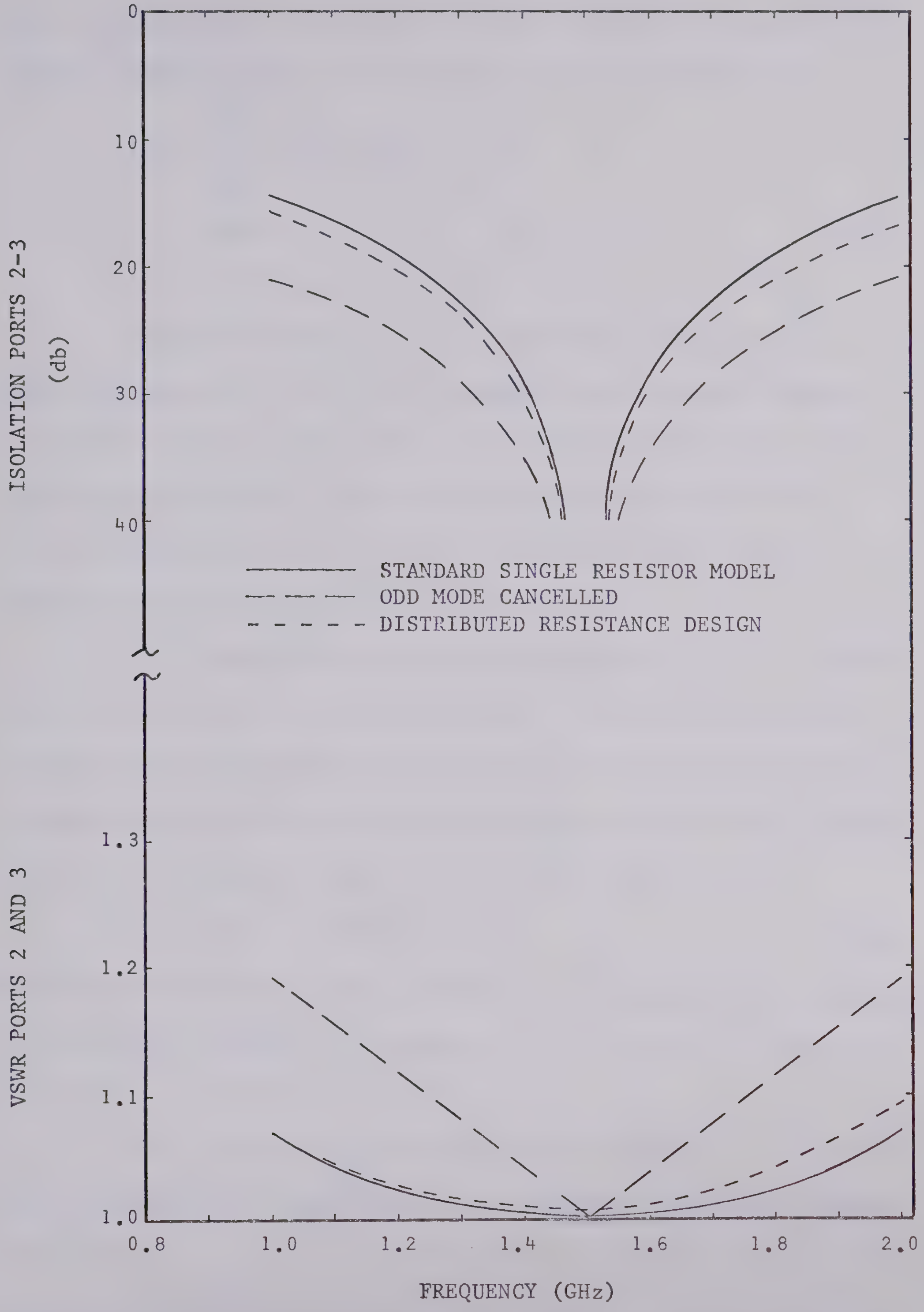

FIGURE 3.5 COMPUTED CHARACTERISTICS OF THE THREE-PORT WILKINSON HYBRID (DISTRIBUTED RESISTANCE MODEL)

plane v (Figure 3.1). The values of these components were as follows, (using a separation of 0.1 cm for the discrete resistors of R_n)

$$R_n = \sum_{n=1}^{50} (1230 + 20n)$$

$$R_a = 526\ \Omega \qquad (3.12)$$

$$C_a = 1.06 \text{ pf}$$

The characteristics of the "minimized" odd mode design, plotted in Figure 3.5, pertain to a model having a center frequency of 1.5 GHz. Characteristics identical in form can be computed for models having any design center frequency that is required. For design frequencies different from 1.5 GHz the frequency scale of Figure 3.5 is multiplied by the factor p, where

$$p = (\text{desired center frequency in GHz})/1.5 \qquad (3.13)$$

As the design frequency changes, the length (L) of the $\frac{\lambda}{4}$ transformer section used in the circuit of Figure 3.1, will change appropriately. This means that the length of the distributed resistance will change also, with the required length (L) now being, using (3.13)

$$L = (\tfrac{\lambda}{4} \text{ at } 1.5 \text{ GHz})/p \qquad (3.14)$$

Referring to Figure 2.6, the separation (ℓ) of the theoretical discrete resistors used to simulate the continuous distribution of resistance will now be

$$\ell = (\ell \text{ for a design frequency of } 1.5 \text{ GHz})/p \qquad (3.15)$$

Also, from Figure 2.6, the value of each theoretical discrete resistor is

$$R_n = \frac{h_n}{\ell} R_s \qquad (3.16)$$

$$n = 1, 2, \ldots 50$$

where h_n is the separation of the port 2 and 3 circuitry and R_s is the sheet resistivity of the thin film resistor. Since the value of ℓ has been modified to account for the new center frequency, the values of h_n and R_s must also be modified to ensure that all the values of R_n are the same as given in Equation (3.12).

It has been shown in this section that it is theoretically possible to use a distributed resistance in the construction of a symmetrical three-port hybrid. The resultant VSWR's of all ports and the isolation between the conjugate ports of this hybrid are at least as satisfactory as the single resistor model. The use of a distributed resistance in lieu of a single resistor will provide more assurance that the power division will produce two equal-amplitude, equal-phase signals as any inherent differences of amplitude or phase will be more severely attenuated. However, the practical usage of this distributed resistance model of the three-port hybrid may be limited by the increased complexities of construction and the smallness of the increase in bandwidth over which the isolation is increased with respect to the single resistor model.

3.3 Effects of Construction Tolerances on Three-Port Hybrid Stripline Circuits

In stripline circuit construction, the actual circuit may have impedance mismatches due to inherent manufacturing tolerances. These mismatches are usually associated with unintentional changes in the design values of the characteristic impedances of the stripline circuits and may occur in any one or all of the steps involved in the design and construction, such as:

(a) the initial drafting of the enlarged model

(b) photo reduction and forming of the negative

(c) transferring the design from the negative to the copper clad stripline board

(d) the chemical etching process

Another contributing factor could be small variations in the dielectric constant and/or the thickness of the copper film of the stripline board itself. These sources of error would be minor if considered separately; however, when considered together, the total error may be significant.

A theoretical study was carried out to determine the effects of characteristic impedance variations upon the VSWR's of all ports and the isolation between ports 2 and 3. It is reasonable to assume that the maximum error that could occur can be limited to ± 5% of the design impedance for any part of the circuit and hence this study of the effects of tolerances was limited to this range of errors. Also, for purposes of analysis, the circuit was divided into three sections and the error associated with each section was assumed to be uniform throughout the section. These sections were (reference Figures 2.3 and 3.1):

section A - That part of the circuit extending from the port 1 coax-to-stripline connector to reference plane u.

section B - The circuit area between reference planes u and v.

section C - That part of the circuit extending from the reference plane v to the stripline-to-coax connectors of ports 2 and 3.

The tolerances under study were confined to one section only and the remainder of the circuit was considered to be correct. This procedure gave the maximum effect of the errors upon the VSWR and isolation characteristics of the hybrid circuit.

The results of this study, for each section, show that

(1) when the tolerance limit is applied to section A or C (here the impedance mismatch between the coaxial line and the stripline has been taken into account) the VSWR curve for port 1 is uniformly shifted higher in magnitude so that the minimum VSWR is now 1.1.

(2) for the tolerance limit applied to section A (using the same procedure as in (1) above) the VSWR for ports 2 and 3 shows some fluctuation in curvature and increases in magnitude to a value near 1.1 in the vicinity of the design frequency while if this limit is applied to section C similar variations in curvature occur but the increase in magnitude is only to a value near 1.05 in the vicinity of the design frequency.

(3) for both the above situations ((1),(2)) the isolation between ports 2 and 3 was reduced by only a small amount.

(4) when the tolerance limit was applied to section B (here there is no coaxial line-stripline mismatch to be accounted for) the effect upon the characteristics of the hybrid was similar to those for section A above, with the minimum of the port 1 VSWR shifted to the vicinity of 1.15. In this case the effect upon the

isolation was more pronounced than that of section A but still only small deterioration resulted.

For all of the combinations studied it was apparent that the effect of possible tolerances upon the VSWR and isolation characteristics was less if the errors were on the plus side. Also apparent from this study is that, if the circuit performance is expected to be reasonably close to design theory, then possible circuit impedance errors will have to be kept below ± 2% of the design values.

3.4 Interpretation of Experimental Results for a Three-Port Wilkinson Hybrid

The main purpose of the experiments reported here was to verify the theoretical results found for the distributed resistance hybrids and to determine if there were any inherent difficulties in construction techniques. In accordance with the theoretical development of Section 3.2, the thin film resistors were cut so that the total resistance was 100 ohms (the parallel combination of the discrete resistors used in the theory resulted in the basic single resistor value of 100 ohm).

These thin film resistors were constructed from a commercially obtained material consisting of a thin, metallic, resistive film deposited on a mylar base, with the total thickness being about 3 mils. The resistivity of this thin film material is given in ohms per square so that any resistor constructed has a value R, where

$$R = (\text{number of squares})(\text{resistivity}) \qquad (3.17)$$

The thin film resistors used for these experiments are shown in Figure 3.5, their value is calculated as

$$R = \frac{h}{w}(200) = 100 \text{ ohms} \qquad (3.18)$$

To ensure good electrical contact between the resistor edge and the copper strips of the circuit shown in Figure 3.7, the w edges of the thin film were covered by a thin coating of silver paint.

As noted in Figure 3.6 there are two different resistors, 23-R and 27-R, corresponding to theoretical models of 23 discrete resistors of 2300 ohms each and 27 resistors of 2700 ohms each, respectively. These thin film resistors were placed in the circuit of Figure 3.7, in the vicinity of the reference plane indicated, in such a manner that the w edges overlapped the copper strips of the circuitry ($h > H$). This overlapping of the edges presented a problem in determining the actual amount of thin film resistor that was used electrically. Hence, the theoretical model of the circuit displayed in Figure 3.7 was developed for both the 23-R and 27-R cases using several different values for the 23 and 27 discrete resistors, respectively. For both the 23-R and 27-R models, the same value of resistance was used for all the discrete resistors at any one time, and the resistor separation was 0.1 cm electrically (corresponding to $\frac{\lambda}{200}$ for a frequency of 1.5 GHz). The theoretically obtained characteristics for both these models are shown in Figures 3.8 to 3.12 inclusive, where the basic frequency scale is for a design center frequency (f_c) of 1.5 GHz.

The procedures used to measure the experimental characteristics were

(a) The VSWR for port 1 was measured with the resistor out of the circuit and both ports 2 and 3 terminated in 50 ohm loads.

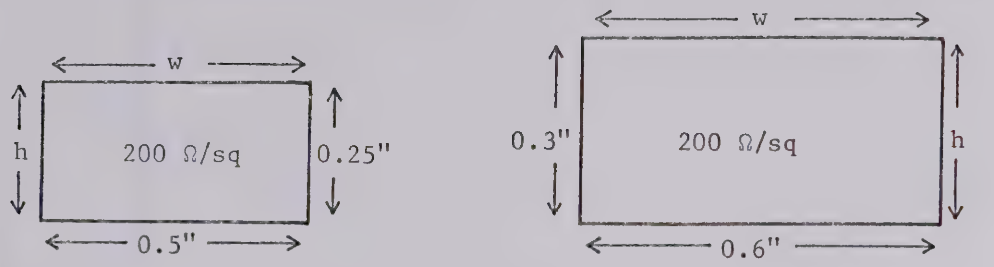

23-R CASE

27-R CASE

FIGURE 3.6 THIN FILM DISTRIBUTED RESISTANCES

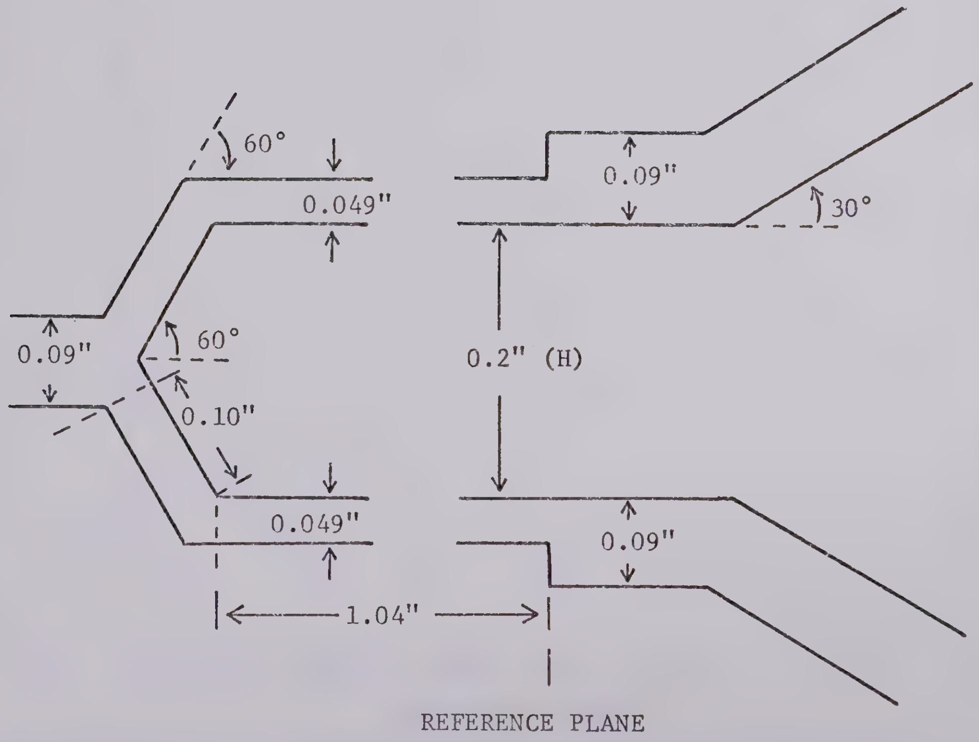

FIGURE 3.7 EXPERIMENTAL MODEL OF THREE-PORT WILKINSON HYBRID (STRIPLINE CENTER CONDUCTOR ONLY)

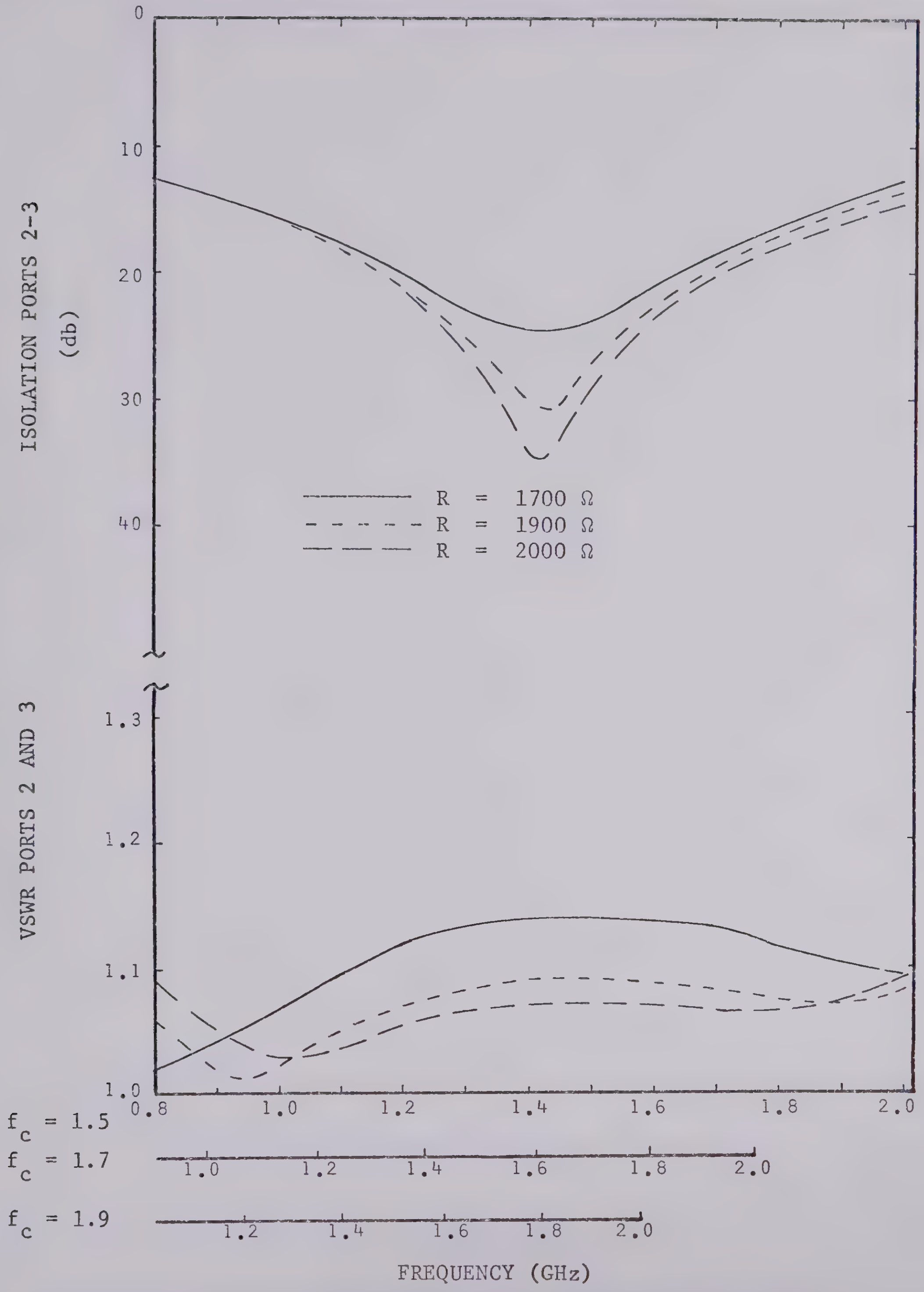

FIGURE 3.8 COMPUTED CHARACTERISTICS OF THREE-PORT WILKINSON HYBRID 23-R MODEL (RESISTANCES CENTERED ON REFERENCE LINE)

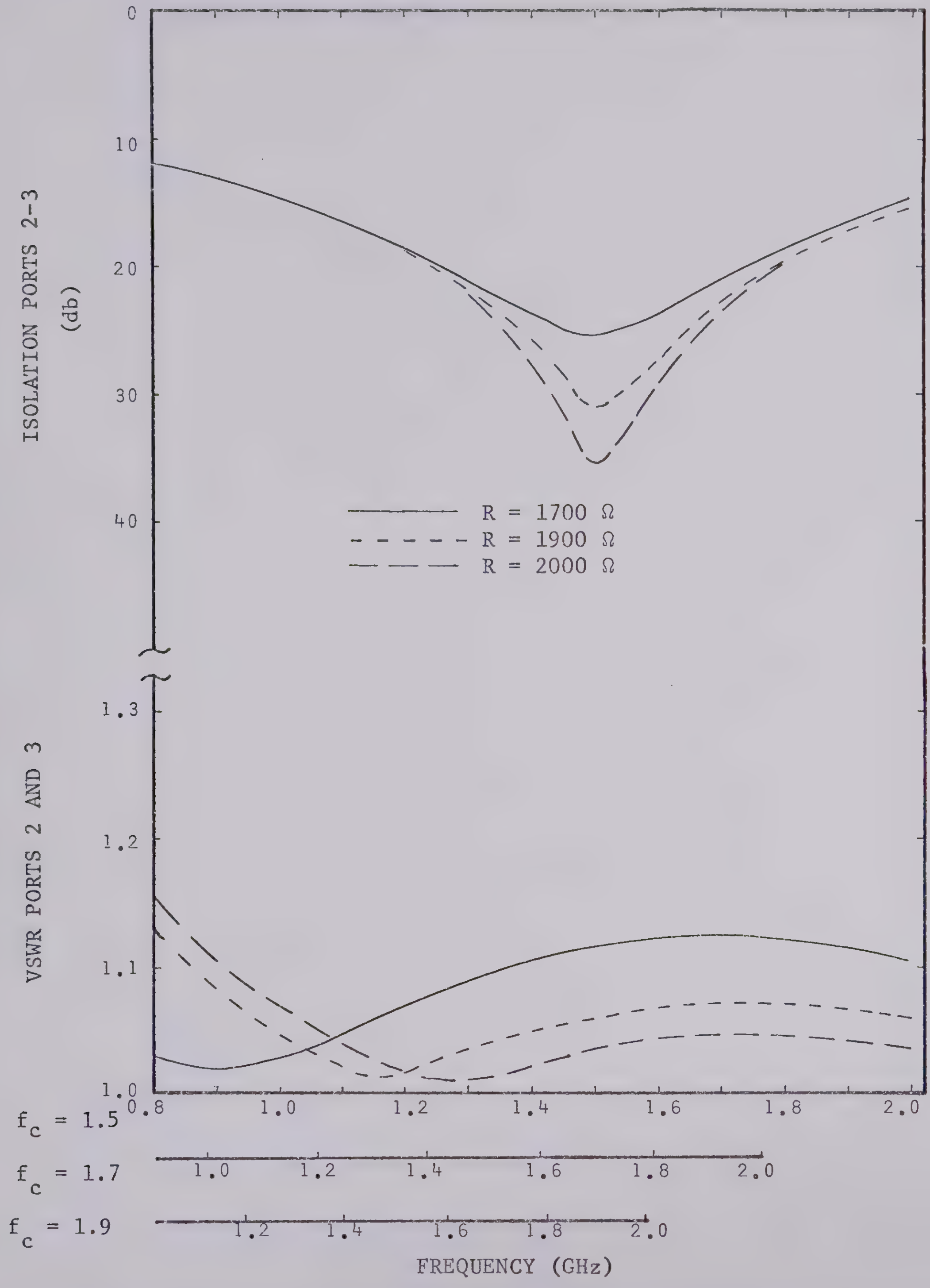

FIGURE 3.9 COMPUTED CHARACTERISTICS OF THREE-PORT WILKINSON HYBRID 23-R MODEL (2/3 OF RESISTANCES ON 70.7 OHM LINE)

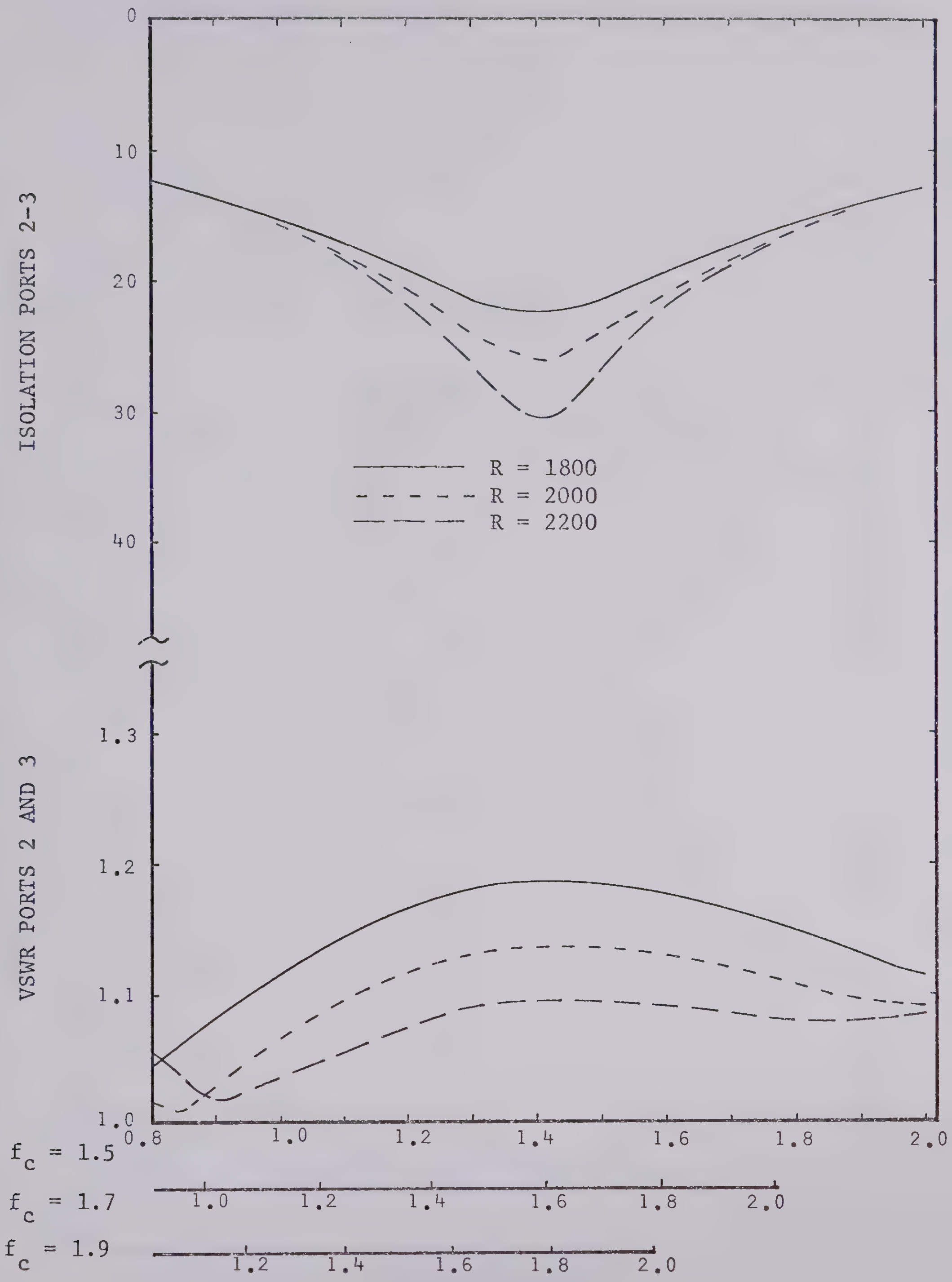

FIGURE 3.10 COMPUTED CHARACTERISTICS OF THREE-PORT WILKINSON HYBRID 27-R MODEL (RESISTANCES CENTERED ON REFERENCE LINE)

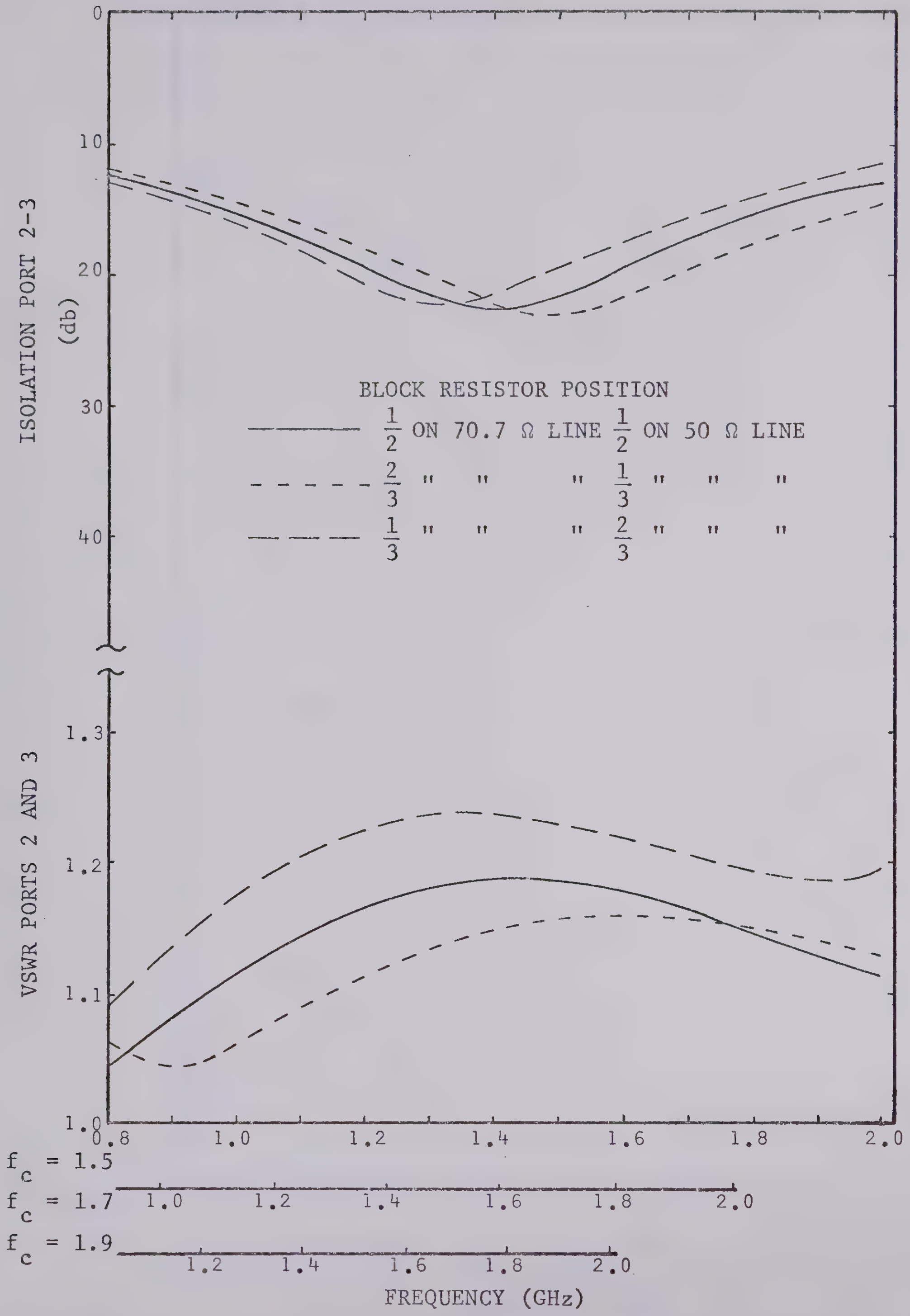

FIGURE 3.11 COMPUTED CHARACTERISTICS OF THREE-PORT WILKINSON HYBRID 27-R MODEL (R = 1800 OHMS)

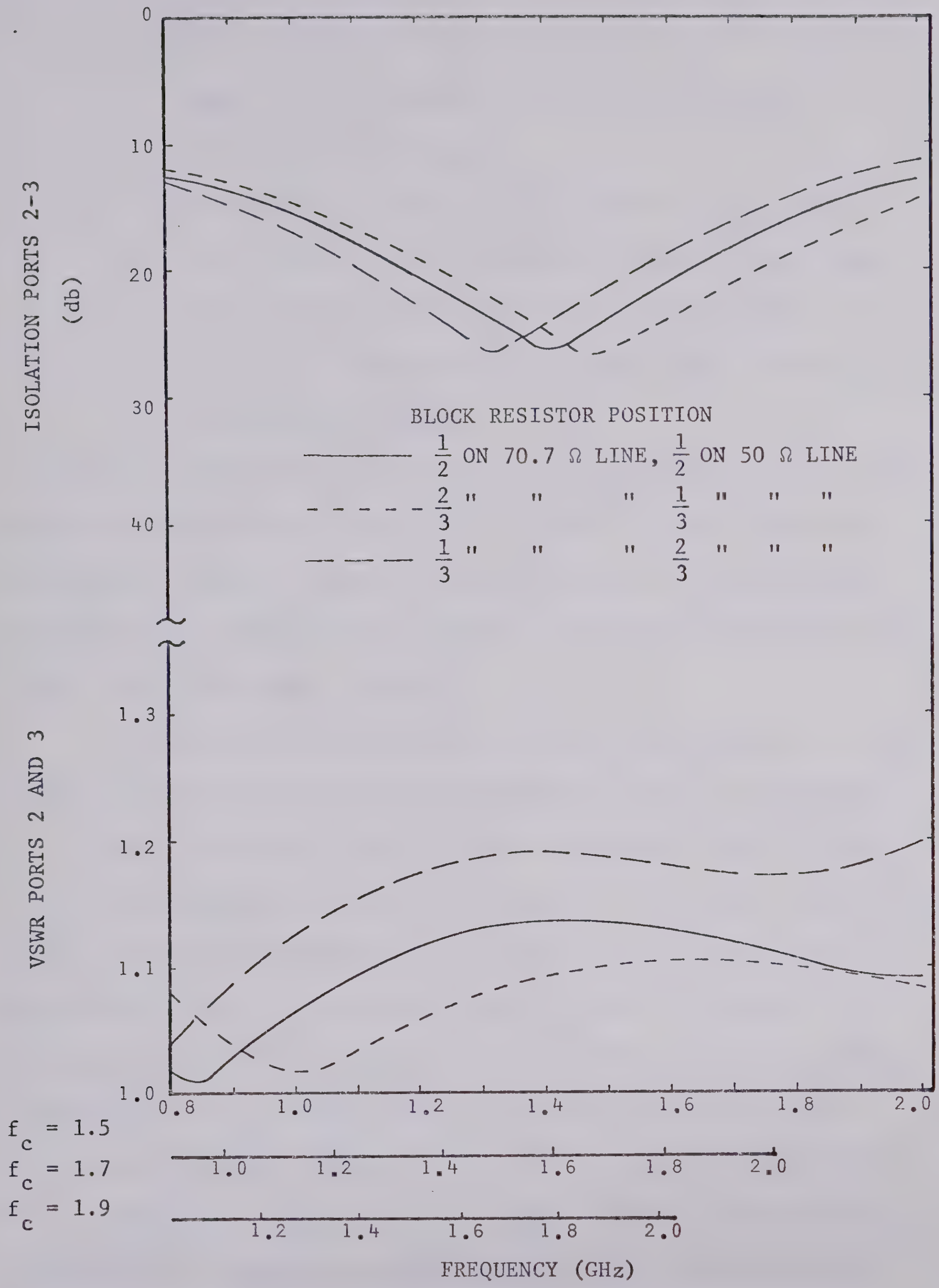

FIGURE 3.12 COMPUTED CHARACTERISTICS OF THREE-PORT WILKINSON HYBRID 27-R MODEL (R = 2000 OHMS)

(b) The port 2 (or 3) VSWR was measured with the ports 1 and 3 (or 2) terminated in 50 ohm loads and the resistor in the circuit.

(c) The isolation between ports 2 and 3 was measured as the difference in db between the power incident upon port 2 (or 3) and the power being emitted from port 3 (or 2). The resistor was in the circuit and port 1 was match terminated.

These measured characteristics are displayed in Figures 3.13 to 3.15 inclusive. The internal isolation is arrived at from an external measurement: however, the error should be small, as power measurements are rather insensitive to VSWR's of less than 1.5 and the port 2 and 3 VSWR's were less than 1.2.

Figure 3.13 shows the VSWR for port 1; the point of minimum VSWR indicates that the impedance transformers are $\frac{\lambda}{4}$ at a frequency of 1.7 GHz. The effects of the corners and junction area of Figure 3.7 on the frequency that gives a $\frac{\lambda}{4}$ length are reported in Appendix A. When the resistor was placed in the circuit and the VSWR for port 1 was measured again, it was noticed that the point of minimum VSWR had shifted to 1.9 GHz. This shift of the characteristics to higher frequencies was also noticed when the VSWR and isolation of ports 2 and 3 were measured. Also, it was known from previous experiments that the coax-to-stripline connectors used, produced increasingly high VSWR's for frequencies greater than 1.5 GHz. Therefore some form of calibration of the measured results were necessary before a comparison with the theory could be made. The calibration procedure used is described in Appendix B and the results for the single 100

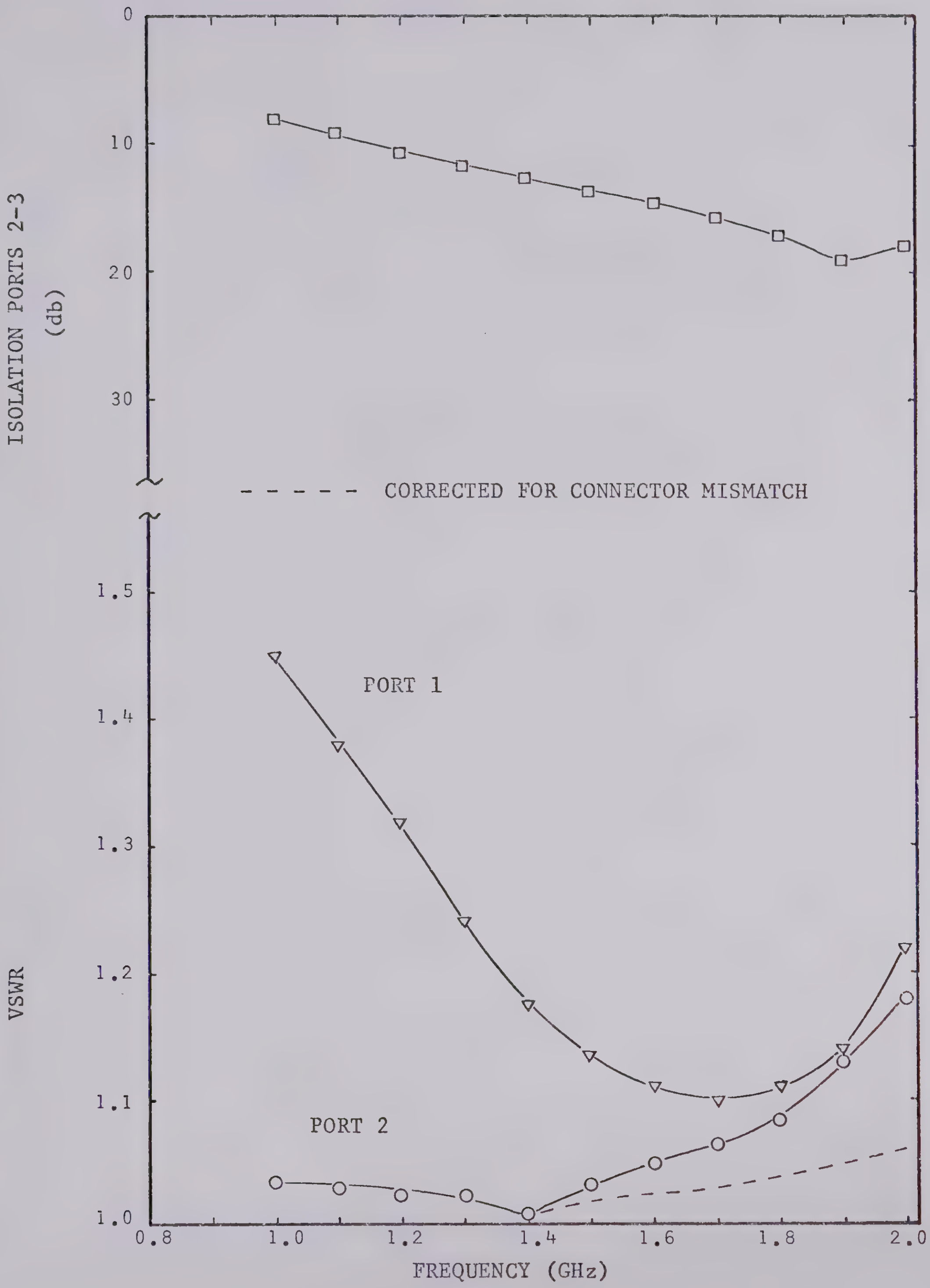

FIGURE 3.13 EXPERIMENTALLY MEASURED CHARACTERISTICS OF THE THREE-PORT WILKINSON HYBRID (SINGLE RESISTOR MODEL)

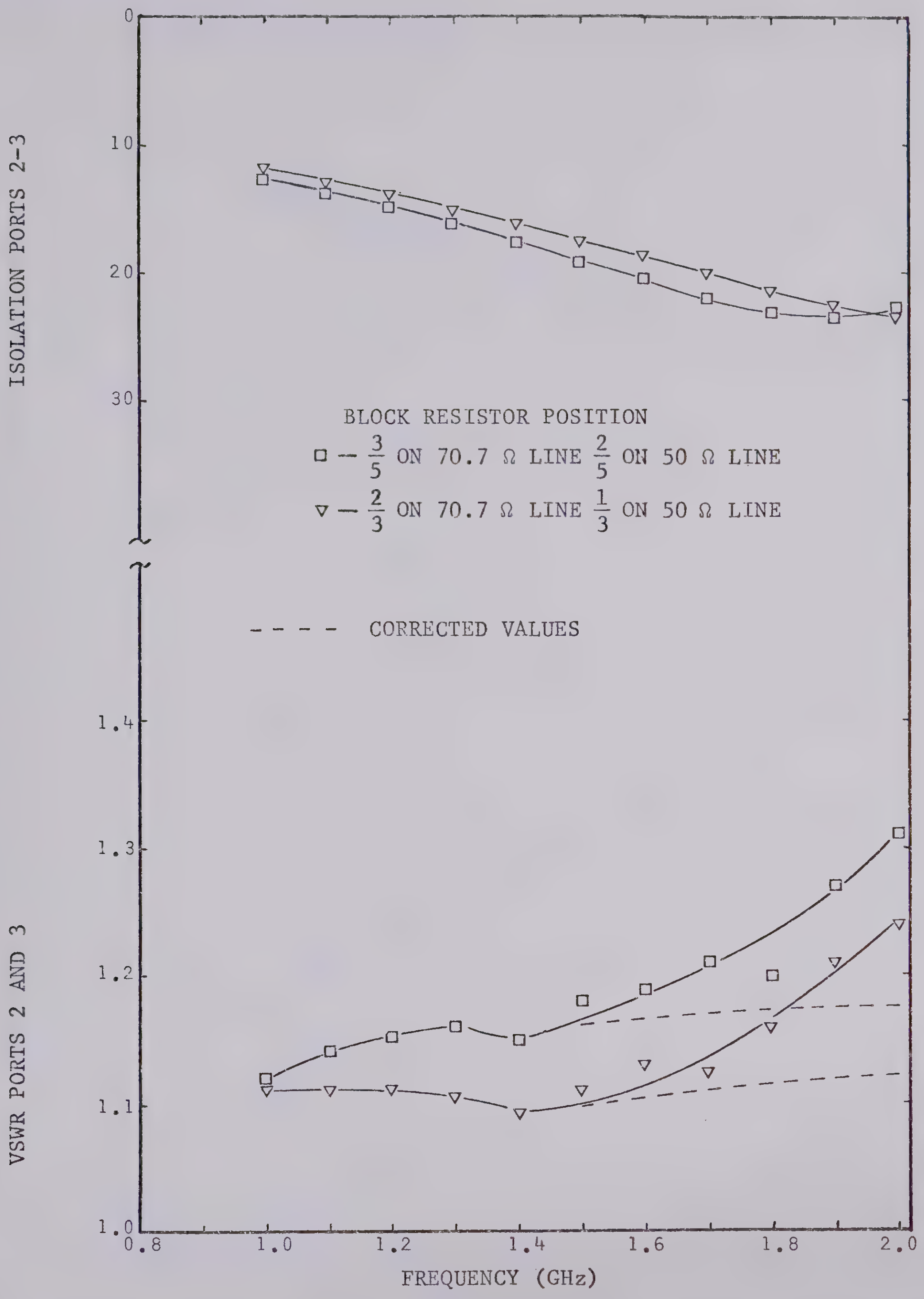

FIGURE 3.14 EXPERIMENTALLY MEASURED CHARACTERISTICS OF THE THREE-PORT WILKINSON HYBRID (23-R MODEL)

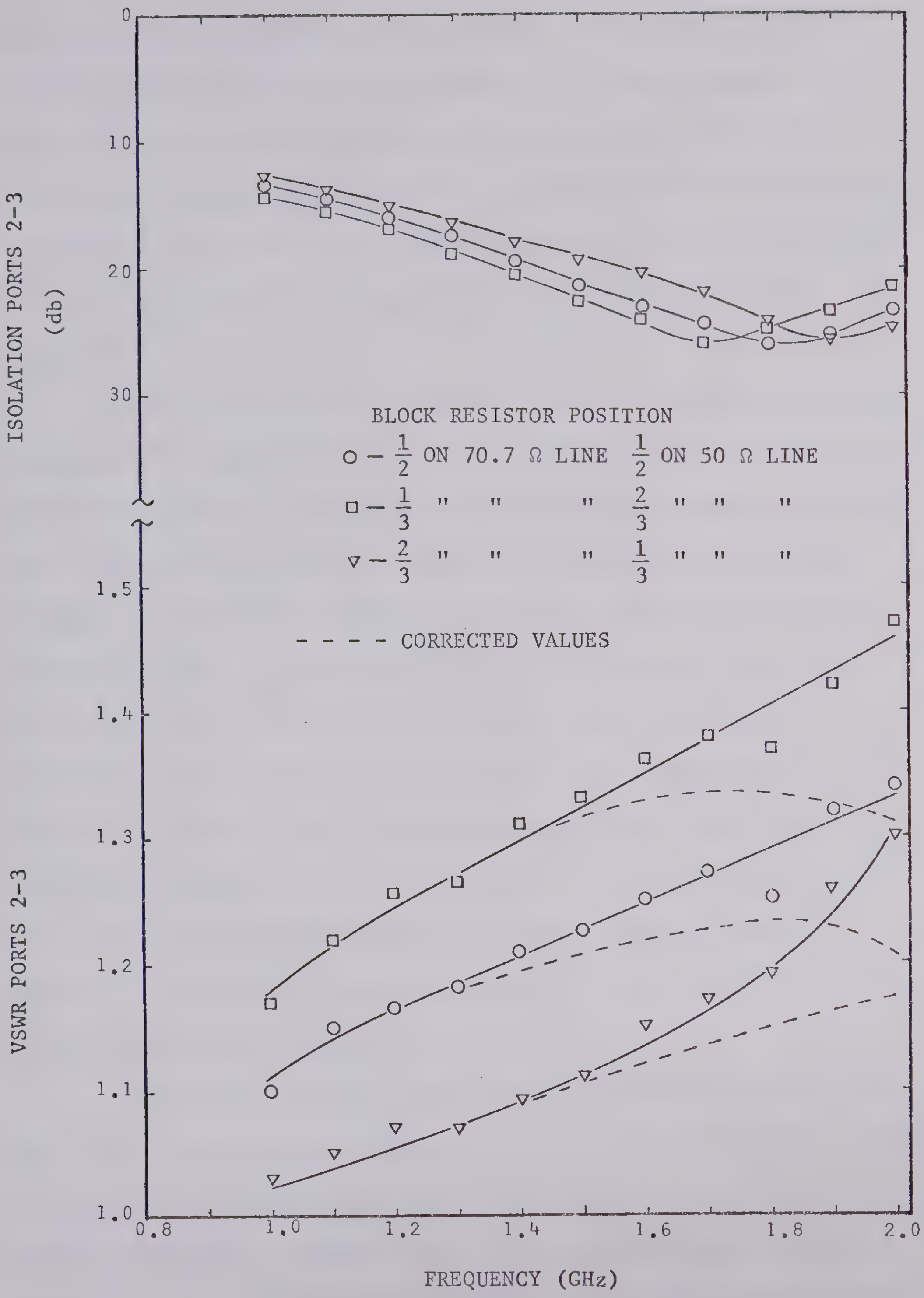

FIGURE 3.15 EXPERIMENTALLY MEASURED CHARACTERISTICS OF THE THREE-PORT WILKINSON HYBRID (27-R MODEL)

ohm resistor case are shown in Figure 3.13. This established the correction factor for the mismatch between the connectors and the stripline circuit and also established the frequency shift to be expected when the distributed resistance was inserted into the circuit. The measured characteristics, along with the appropriate corrections, for both the 23-R and 27-R cases are shown in Figures 3.14 and 3.15 respectively.

Using the frequency scale for a center frequency of 1.9 GHz, a comparison of Figures 3.8 and 3.9 with Figure 3.14, shows that the experimental results of the 23-R case follows the theoretical pattern for all the discrete resistors having a value of 1900 ohms. This value of 1900 ohms for the discrete resistors, produces a parallel combination, that is very close in value to that part of the thin film resistor that lies between the copper strips of the ports 2 and 3 circuitry. That part of the thin film resistor which overlaps the copper strips appears to be electrically neglected. When the experimental results of the 27-R case are studied and Figures 3.10, 3.11, 3.12 and 3.14 are compared, the results indicate that the value of the theoretical discrete resistors is about 1900 ohms each, substantiating the findings of the 23-R model.

The shift in center frequency of the characteristics of the hybrid, when the resistor is inserted into the circuit, can be attributed to the inductance and capacitance added to the circuit by the resistor construction (Appendix B). From Equations (B.2) and (B.6) it is evident that the reactance inherent in the resistor construction can be reduced by closer spacing of the ports 2 and 3 circuitry. This spacing can only be reduced a limited amount. A certain minimum separation must be maintained to avoid appreciable electromagnetic

coupling between the stripline circuitry and also to enable the formation of a proper junction area (Appendix A).

It is interesting to note that the reactance attributed to the resistor construction (Appendix B) is produced by a section of transmission line that is $\frac{\lambda}{50}$ in length at the design frequency. This reactance produces a shift in frequency of about 14% of the design frequency. Since the shift in frequency characteristics is present at all ports, the amount of the shift can be computed (Appendix B) and the length of the $\frac{\lambda}{4}$ transformers adjusted accordingly. This would permit the use of a single resistor in stripline construction, without involvement of the circuit design in complicated compensation procedures, while still maintaining the symmetry of the circuit characteristics.

CHAPTER IV

THREE-PORT HYBRIDS USING MULTIPLE-SECTION QUARTER-WAVELENGTH IMPEDANCE TRANSFORMERS

4.1 Introduction

As shown in Chapter II, the characteristic impedance(s) of the quarter-wavelength $(\frac{\lambda}{4})$ section(s) of transmission line serve to match the impedances of the junction area to those of ports 2 and 3 (reference planes u and v respectively, Figure 4.1). The characteristic impedances of these transformer sections are designed to match the even mode impedances of the reference planes u and v. This means that the VSWR for port 1 is essentially that of the transformer section(s) alone, hence, by varying the impedance of these section(s), various VSWR characteristics for port 1 can be obtained. A single transformer section provides a satisfactory impedance match over a narrow range of frequencies; however, by using more than one section, a satisfactory impedance match can be obtained over a band of frequencies. The greater the number of transformer sections, the wider the bandwidth of the satisfactory impedance match and the more varied the VSWR characteristics can be. However, since each section is $\frac{\lambda}{4}$ long, as the number of sections increase, so does the overall length of the complete impedance transformer and the total length of even a few sections can become unwieldy. The commonly used multiple-section transformer is the two section model, as this provides a relatively large bandwidth,

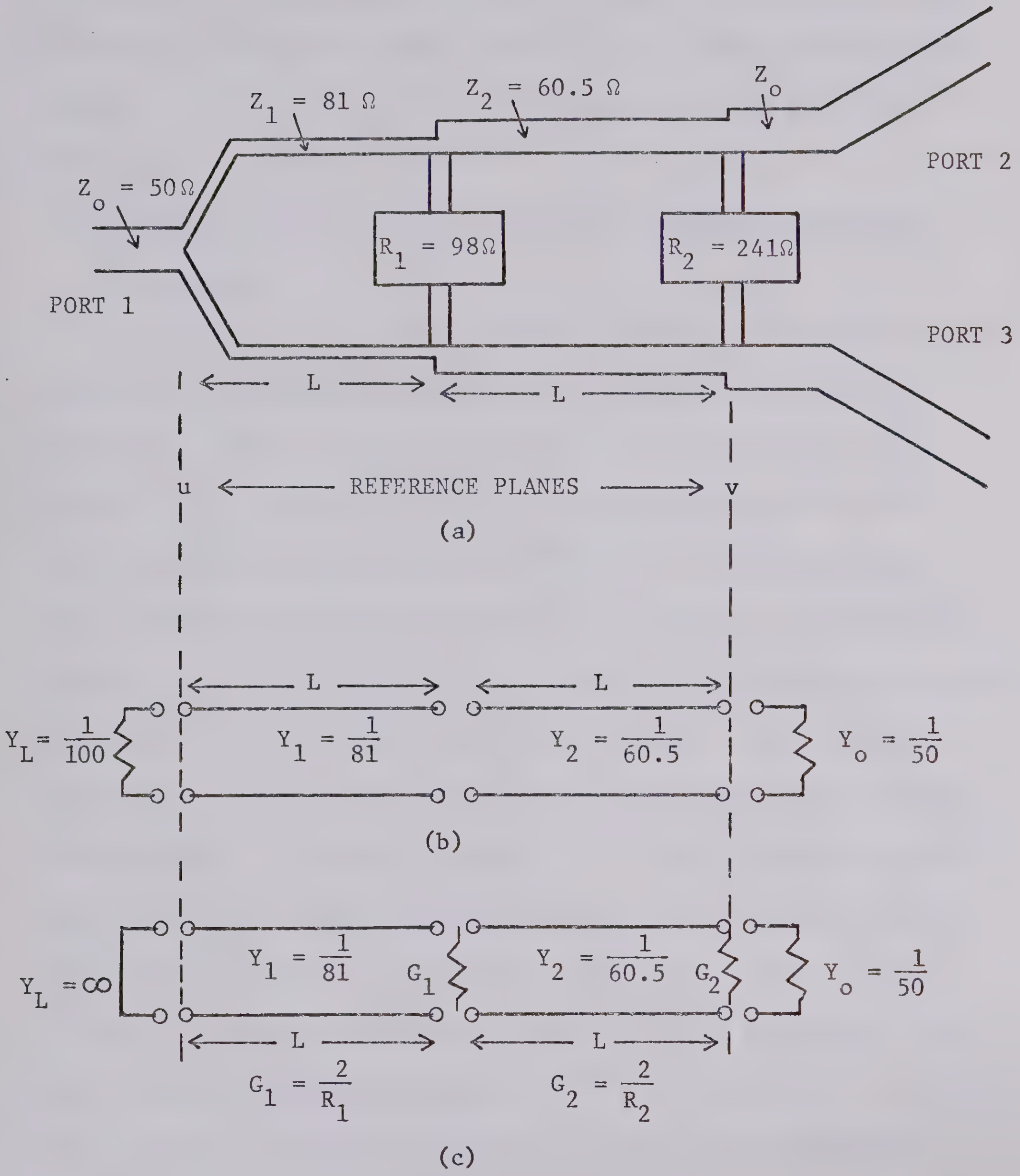

$L = \frac{\lambda}{4}$ AT THE DESIGN CENTER FREQUENCY

FIGURE 4.1 THREE-PORT HYBRID USING TWO-SECTION CHEBYSHEV IMPEDANCE TRANSFORMER
(a) CENTER CONDUCTOR STRIPLINE MODEL
(b) EQUIVALENT CIRCUIT FOR THE EVEN MODE
(c) EQUIVALENT CIRCUIT FOR THE ODD MODE

with a reasonably short overall length. Since the use of three or more impedance transformer sections is merely an extension of the two-section catagory and this catagory is well represented by the Chebyshev and Binomial models, only these two models will be discussed here.

4.2 Three-Port Hybrid Using a Two-Section Chebyshev Impedance Transformer

The stripline circuit of this device, along with its associated even and odd mode equivalent circuits, is shown in Figure 4.1. Here the necessary impedance matching between the junction area and the ports 2 and 3 is accomplished by the use of a two-section Chebyshev transformer(16). For a given maximum acceptable VSWR in the frequency range of interest, this particular impedance transformer provides the desired operating frequency bandwidth, while utilizing the least circuit length. By setting the maximum permissible reflection coefficient at 0.05 (VSWR = 1.105) and designing for a center frequency of 1.5 GHz, the characteristic impedances of the two, $\frac{\lambda}{4}$ sections, are 81.0 and 60.5 ohms respectively. These impedances provide a usable bandwidth of an octave. The use of a Chebyshev impedance transformer in a symmetrical three port hybrid has been described by Cohn(16), who found that the values of the resistors, R_1 and R_2 (Figure 4.1) were 98 and 241 ohms, respectively.

Using the procedures (mainly Equations (2.11) and (2.13)) outlined in Section 2.2, for extending the analysis of Section 3.1 to include one more length of transmission line, the circuit described above can be readily characterized. These characteristics of

VSWR and isolation are shown in Figure 4.2. Similar to the single section transformer model discussed in Chapter III, the odd mode can be controlled by the resistances used, while the even mode is independent of these resistances. Again, the "theoretically optimum" model is taken to be the case in which the odd mode is completely cancelled. These "optimum" characteristics are arrived at by applying Equation (3.9) and, for purposes of comparison, these characteristics are shown in Figure 4.2. The "optimum" characteristics provide an increase in isolation of about 5 db at the center frequency, while still maintaining an acceptable VSWR at ports 2 and 3.

A theoretical investigation was carried out to see if the odd mode could be cancelled by using various distributions of resistance. These distributions were placed along the $\frac{\lambda}{4}$, impedance transformer sections, extending from reference planes u to v in Figure 4.1. By keeping the resistive distributions between only the impedance transformer sections of the circuitry, there is greater flexibility in the manner in which ports 2 and 3 can be terminated. The theory was developed in a similar manner to that of Section 3.2 where, for theoretically optimum conditions,

$$\Gamma_o = 0.0 \quad \text{and} \quad Y_{odd} = \frac{1}{50} \qquad (4.1)$$

Hence, the search for a suitable resistive distribution involved equating the real part of the calculated odd mode admittance to $\frac{1}{50}$ while simultaneously attempting to obtain an imaginary part of the odd mode admittance that could be cancelled out. The spacing of the discrete resistors (used to simulate a continuous distribution of resistance) was taken as 0.1 cm. This was $\frac{1}{100}$ of the total length

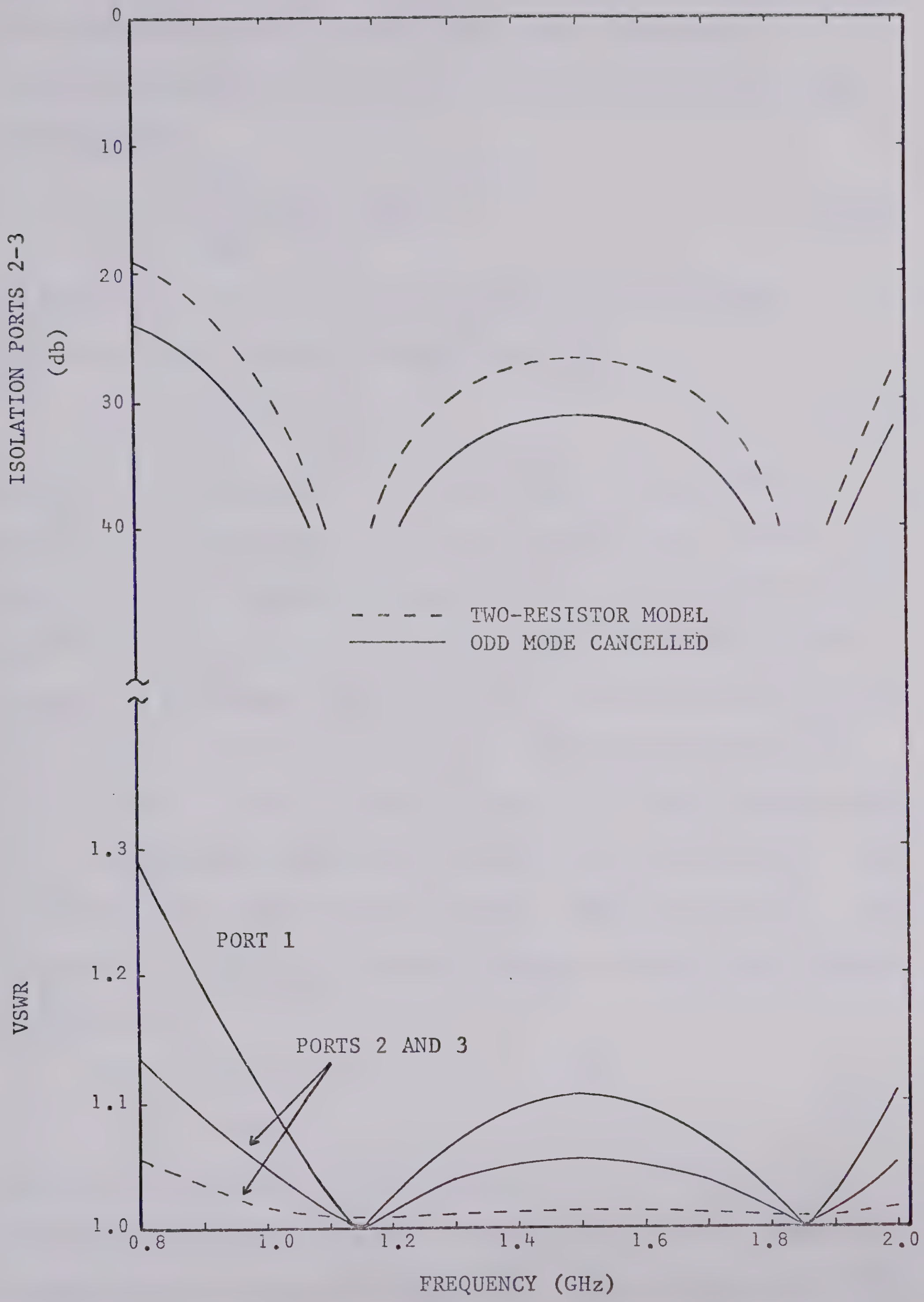

FIGURE 4.2 COMPUTED CHARACTERISTICS OF THREE-PORT HYBRID USING TWO-SECTION, CHEBYSHEV IMPEDANCE TRANSFORMER (TWO - RESISTOR MODEL)

of the impedance matching sections for a center frequency of 1.5 GHz. Using only resistances, "best" results were obtained for the linear distribution (R_n)

$$R_n = \sum_{n=1}^{100} (90n + 920) \tag{4.2}$$

Each value of R_n represents a narrow section of the thin film resistor and (with reference to Figure 2.6)

$$R_n = \frac{h_n}{\ell_n} R_s \tag{4.3}$$

where R_s is the resistivity of the thin film resistance material given in units of ohms/square. In this particular case the width (ℓ_n) of each one of the resistive sections is fixed at an electrical length of 0.1 cm and the height (h_n) of each section is determined by the separation of the ports 2 and 3 circuitry. The characteristics (VSWR and isolation) of ports 2 and 3 when the resistive distribution of Equations (4.2) is used, are shown in Figure 4.3. These characteristics can be improved upon somewhat by the addition of a fixed resistor (R_e) and capacitor (C_e) located at the reference plane v (Figure 4.1). This improvement is also shown in Figure 4.3 and the values of the additional components are

$$\begin{aligned} R_e &= 1820\ \Omega \\ C_e &= 0.202\ \text{pf} \end{aligned} \tag{4.4}$$

In general, it was found that the calculated value of the odd mode admittance at the reference plane v (Figure 4.1), was such that the real part could not be equated to $\frac{1}{50}$, over the entire octave bandwidth. Also, neither could the imaginary part be reduced to a negligible quantity over the entire octave bandwidth. The best compromises were those given by the use of Equations (4.2) and (4.4).

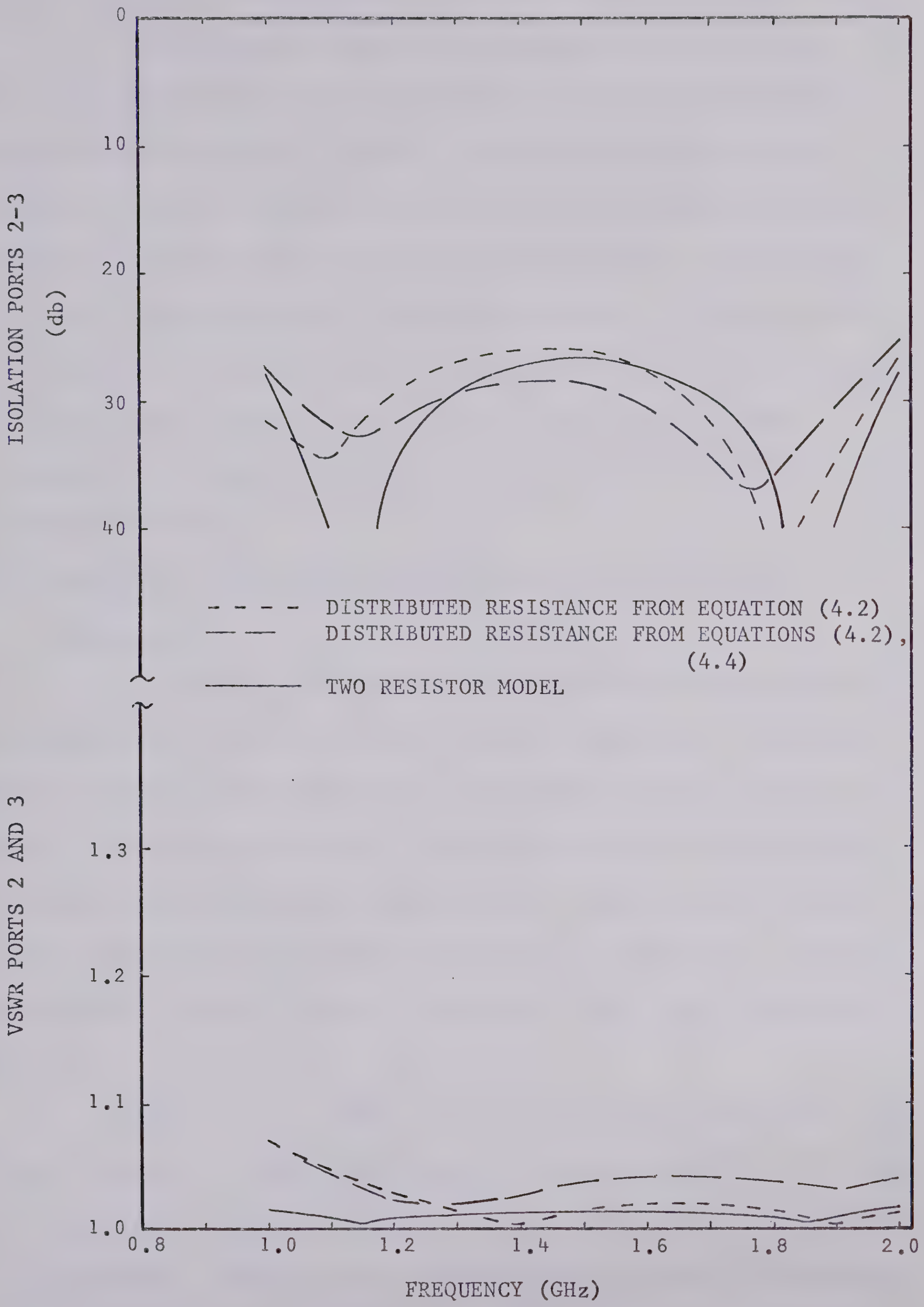

FIGURE 4.3 COMPUTED CHARACTERISTICS OF THREE-PORT HYBRID USING TWO-SECTION CHEBYSHEV IMPEDANCE TRANSFORMER (DISTRIBUTED RESISTANCE MODEL)

It was found, similar to the findings of Chapter III, that the odd mode could not be completely cancelled by only using resistive distributions. However, it was possible to design the hybrid circuit such that it could use a continuous distribution of resistance, located along the impedance transformer sections, with no significant degradation of the characteristics. In this section, both graphical results and equations are for a design frequency of 1.5 GHz, however, they can be adjusted to apply to any design frequency by following the same procedure outlined by Equations (3.13) to (3.16) inclusive.

4.3 Three-Port Hybrid Using a Two-Section Binomial Impedance Transformer

By changing the values of the characteristic impedances of the transformer sections, in the circuit of Figure 4.1, a maximally flat or Binomial characteristic(25) can be obtained for the VSWR of port 1. For the same length of impedance transformer sections and the same maximum permissible VSWR (1.105), as set for the Chebyshev model, the frequency bandwidth is 0.75 GHz, as compared to 1 GHz for the Chebyshev model. However, it does have other useful characteristics.

Using the same method of analysis as for the Chebyshev two-resistor model, the VSWR and isolation characteristics for this device were computed, and are illustrated in Figure 4.4. From this analysis it was apparent that there were two possible solutions for the values of the resistances to be used and also that there was little to be gained from attempting to further minimize the odd mode. Design 1 ($R_1 = 95\ \Omega$, $R_2 = 235\ \Omega$) provides an isolation between ports 2 and 3,

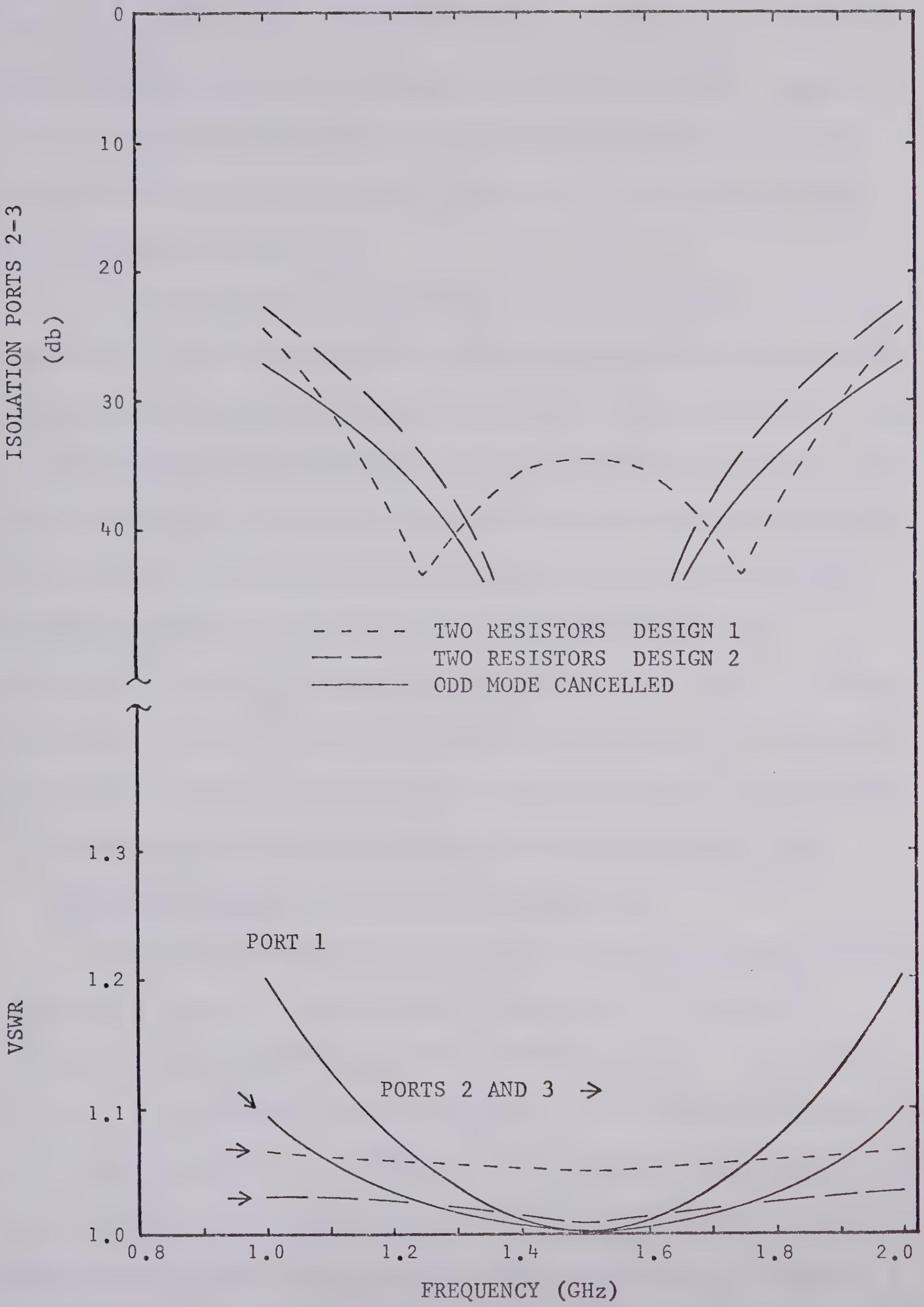

FIGURE 4.4 COMPUTED CHARACTERISTICS OF THREE-PORT HYBRID USING TWO-SECTION BINOMIAL IMPEDANCE TRANSFORMER (TWO RESISTOR MODEL)

that is, about 8 db better than that given by the Chebyshev model, over their respective bandwidths (maximum VSWR of 1.105). Design 2 (R_1 = 85 Ω, R_2 = 240 Ω) provides an isolation characteristic that follows the Binomial pattern more closely and also provides a lower VSWR at the ports 2 and 3.

The characteristic impedances of the two-section impedance transformers can be choosen to provide the different impedance matching characteristics which may be required for various purposes. From the above work it is apparent that the theory used could apply to any choice of impedance matching characteristics and also that the values of the necessary resistances will be close to the values used for the Chebyshev model. Using this procedure, the design of the Binomial model was accomplished in very short order, and it is suggested that this procedure will enable the rapid design of the three-port-hybrid using similar combinations of impedance matching transformers.

4.4 Circuit Design Considerations for Three-Port Hybrids Using Multiple Quarter-Wave Impedance Transformers

The design of the three-port hybrid shown in Figure 4.1 uses a two-section, quarter-wave impedance transformer to provide the necessary impedance matching between reference planes u and v (Figure 4.1). The use of a two (or more) section impedance transformer will mean that one of these lengths will be influenced by junction and/or corner effects that may vary its electrical length. The electrical length variation associated with corners and junction areas is discussed in Appendix A. In this Appendix, certain methods of forming these corners and junctions are suggested that would eliminate possible electrical length variations in the quarter-wave sections. However, it is entirely possible that

circuit conditions or construction methods will prevent the use of these suggested methods of corner and junction formation. In the interests of gaining more information from experimental results, and also to emphasize the results of improper construction techniques, the effects of these possible electrical length variations were computed.

The circuit model used for these computations had a similar configuration to that shown in Figure 4.1 and the quarter-wave section labelled Z_1, was allowed to vary in electrical length. The amount of electrical length variation that was allowed in the computations was ± 12%. This variation of ± 12% was empirically selected from the results observed during the testing of the various circuits constructed in this work. From the results of this study, for both the Chebyshev and the Binomial models, it was apparent that the effect of these ± 12% length variations on the VSWR of ports 2 and 3 was negligible. However, the effects upon the VSWR of port 1 and the isolation between ports 2 and 3 were more noticeable. These effects are illustrated in Figures 4.5 and 4.6, which pertain to the Chebyshev model and design 1 of the Binomial model, respectively. The effects upon design 2 of the Binomial model were similar to those of design 1.

Another factor that must be considered for any practical design, is the allowable tolerance on the values of the resistors that are used. This tolerance is often of the order of ± 10% and a study was carried out as to what effect this resistive tolerance has on the device characteristics. The results of this study showed that, for the Chebyshev model, a variation of ± 10% had only minor effects upon the VSWR of ports 2 and 3, while changes in the isolation characteristics

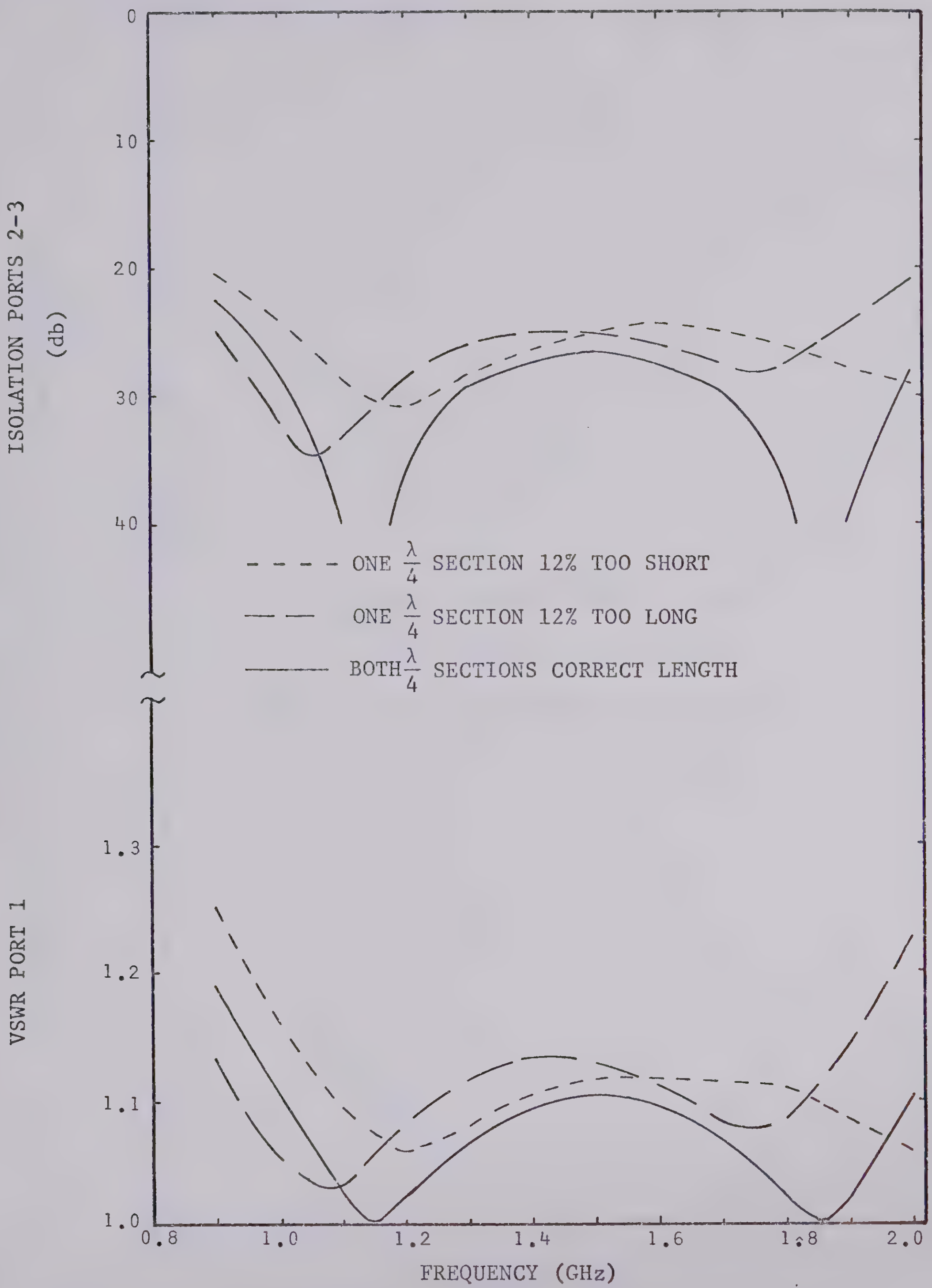

FIGURE 4.5 COMPUTED EFFECTS OF LENGTH VARIATIONS IN CHEBYSHEV TWO-SECTION IMPEDANCE TRANSFORMER MODEL OF THREE-PORT HYBRID (TWO RESISTOR CASE)

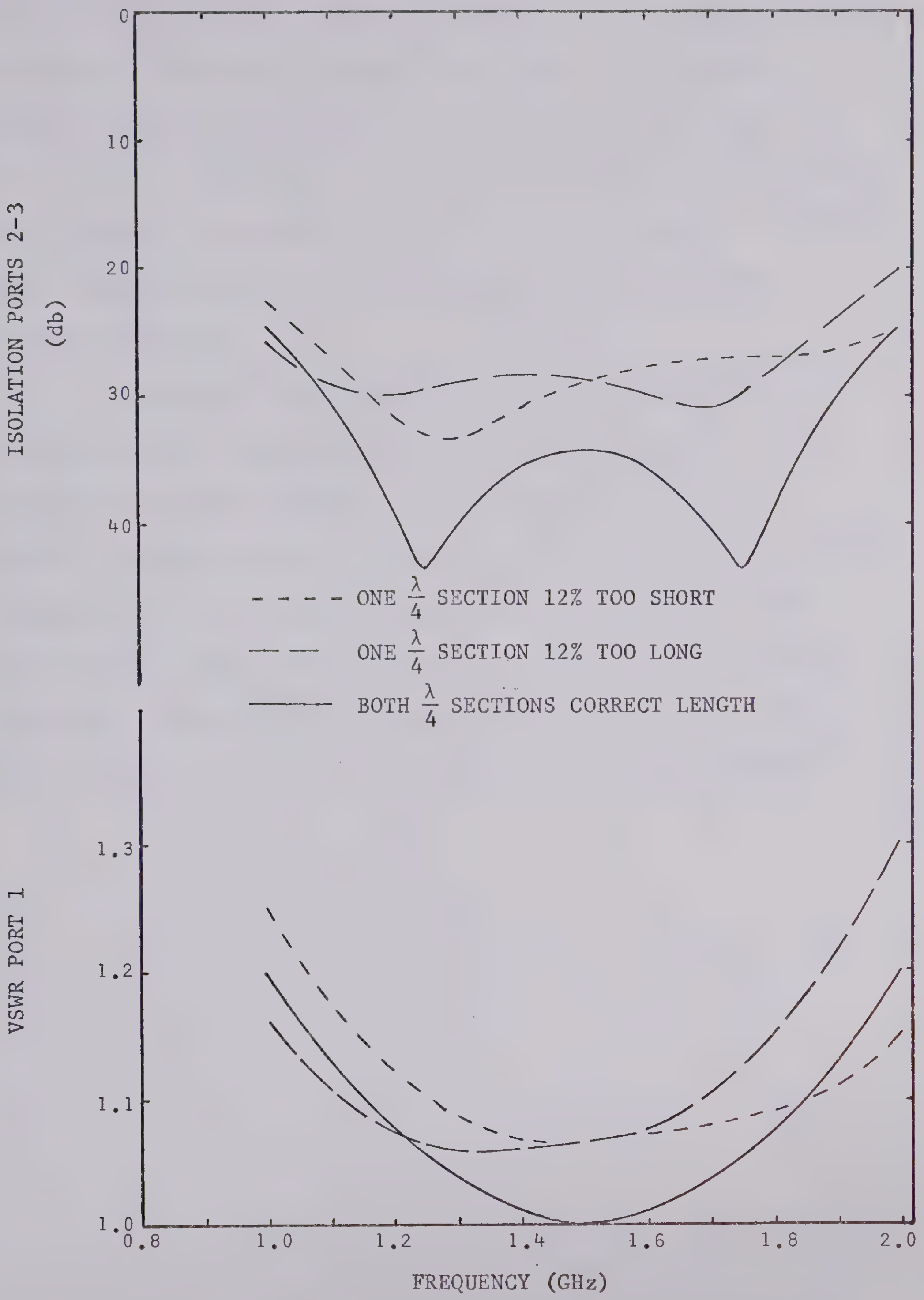

FIGURE 4.6 COMPUTED EFFECTS OF LENGTH VARIATIONS IN BINOMIAL TWO-SECTION IMPEDANCE TRANSFORMER MODEL OF THREE-PORT HYBRID (TWO RESISTOR CASE)

were small also (of the order of 2-3 db). For both Binomial models, the results of the study indicated, that for a ± 10% variation in resistance values, the effects upon the VSWR for ports 2 and 3 was small, but that variations of about 5-6 db occurred in the isolation. Hence, although a tolerance of ± 10% on resistor values is acceptable for the Chebyshev model, the Binomial model may require more stringent tolerances.

It should be noted that the above discussion on the effects of various circuit design problems, for three-port hybrids using multiple quarter-wave impedance transformers, applies to any applicable construction method where the TEM mode is dominant. Also, the graphs of Figures 4.5 and 4.6 are drawn for a design center frequency of 1.5 GHz. Since these figures apply to the standard two-resistor models, they can be adjusted to apply to any design center frequency by following the procedure outlined by Equation (3.13).

CHAPTER V

THREE-PORT HYBRID UTILIZING TAPERED IMPEDANCE TRANSFORMERS

5.1 Introduction

By extending the general theory of Chapter II, beyond that of Chapters III and IV, it is possible to utilize a tapered transmission line to provide the necessary impedance matching in the design of three-port hybrids. There are some distinct advantages to being able to use a taper in place of multiple sections of quarter-wave impedance transformers. The more significant of these are the following:

(a) The physical length of a taper is usually less than the length of a two-section, quarter-wavelength impedance matching network. Also, the taper will provide acceptable impedance matching over a much broader frequency range. Therefore, the use of tapered impedance transformers should permit a significant broadbanding of the three-port hybrid with no increase in physical size.

(b) When used in construction techniques where the TEM mode dominates, the taper has only a lower cut-off frequency. Therefore, many octaves of frequency bandwidth are then theoretically possible. Usually, practical circuit construction considerations limit this bandwidth to three or four octaves.

(c) Using synthesis procedures, it is possible to design

tapers which have some rather unique characteristics. This should make the three-port hybrid, which utilizes a taper, a versatile device. This versatility of design will undoubtedly increase the device's usefulness.

5.2 Theory of Tapers

The stripline circuit configuration employed, along with its associated even and odd mode equivalent circuits, is illustrated in Figure 5.1. The analysis of this circuit is slightly more involved than the previous cases. Here, the characteristic admittances for both the even and the odd modes are not constant but are continuously changing with distance between the reference planes. The even mode is readily calculable, as this is the matched situation where the taper is terminated in the impedances for which it was designed. Therefore the reflection coefficient (and hence VSWR) can be rapidly calculated by following the approximate method outlined by Collin(26). This approximate method has good accuracy as long as the taper provides a continuous and gradual transition of impedances.

The derivation of this approximate theory will be repeated here for purposes of illustration and for later reference. The incremental approach used in the approximate theory is shown in Figure 5.2. Since the theory only holds for small reflection coefficients, the magnitude of Y_1 is practically the same as the termination Y_L, so that the incremental reflection coefficient ($d\Gamma_1$) is very small

$$d\Gamma_1 = \frac{Y_1 - Y_L}{Y_1 + Y_L} \tag{5.1}$$

The incremental reflection coefficient at any point along the taper is $d\Gamma_n$, where

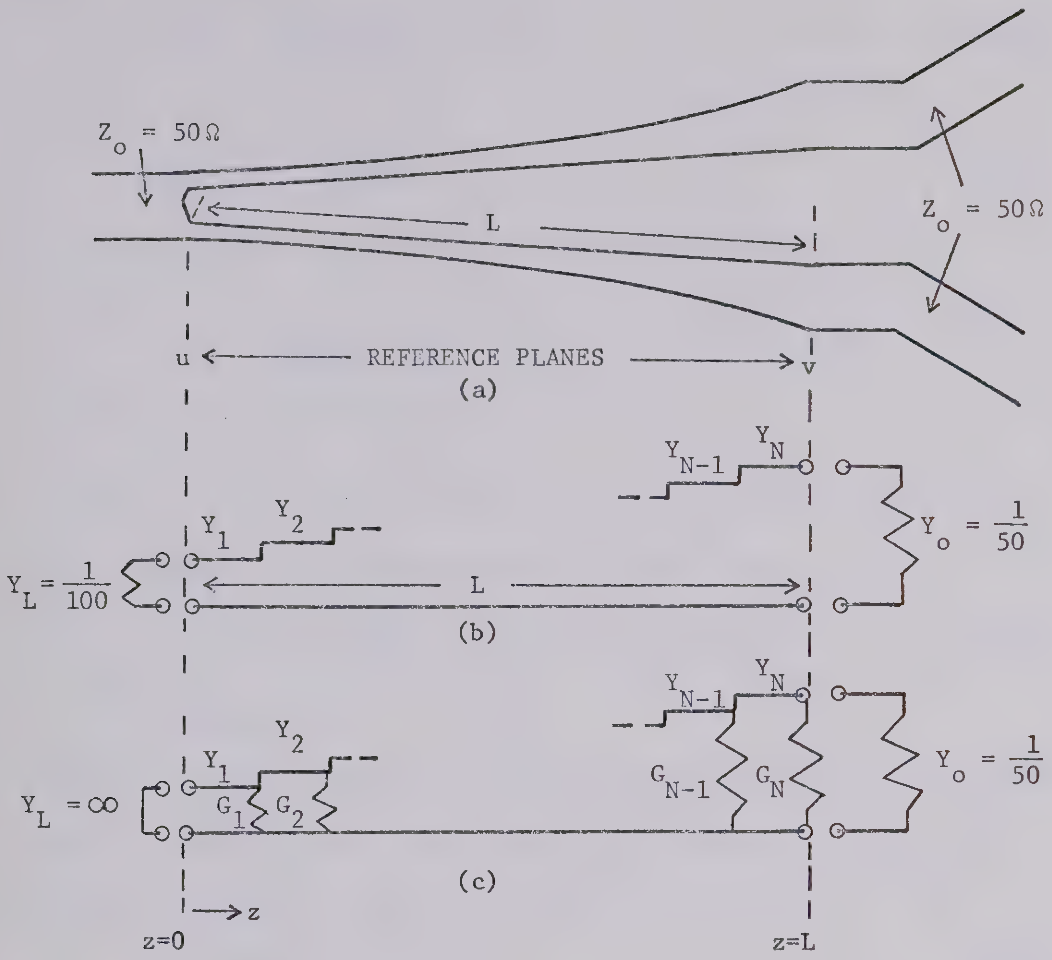

FIGURE 5.1 THREE-PORT HYBRID USING A TAPERED IMPEDANCE TRANSFORMER
(a) STRIPLINE MODEL (CENTER CONDUCTOR)
(b) EQUIVALENT CIRCUIT FOR EVEN MODE
(c) EQUIVALENT CIRCUIT FOR ODD MODE

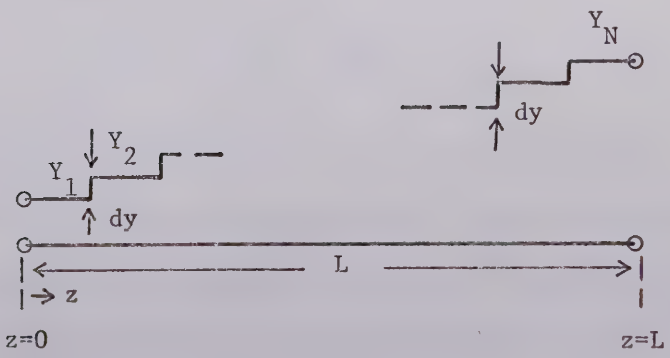

FIGURE 5.2 APPROXIMATE MODEL FOR A TAPER

$$d\Gamma_n = \frac{Y_n - Y_{n-1}}{Y_n + Y_{n-1}} \qquad (5.2)$$

and

$$Y_{n-1} = Y_n - dy \qquad (5.3)$$

so that the expression for $d\Gamma_n$ can be rewritten as

$$d\Gamma_n = \frac{+dy}{2y_n - dy} \approx \frac{dy}{2y_n} = \frac{1}{2}\, d(\ell n\ y_n) = \frac{1}{2}\frac{d}{dz}(\ell n\ y_n)dz \qquad (5.4)$$

since $dy << y$ and $1 \leq n \leq N$

When this $d\Gamma_n$ is referred to the terminated end of the taper ($d\Gamma'_n$ at $z = 0$) and writing the expression in polar form

$$d\Gamma'_n = d\Gamma_n\, e^{-j2\beta z_n} = \frac{1}{2}\, e^{-j2\beta z_n} \frac{d}{dz}(\ell n\ y_n)dz \qquad (5.5)$$

where $\beta = \frac{2\pi}{\lambda}$

Since all $d\Gamma'_n$ are small, only the first-order reflection coefficients have to be taken into account, hence at the reference point ($z = 0$) the total reflection coefficient (Γ) is

$$\Gamma = \sum_{n=1}^{N} d\Gamma'_n \qquad (5.6)$$

As the size of the incremental step is decreased the accuracy of the calculations improves so that the sum can be placed in the form of an integral equation and

$$\Gamma = \int_n d\Gamma'_n = \frac{1}{2}\int_o^L e^{-j2\beta z}\, \frac{d}{dz}(\ell n\ y)dz \qquad (5.7)$$

where L is the total length of the taper and $Y = Y(z)$. The foregoing theory can be written using either end of the taper as the reference and the same result (Equation (5.7)) will be arrived at, however, the choice of reference planes used above ensures that all quantities are

positive and equation formulation is easier. It should be noted that Equation (5.7) is reasonable to solve only for certain functions y(z).

5.3 Even and Odd Mode Analysis

The equivalent circuits for this analysis are shown in Figure 5.1. For the even mode it is seen that the equivalent circuit is similar to that in Figure 5.2; hence, the even mode is readily solved. One selects the taper desired and uses Equation (5.7) to solve for the even mode reflection coefficient.

Solving for the odd mode is not as straight forward because of the large impedance (admittance) mismatch at one end of the taper (Figure 5.1(c)). This invalidates the use of the small reflection coefficient theory and some other method must be found. The general solution procedure outlined in Chapter II (Equation (2.13)) can be readily adapted to the equivalent circuit shown in Figure 5.1(c), with the provision that the value of the taper admittance be known for all points along its length. This provision should not present any difficulty, as for most tapers normally used, the distribution of impedance (admittance) with distance along the taper can be described mathematically. Since use of the transmission line equations necessitates a finite length for each increment, a decision must be made as to the incremental length that will give acceptable accuracy consistent with a reasonable use of computer time. The error due to discretization of the taper decreases as the selected incremental length decreases, however, this error must be balanced against the acceptable cost of computing time. For this work, a value for the incremental length of $\frac{L}{100}$ (Figure 5.1) produces very good accuracy (see Appendix C) and required the use of

a reasonably small amount of computing time. However, if the allowable computing time is quite limited then good results can be obtained using a length of $\frac{L}{50}$ for each incremental distance (Appendix C). This type of calculation has the advantage of being independent of the limitations of small reflection coefficients. The even and odd modes can now be solved for their respective reflection coefficients and the VSWR and isolation characteristics of ports 1, 2 and 3 can be calculated.

All the theoretical and experimental results that follow are for tapers whose lower cut-off frequency is 1.0 GHz. To interpret these graphs for tapers having different lower cut-off frequencies, the frequency scale on the following graphs is multiplied by the factor p, where

$$p = (\text{lower cut-off frequency desired in GHz})/1.0\text{ GHz} \quad (5.8)$$

The resistive distribution used in this work also applies to a taper whose electrical length (L) corresponds to a lower cut-off frequency of 1.0 GHz and the theoretical discrete resistor separation used was (ℓ) where

$$\begin{aligned} \ell_e &= \frac{L}{100} && \text{electrical length} \\ \ell_p &= \left(\frac{L}{100}\right)\left(\frac{1}{\sqrt{\varepsilon_r}}\right) && \text{physical length} \end{aligned} \qquad (5.9)$$

and ε_r is the relative dielectric constant of the stripline dielectric. As the length of the taper varies, so does the value of ℓ_p, and hence the width of the thin film resistor section represented by the discrete resistor (Figure 2.6). Since for most tapers the frequency-length product is a constant, the width of resistance section (ℓ_d) corresponding to the desired taper is, using Equations (5.8) and (5.9),

$$\ell_d = (\ell_p)/p \tag{5.10}$$

The height (h) of the resistance section is determined by the physical separation of impedance transformer sections of ports 2 and 3 and is independent of the theory, as is the resistivity (R_s) of the thin film used. Hence, the theory only fixes the width (ℓ_d) of the resistance section, and the value of the discrete resistor (R) representing this section is (from Figure 2.6)

$$R = \frac{h}{\ell_d} R_s \tag{5.11}$$

The designer chooses the values of h and R_s to give the value of R that corresponds to the value given in the following theory, then all the resistance sections are placed together, in sequence and the dimensions of the thin film resistor, are determined.

5.4 Three-Port Hybrid Using a Chebyshev-Taper Impedance Transformer

For a given maximum allowable reflection coefficient the taper that gives a required impedance transformation within the shortest length is the Chebyshev taper(26). This taper has an equal ripple reflection characteristic with a sharply defined cut-off frequency. For the case where the maximum permissible reflection coefficient and the lower cut-off frequency are set to 0.05 (VSWR = 1.105) and 1.0 GHz respectively, this taper will have the VSWR characteristics shown in Figure 5.3. This characteristic is also equivalent to that of the even mode, hence, Figure 5.3 shows the VSWR of port 1 of the three-port hybrid.

The VSWR's and isolation of ports 2 and 3 depend upon the value of the distributed resistance R(z). As in the quarter-wave impedance transformer case, theoretically optimum performance will be

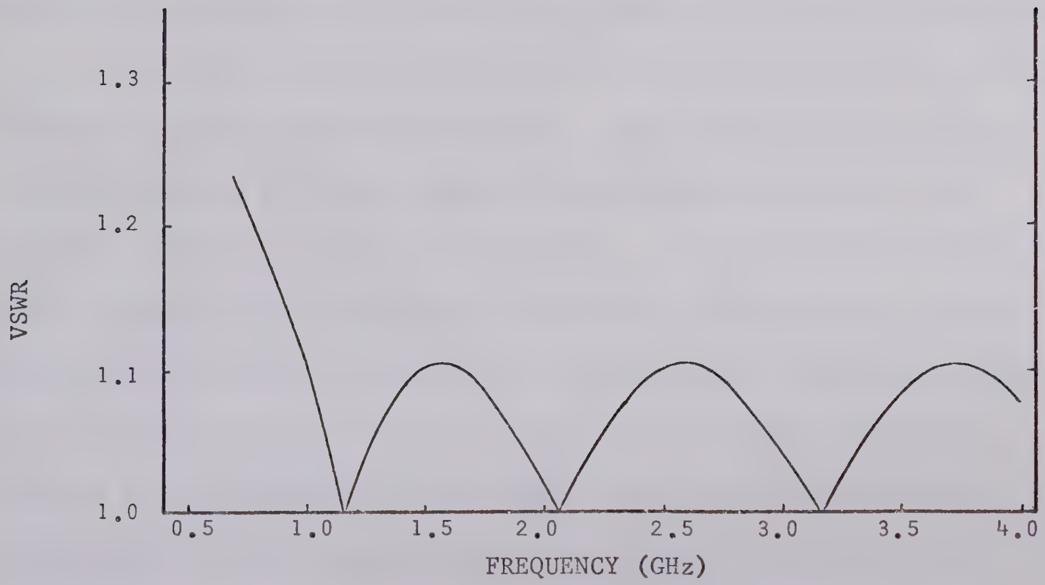

FIGURE 5.3 CHARACTERISTICS OF CHEBYSHEV TAPER

obtained when the odd mode is completely cancelled. An investigation was carried out to find a practical "optimum" result obtainable, utilizing only real functions of $R(z)$. During this investigation it was observed that there was no practical advantage to using non-linear variations of $R(z)$ and the required "optimum" result was obtained by the use of linear variations of $R(z)$. This linearity of the distributed resistance has the advantage of simplifying construction of the actual device. The "optimum" distribution of resistance extended the full length of the taper and had the following theoretical discrete resistor model

$$R(z) = \sum_{n=1}^{100} 100n \tag{5.12}$$

Characteristics resulting from the use of this particular $R(z)$ are shown in Figure 5.4; also shown in this Figure, for comparison purposes, are the characteristics of ports 2 and 3 when the odd mode is cancelled.

It can be seen from Figure 5.4 that the use of Equation (5.12) does not completely cancel the odd mode. The theory indicates that it will be difficult to further reduce the odd mode, as the real and imaginary parts of the odd mode admittance, calculated at the reference plane v (Figure 5.1), oscillate in magnitude as the frequency varies. This limits the range of frequencies over which any practical modification to the characteristics can be made. If the designer is only concered with a bandwidth of two octaves, then some improvement can be obtained by using Equation (5.12) plus a capacitor of 0.079 pf between the tapers at the reference plane v. This modified result is also shown in Figure 5.4.

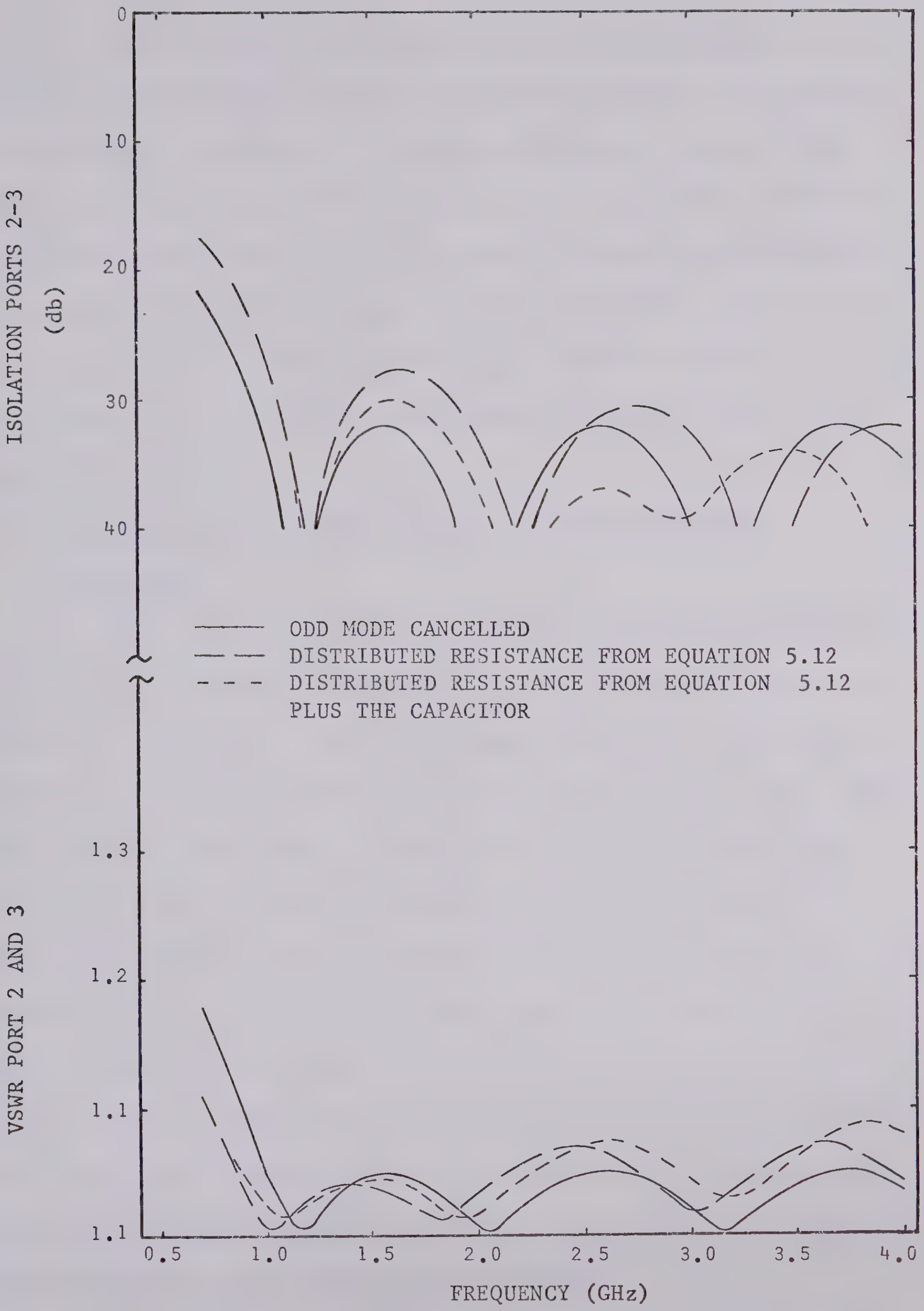

FIGURE 5.4 COMPUTED CHARACTERISTICS OF THREE-PORT HYBRID USING CHEBYSHEV TAPER IMPEDANCE TRANSFORMER

The Chebyshev taper has an equal ripple characteristic and this feature is evident in the characteristics of all three ports of the hybrid, as the odd mode is nearly cancelled and the even mode dominates. Therefore, if the designer wants a particular characteristic, he should choose the type of taper that produces the desired variations of VSWR with frequency and then design the circuit around it. Noting that the VSWR at ports 2 and 3 will be similar in its variations with frequency but approximately $\frac{1}{2}$ the magnitude of the port 1 characteristic.

5.5 Three-Port Hybrid Using an Exponential Taper Impedance Transformer

The variation of the characteristic impedance with distance along the taper creates individual reflection coefficient characteristics for each taper. However, the magnitude of the characteristic impedance for the same distance along each taper, varies only a small amount for different tapers. The odd mode reflection coefficient is calculated using the magnitude of the characteristic impedance for each point along the taper. Therefore, it should be reasonable to assume that the resistive distribution required to reduce the odd mode will be somewhat similar for most tapers. Hence, the search for the practical, "optimum" resistive distribution, should be started by using the values arrived at for the Chebyshev taper. This procedure should significantly simplify the design of the three-port hybrid which utilizes the more common types of tapers.

To illustrate the effects of choosing different types of tapers, the exponential taper(27) was analyzed. This particular type

of taper has a characteristic impedance (Z) that varies with distance (z) along the taper, terminating load impedance (Z_L) and overall length of the taper (L), as follows:

$$\ln Z = (\frac{z}{L})\ \ell n\ Z_L \tag{5.13}$$

Using Equation (5.7), the reflection coefficient characteristic of the taper is given by

$$\Gamma = \frac{1}{2}\ e^{-j\beta L}\ \ell n\ Z_L\ \frac{\sin \beta L}{\beta L} \tag{5.14}$$

$$\text{where}\quad \beta = \frac{2\pi}{\lambda}$$

By requiring that

$$\beta L = \pi \tag{5.15}$$

at 1.0 GHz, the overall length of the taper (L) is set to 15 cm. and its reflection coefficient, plotted as VSWR, is shown in Figure 5.5.

Analogously to the Chebyshev model discussed in Section 5.4, the VSWR characteristic of the exponential taper and hence port 1 of the hybrid, is shown in Figure 5.5. Investigation of possible resistive variations, revealed that the practically "optimum" resistive distributions were all linear in their variation with distance along the taper. In determining the VSWR and isolation characteristics of ports 2 and 3, it was found that near optimum results were obtained utilizing the distribution of resistances, R(z), where

$$R(z) = \sum_{n=1}^{100} (600 + 100n) \tag{5.16}$$

A slightly different characteristic can be obtained using two stages of linear distributions of resistances whose theoretical models are

$$R_1(z) = \sum_{n=1}^{50} (225 + 75n) \tag{5.17}$$

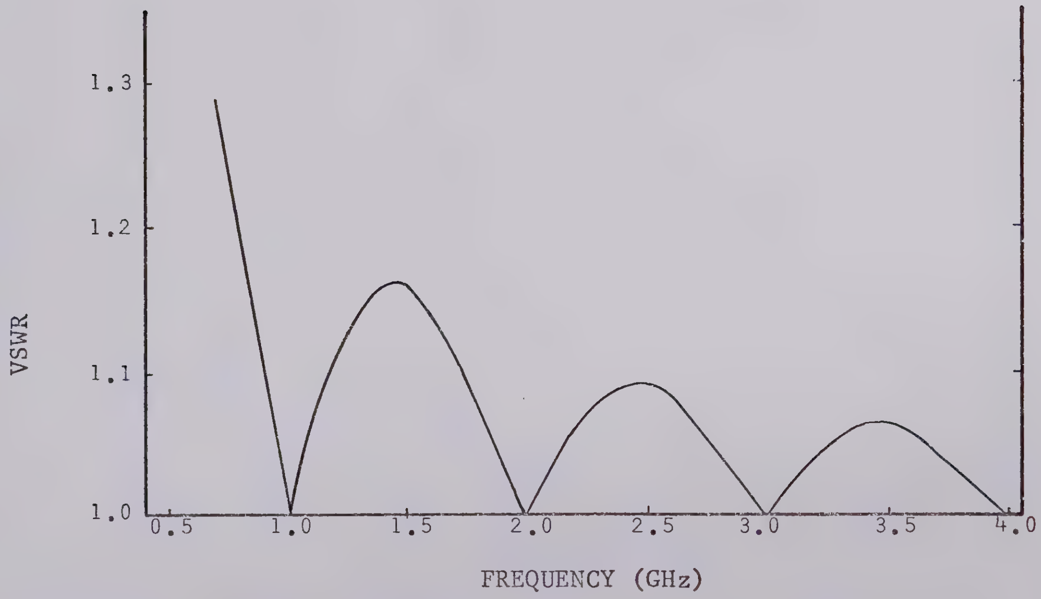

FIGURE 5.5 CHARACTERISTICS OF EXPONENTIAL TAPER

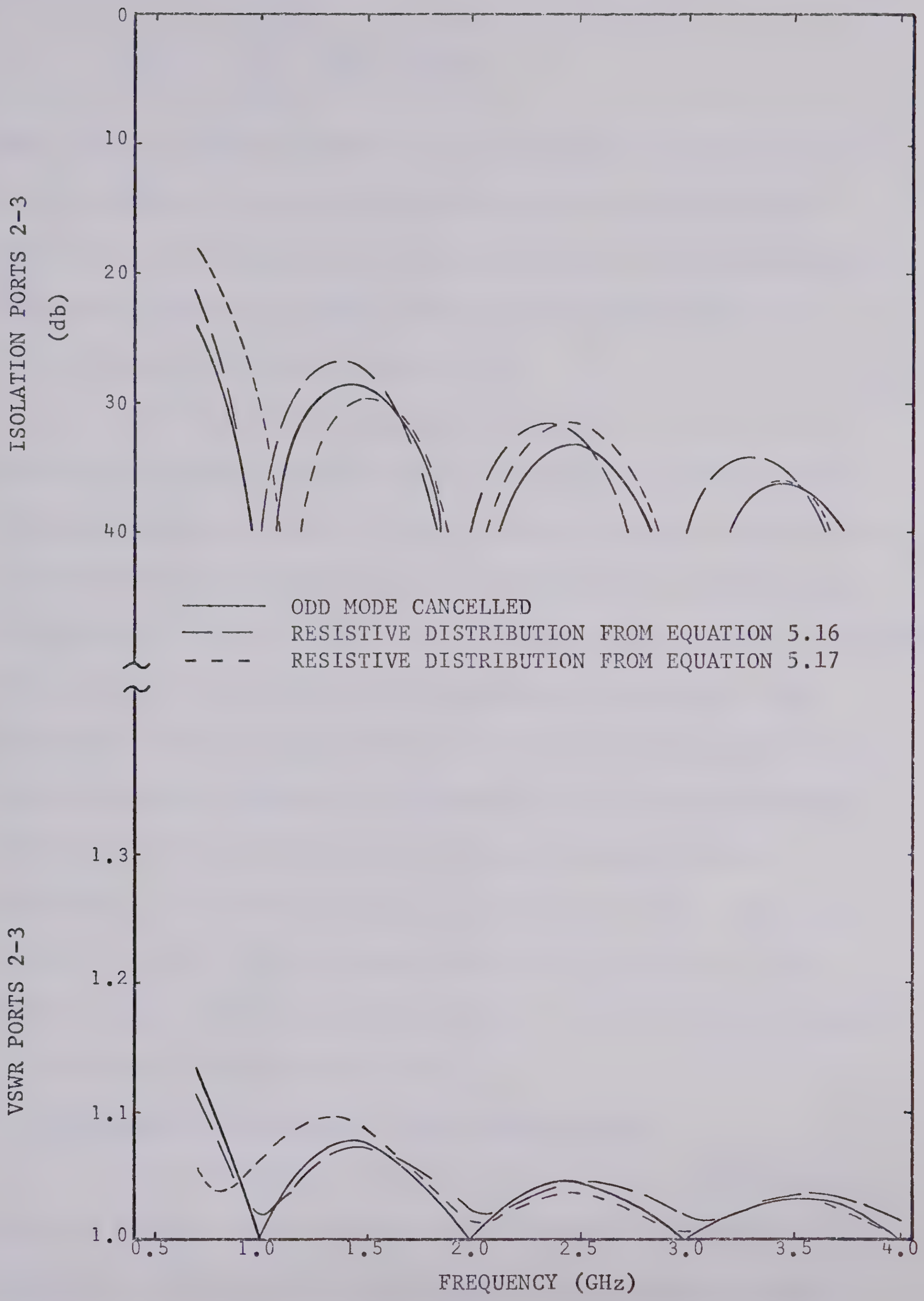

FIGURE 5.6 COMPUTED CHARACTERISTICS OF THREE-PORT HYBRID USING EXPONENTIAL-TAPER IMPEDANCE TRANSFORMER

$$R_2(z) = \sum_{n=1}^{50} (4050 + 150n)$$

where $R_1(z)$ is effective from the reference plane u (Figure 5.1) to $\frac{1}{2}$ the distance to reference plane v and $R_2(z)$ is effective the remainder of the distance to reference plane v. The VSWR and isolation characteristics of ports 2 and 3, for the above resistive distributions, are shown in Figure 5.6.

In the case of the exponential taper, the use of real components R(z) only, produces results that are very close to the theoretical optimum, i.e. when the odd mode is completely cancelled. The linear variation with distance of the resistive distributions of Equations (5.16) and (5.17), plus the similarity of their magnitudes with Equation (5.12), verify the assumptions made in the first paragraph of this section. Hence, the design of three-port hybrids, utilizing tapered impedance transformers, can be accomplished by restricting the search for the practically optimum resistive distribution to linear variations of resistances whose values are reasonably close to those of Equations (5.12), (5.16) or (5.17). This procedure produces a design with near optimum characteristics in a relatively short period of time.

5.6 Experimental Results and Their Interpretation

To verify that the type of analysis used in this chapter, (discrete resistors separated by small intervals to simulate a continuous distribution) was reproducable in a practical model, a three-port hybrid using a Chebyshev taper was constructed. This taper was designed to have a lower cut-off frequency of 1.0 GHz and a maximum reflection coefficient of 0.05 (VSWR = 1.105) for

frequencies equal to or greater than the lower cut-off. Due to problems caused by high VSWR's associated with the coaxial-to-strip-line connectors (Section 3.4) it was decided to utilize a resistive distribution that would produce measurable VSWR's and to forego an attempt to build the circuit associated with Equation (5.12). Therefore a resistive distribution (R(z)) whose theoretical model is

$$R(z) = \sum_{n-1}^{100} (600 + 40n) \tag{5.18}$$

was used. Similar to the procedures of Section 3.4, the thin film tapered resistors used, had their edges thinly covered with silver paint, to ensure good electrical contact with the copper. Also, as in Section 3.4, the thin film resistor overlapped the tapered arms of the hybrid circuit, so it was not possible to determine, prior to the experiment, the exact resistive distribution used. Hence, the theoretical calculations were carried out for a range of resistive distributions, as follows;

$$R(z) = \sum_{n=1}^{100} (570 + 30n) \tag{5.19}$$

$$R(z) = \sum_{n=1}^{100} (560 + 40n) \tag{5.20}$$

$$R(z) = \sum_{n=1}^{100} (550 + 50n) \tag{5.21}$$

The computed results of using the above distributions are shown in Figure 5.7. To determine the behaviour of the thin film resistor in the junction area Equation (5.20) was used with the following modifications

$$R(z) = \sum_{n=1}^{100} (200 + 40n) \tag{5.22}$$

$$R(z) = \sum_{n=1}^{100} (560 + 40n) \tag{5.23}$$

$$R(z) = \sum_{n=1}^{100} (960 + 40n) \tag{5.24}$$

and the effect upon the characteristics of ports 2 and 3 are shown in Figure 5.8.

The experimentally measured characteristics are shown in Figures 5.9 and 5.10. It can be seen from Figure 5.9, which shows the VSWR of port 1 when the resistor is out of the circuit, that this characteristic is significantly different from the theoretical model shown in Figure 5.3. Part of this difference is relatively constant with frequency and is due to tolerances in material parameters and in the actual construction techniques used. The other component of the difference can be attributed to the impedance mismatch of the coax-to-stripline connectors and this factor does not remain constant, but usually increases in magnitude as the frequency increases. The effects of the connectors can be corrected for (Appendix B section B.3) and the corrected results are shown in Figure 5.9 and 5.10. From the corrected curve of Figure 5.9 it can be seen that the lower cut-off frequency for the constructed taper is 1.05 GHz. This compares favorably with the design frequency of 1.0 GHz, indicating that the junction area has contributed a minimum of reactive effects (Appendix A).

Comparing Figure 5.10 with Figures 5.7 and 5.8 it can be seen (remembering to apply Equation (5.8)) that the experimental results

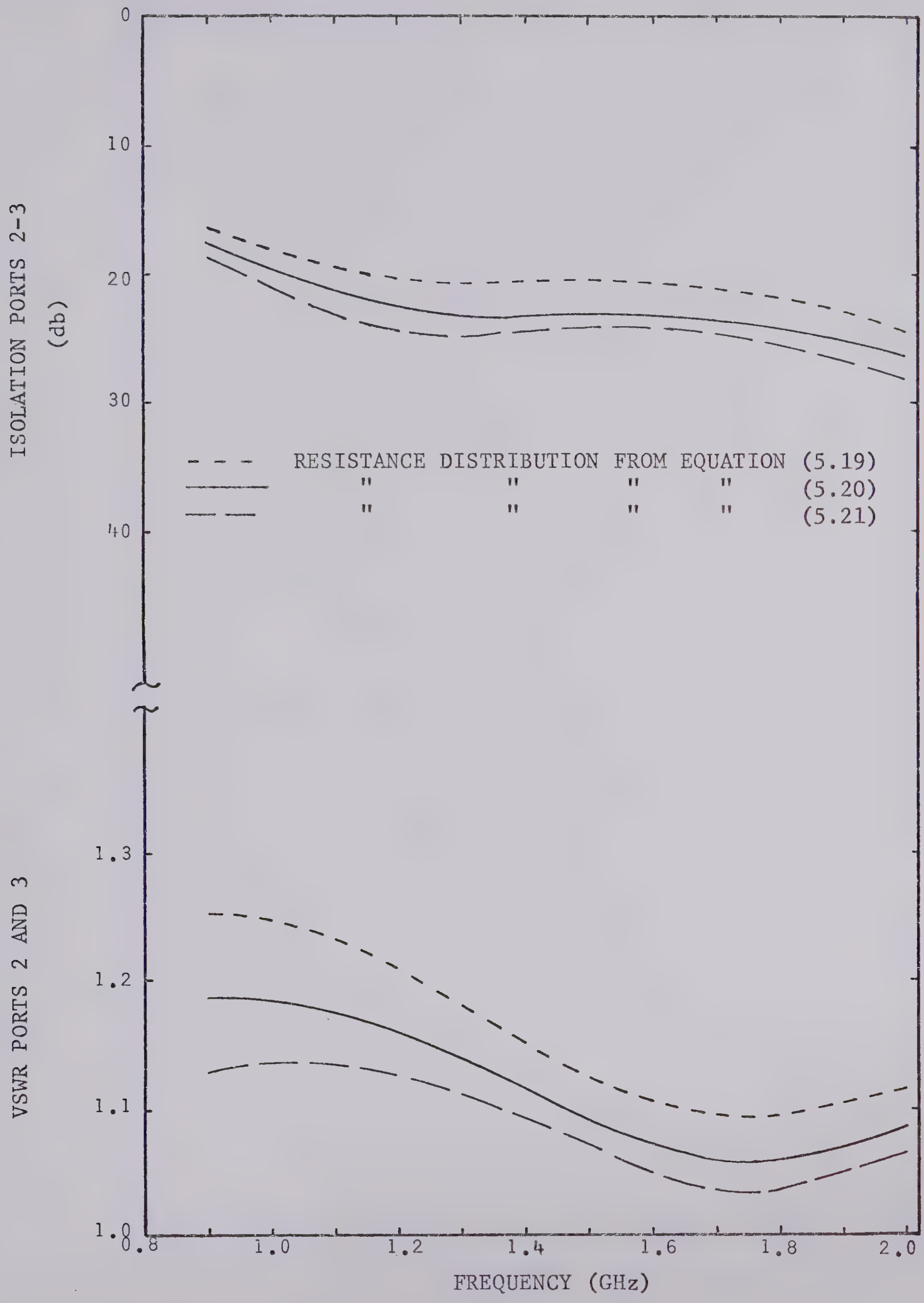

FIGURE 5.7 COMPUTED CHARACTERISTICS OF THREE-PORT HYBRID USING CHEBYSHEV TAPER IMPEDANCE TRANSFORMER (VARIOUS DISTRIBUTED RESISTANCES)

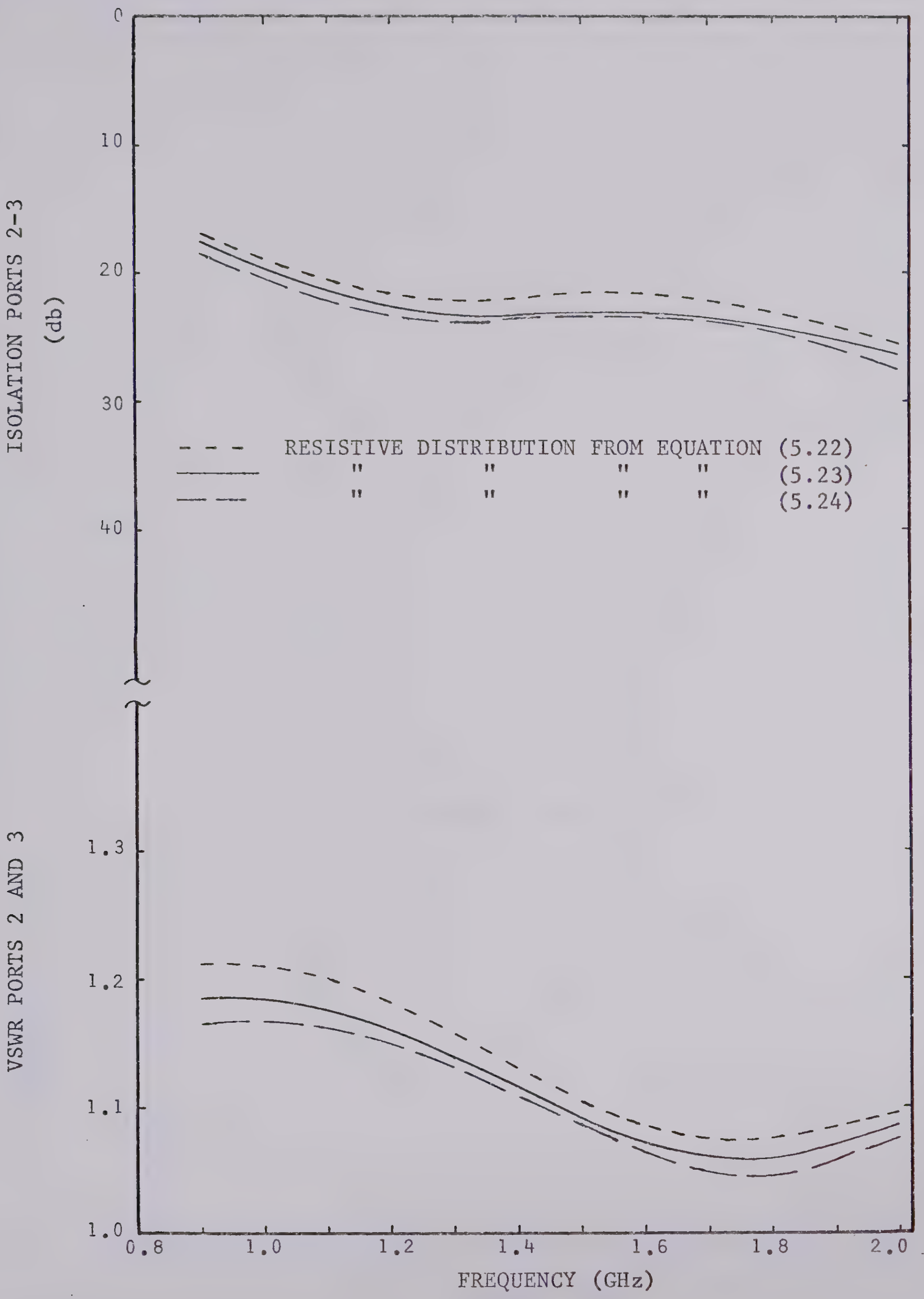

FIGURE 5.8 COMPUTED CHARACTERISTICS OF THREE-PORT HYBRID USING CHEBYSHEV TAPER IMPEDANCE TRANSFORMER (VARIOUS DISTRIBUTED RESISTANCES)

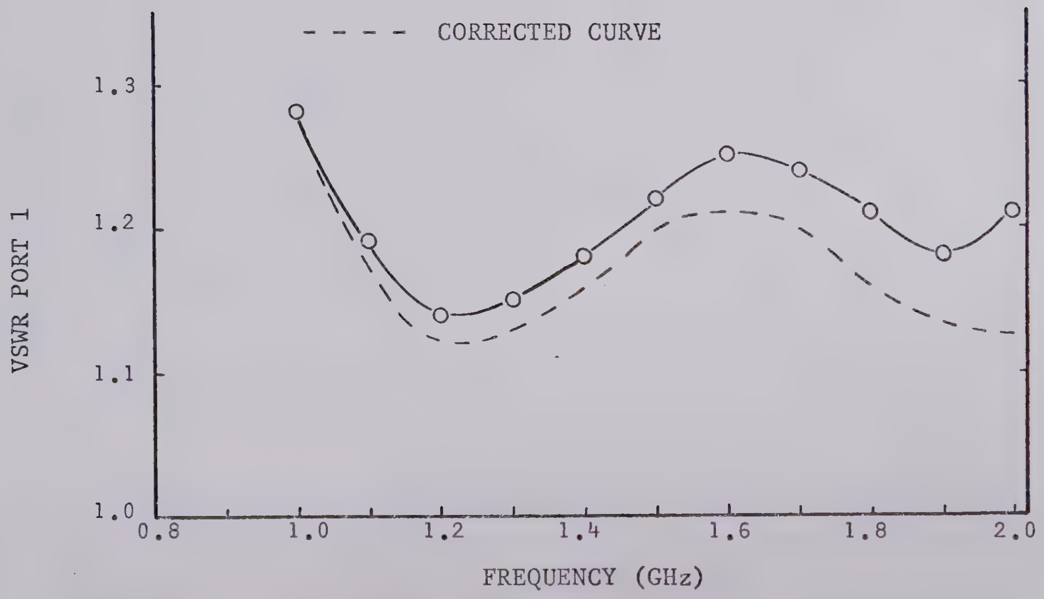

FIGURE 5.9 EXPERIMENTALLY MEASURED CHARACTERISTICS OF CHEBYSHEV IMPEDANCE TRANSFORMER

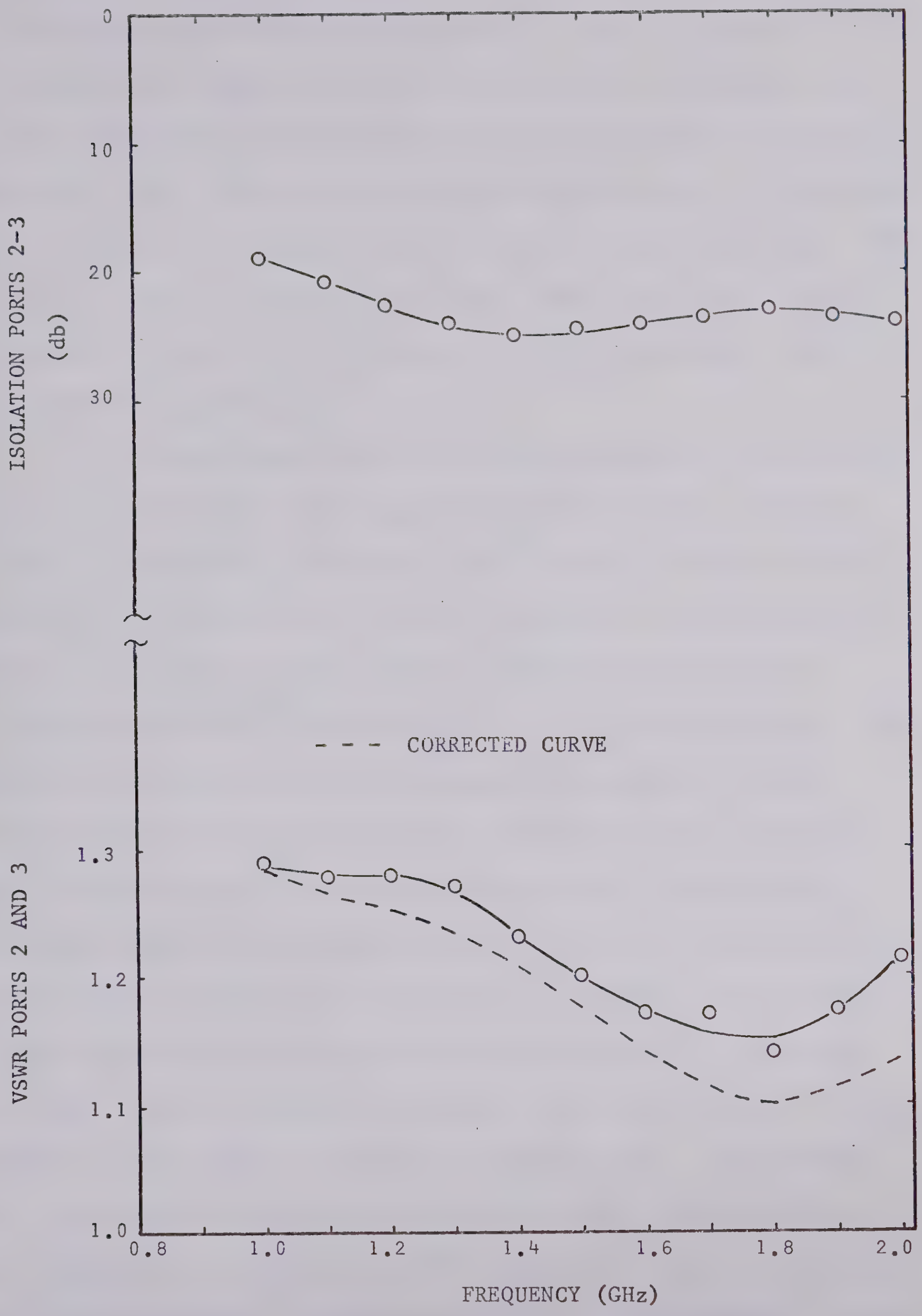

FIGURE 5.10 EXPERIMENTALLY MEASURED CHARACTERISTICS OF THE THREE-PORT HYBRID USING CHEBYSHEV TAPER IMPEDANCE TRANSFORMER

correspond to the region represented by the theory of Equation (5.20). By referring to Figure 5.8, it is evident that the resistance value in the junction area is about 600 ohms, which is also in agreement with Equation (5.20). These results indicate that the amount of the resistor that overlapped the copper strips was generally fully utilized by the circuit. The use of a thin film resistor whose theoretical model differed from Equation (5.18) produced a similar agreement between experiment and theory.

The experimental results for the VSWR and for the isolation of ports 2 and 3 do not show any shift of the frequency scale with respect to the theory, as was the case in Section 3.4 and Section B.2. By applying the equivalent circuits of Figure B.2 to the section of the thin film resistor that each theoretical discrete resistor represents and using procedures similar to those of Section B.2, the possible effects of the inductance and of the capacitance added to the odd and even modes, was studied. From Equation B.4, it can be seen that for large values of discrete resistors, such as used in the taper model, the magnitude of the inductive susceptance that can be attributed to the resistive section is negligible. The magnitude of the capacitive susceptance that could be added to the even mode was small and it was found that the only effect was to increase the magnitude of the VSWR all across the frequency band. By increasing the capacitive susceptance added, the entire VSWR characteristic was adjusted to a higher value, with very little shift in the frequency characteristics. Hence, the theory and the experimental results support one another and there should be no need to apply any correction factors to the design, as was necessary in the single section

quarter-wavelength impedance transformer case.

A disturbing feature of using distributed resistances became apparent when the insertion loss between ports 1 and 2 (or 3) was measured, with the thin film resistor in the circuit. Insertion loss (I.L.) is defined as

I.L. = (power theoretically present) - (power measured)

and is usually expressed in decibels (db). It is reasonable to expect the I.L. to be about $\frac{1}{2}$ db when measuring the power loss from port 1 to port 2 or vice-versa; however, the values of I.L. measured, were as high as 2 db. Increased signal dissipation can occur if there are components of the signal in the port 2 arm of the circuit that are out of phase and/or of uneven magnitude with respect to their counterparts in the port 3 arm of the circuit. The use of a distributed resistance will provide a large area over which this signal dissipation could occur. A contributing factor to this increased insertion loss may be the difficulty of placing the thin film resistor in the circuit so that it is positioned with electrical symmetry between the two arms of the circuit. This lack of symmetry could result in the reactance associated with the resistor being unequally divided between the port 2 and 3 arms of the circuit. Thereby, causing an unbalancing effect in the characteristic impedances of the circuit arms, that would produce out of phase and/or uneven magnitude components in the associated signals. This high insertion loss has been observed previously(29) and the thin film resistor had to be limited to an area extending from the junction to a point about $\frac{1}{2}$ to $\frac{2}{3}$ the length of the taper, to keep the insertion loss within acceptable limits.

It is believed that the unbalancing effect of the distributed resistor is due to the stripline construction, and the use of the tapered transmission line along with its associated distributed resistance may have to be restricted to microstrip or similar construction techniques. In this way the sandwiching of the thin film resistor between dielectric sheets is avoided and overlay deposition techniques can be used to raise the resistive film off the dielectric substrate, thereby reducing any capacity added to the even mode.

CHAPTER VI

CONCLUSION

A class of four-port hybrids, having a three-port exterior physical configuration, has been studied with the purpose of extending the usable frequency range. The three-port configuration is obtained by internally terminating the fourth port. The manner in which this internal termination was accomplished and the types of impedance transformations used, were found to be the principal means by which the frequency bandwidth could be varied.

It was found that a distributed resistance could be employed to terminate the internal port. This distributed termination produced a more even division of power, when used in working circuits, while the VSWR and isolation characteristics of the conjugate ports were not significantly changed from those of the single resistor/quarter wavelength section models. The theoretical and experimental findings indicated that suitable distributed terminations could be provided with a linear variation of resistance. This finding increased the practicality of using a hybrid with a distributed resistor, as a linear variation is relatively simple to realize in a working model.

The use of a distributed termination for the internal port did not produce any significant broadbanding effect by itself. Any substantial increase in the usable frequency range for these devices had to be achieved by using different methods of internal impedance transformation. These methods were extended from the use of quarter-

wavelength impedance transformers, to incorporate a tapered transmission line, providing as much as several octaves of frequency bandwidth and still maintaining good isolation and VSWR characteristics at all ports. A significant feature of being able to utilize a tapered impedance transformer, is that the overall physical length of the circuit is usually less than, or equal to, the circuit length associated with the use of only two sections of quarter wave transformers.

It has been found that the impedance transformation used governs the type of VSWR characteristic obtained at all three ports. While the form of resistive termination used mainly determines the isolation characteristics of the conjugate ports. The results of this study can be used to design three-port hybrids, using some desired impedance transformation, such that a suitable resistive termination can be determined with a minimum of engineering and computer time.

Experimental evidence showed that the corners and junction areas, necessary in the construction of the three-port hybrid, have a significant effect upon the overall characteristics of the device. These effects are mainly upon the effective electrical length of the impedance transformers used, thus causing a shift in the frequency characteristics of the device. The effective electrical length of standard corners has been tabulated and a method of designing the junction area has been found that eliminates the necessity of adding extra length to the impedance transformer system used.

Experimental and theoretical results show that the benefits derived from the use of a distributed resistance to terminate the

internal port may be limited, at least in stripline construction. The distributed resistance adds a certain amount of reactance to the circuit and the nature of the closed sandwich effect of stripline construction makes it difficult to reduce this reactance. Hence, open construction techniques, such as microstrip, may have to be used, as here overlay metallization and a further reduction of circuit size can be used to effectively reduce the reactance of the distributed resistance.

The use of those three-port hybrids that utilize single or multiple quarter-wave impedance transformers, along with a distributed resistance instead of single or multiple discrete resistors, will probably be somewhat restricted. Additional construction complexities will limit their use to areas that place heavy emphasis on equal-power-equal-phase power division.

Further study could be carried out on the problem of phase shift in the arms of the device, and perhaps some method of adjusting the phase shift in each arm could be incorporated into the design. Also, further work could be done to develop these broadbanding techniques for three-port hybrids which have unequal power division and power addition.

APPENDIX A

EFFECTIVE ELECTRICAL LENGTH OF CORNERS AND JUNCTIONS

A.1 Introduction

In stripline circuits, corners are used to change the direction of the center conductor, while a junction occurs whenever three or more center conductors are brought together. Both corners and junctions contribute a certain amount of additional reactance to the circuits they are associated with. When corners and/or junctions are associated with transmission line impedance transformers (quarter-wave length sections or tapers) the additional reactance added to the circuit, has the effect of varying the electrical length of the transformer section. This variation in the electrical length has a detrimental effect upon the properties of the impedance transformers. Some problems associated with the use of corners have been discussed in the literature,(30,31) however, little of this information applies directly to the circuits used in the three or four-port hybrids. In this study of corners and junctions, the stripline board used was manufactured by Tellite Corporation and had the physical and electrical properties shown in Figure A.1. It should be noted that the results of this study are mainly empirical.

A.2 Corners in Stripline Circuits

A.A. Oliner(30) has published an equivalent circuit for corners (in the center conductor of stripline) which indicates that the electrical length for the corner should increase approximately in proportion to the corner angle. However, this equivalent circuit is

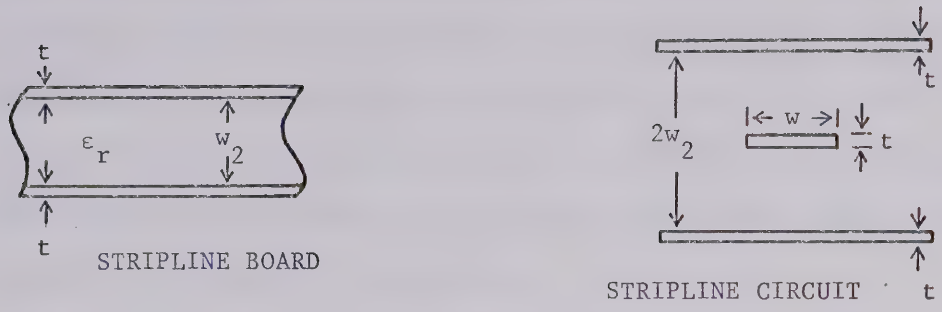

STRIPLINE BOARD

STRIPLINE CIRCUIT

t = 0.0028" THICKNESS OF COPPER
w_2 = 0.0625" THICKNESS OF DIELECTRIC
ε_r = 2.32 RELATIVE DIELECTRIC CONSTANT
w = WIDTH OF ETCHED CENTER CONDUCTOR

FIGURE A.1 STRIPLINE MATERIAL

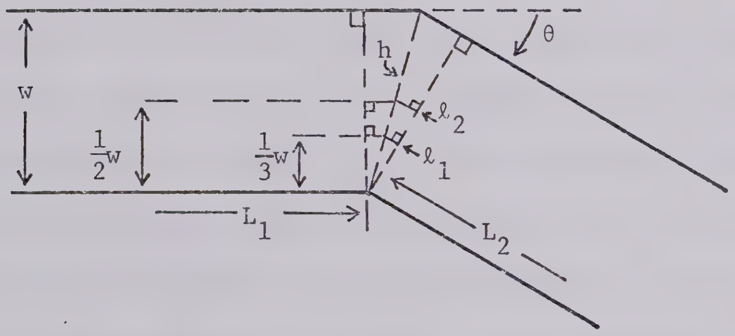

h - MAXIMUM WIDTH OF CORNER
w - WIDTH OF CENTER CONDUCTOR
θ - CORNER ANGLE
ℓ_1 - 0.268w FOR θ = 30°
ℓ_2 - 0.385w FOR θ = 60°

FIGURE A.2 CORNERS IN STRIPLINE CIRCUITS
(CENTER CONDUCTOR ONLY)

based upon an idealized version of the stripline and it does not account for the now-common practice of trimming the outside edges of the corners. For the circuits constructed in the work of this thesis, it was found that the electrical length of a 60° corner was about 1.5 times that of a 30° corner, while the use of trimming further reduced the electrical length of the corners.

It would appear that the equivalent circuits given for corners do not take sufficient account of the distortion of the normal TEM mode that is caused by the corners. In stripline circuits the electric field vectors are perpendicular to the center conductor, while the magnetic field forms closed loops about the center conductor. When this center conductor is bent in the plane of the magnetic field, the magnetic intensity will be increased on the inside and decreased on the outside of the corner. This would require more current to flow near the inside edge of the center conductor; that is, one could say that there is current crowding near the inside edge of the corner. Normally, on a straight section of center conductor, the current is concentrated near the edges because of the electric field configuration associated with a rectangular conductor. In this "normal" situation the current is evenly divided between the two sides of the center conductor and the mean path of the current can be taken as the center of this conductor. Under the influence of corners the mean path of the current is pulled toward the inside edge and hence the electrical length can no longer be taken at the center of the conductor. This displacement of the mean path of the current toward the inside edge produces an electrical length that is a little shorter than expected.

The extend to which the current is concentrated toward the inside edge of the corner depends upon the angle of the corner and the trimming used.

To determine this angular dependence and hence the electrical length of the corner, several circuits similar to that shown in Figure 3.1 were built. A variety of corners were tested and the following results were obtained (with reference to Figure A.2).

- for 30° corners the electrical length should be taken as ℓ_2
- for 60° corners the electrical length should be taken as ℓ_1

A common practice in stripline construction is to use right angle corners and then to trim the corners, to reduce the contribution of the corner to the overall VSWR, as shown in Figure A.3. It was found from this study that

- corners of 30° and even 60°, contribute very little to the overall VSWR of the circuit and therefore do not have to be trimmed.
- trimming the corner will reduce the electrical length of the corner. If a 60° corner, of the type shown in Figure A.2, is trimmed so that the maximum width of the corner is $\frac{2}{3}$ h, the electrical length is reduced to approximately zero.

Mortized corners (Figure A.3 (4) and (5)) are useful for experimental purposes as this type of corner allows the electrical length of the corner to be either reduced or lengthened. This type of corner can have its electrical length increased by notching the inside edge, and decreased by trimming the outside edge. An example of a mortized corner was tested and the electrical length (ℓ), of this

corner was found to be as shown in Figure A.3 (5). Previously published work(31) gave an empirical formula for the electrical length of mortized corners; however, no agreement could be found between the formula and the results of this study. It is believed that the electromagnetic coupling effects that were present in the previous work and not present in this study, contributed to the lack of similarity in the resultant electrical lengths. Apart from this difference, the two studies arrived at similar observations as to the characteristics of these corners.

A.3 Junction Areas in Stripline Circuits

The effects of the junction area upon the overall characteristics of the hybrid were noted by using the circuit of Figure 3.1 as a test model. It was found that these effects could be significant in the form of increased VSWR's at all ports and of electrical length variations in the connected circuits. Various methods of forming these junction areas are illustrated in Figure A.4. The basic Tee junction provides an accurately defined plane of the junction, which enables the electrical lengths of the joined circuits to be accurately designed. However, the resultant VSWR's at all ports are too high to be acceptable. The Vee junction produces an acceptable VSWR at all the ports but the plane of the junction is not well defined. In this type of junction, if the angular separation is not large enough, there is an appreciable area where the joined circuits are physically close enough for electromagnetic coupling to exist. This coupled area is not well defined and creates a significant problem when the electrical lengths of the joined circuits are needed for design purposes.

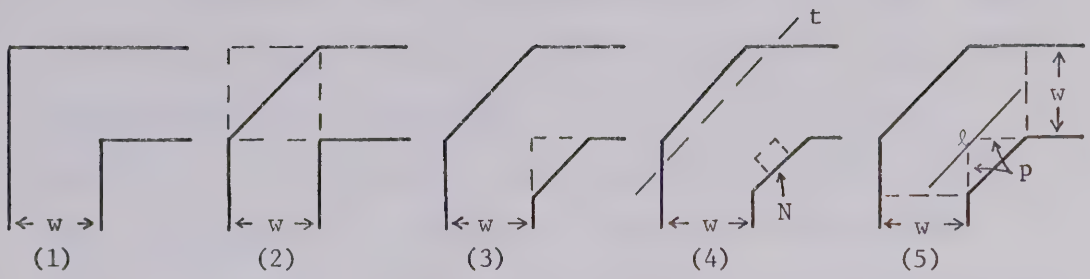

t - FURTHER TRIMMING
N - NOTCH
$P = \frac{w}{2}$ $\ell = 2\sqrt{2}\,P$

FIGURE A.3 VARIATIONS OF RIGHT ANGLE CORNERS IN STRIPLINE CENTER CONDUCTORS
(1) BASIC
(2) TRIMMED
(3) MORTIZED
(4) MODIFICATIONS TO MORTIZATION
(5) TEST CASE

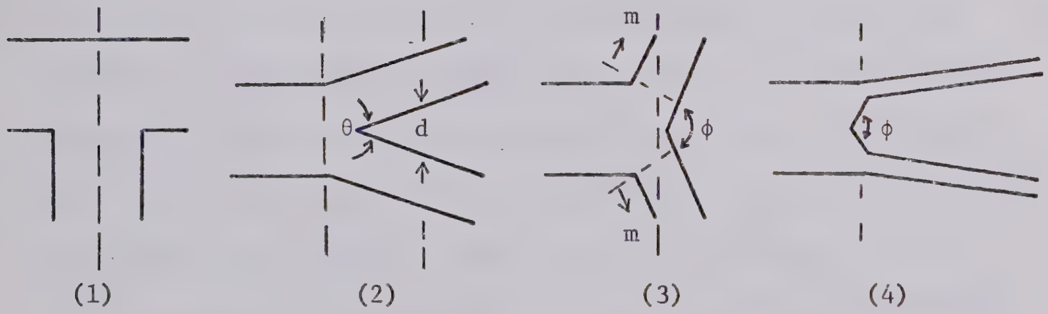

d = MINIMUM COUPLING DISTANCE   ϕ = 120°
- - - - PHYSICAL LOCATION OF PLANE OF JUNCTION
m = REFERENCE PLANE FOR ELECTRICAL LENGTH MEASUREMENTS

FIGURE A.4 METHODS OF FORMING JUNCTION AREAS
(1) BASIC TEE JUNCTION
(2) VEE JUNCTION
(3) WYE JUNCTION
(4) MODIFIED WYE JUNCTION

The form of the junction that produced the "best" results was the Wye junction. This is a type of Vee junction where the angular separation of the joined circuits is 120°, as shown in Figure A.4. Here, the plane of the junction is well defined and there is negligible area where electromagnetic coupling exists. A modified form of the Wye junction is shown in Figure A.4 (4). This modified Wye functions well, as long as the widths of the joined circuits are sufficiently narrow. The joined circuits have to be separated far enough so that there is no electromagnetic coupling between them, even in the immediate vicinity of the junction.

Although the Wye type of junction produces near optimum results with respect to the measured VSWR at all ports and enables one to accurately define the plane of the junction, it has some circuit complexities. In the three-port hybrid, the separation between the ports 2 and 3 arms of the circuit has to be small so that the resistive elements can be added. This limit on the separation of the arms of the circuit necessitates the inclusion of a corner in each arm of the circuit; hence, the designer has to contend with both corners and junction areas. However, no serious problems were encountered when the hybrid circuits were designed according to the information given in this appendix.

APPENDIX B

COMPENSATION FOR COAX-STRIPLINE CONNECTOR DISCONTINUITIES

B.1 Introduction

The coax-stripline connectors used were of the end launch type and were designed to transform the coaxial TEM mode to the stripline TEM mode where both media have a characteristic impedance of 50 ohms. From Figure B.1, which gives the relevant dimensions of the connectors and of the stripline board, it can be seen that there is a dimensional mismatch. These differences in the physical dimensions of the connectors and of the stripline board were compensated by the methods shown in Figures B.1 (b) and (c). Here the electrical connection between the connector center tab and the stripline circuit depends upon pressure applied by the screws in the connector. By using two aluminum plates, as shown in Figure B.1 (b), the modified stripline circuit has sufficient volume for the connector to be properly applied. This procedure has the advantage that the circuit now has a high degree of rigidity and very few additional clamping screws are required. The dimensional (width) mismatch between the connector center tab and the 50 ohm stripline circuit was compensated by trimming the center tab as shown in Figure B.1 (c).

The circuit construction described above was initially most successful. A test circuit was built that consisted of a short length of stripline whose characteristic impedance was 50 ohms, placed between two coax-stripline connectors. For this two-port circuit, with one port terminated in a fifty ohm load, the VSWR measurements

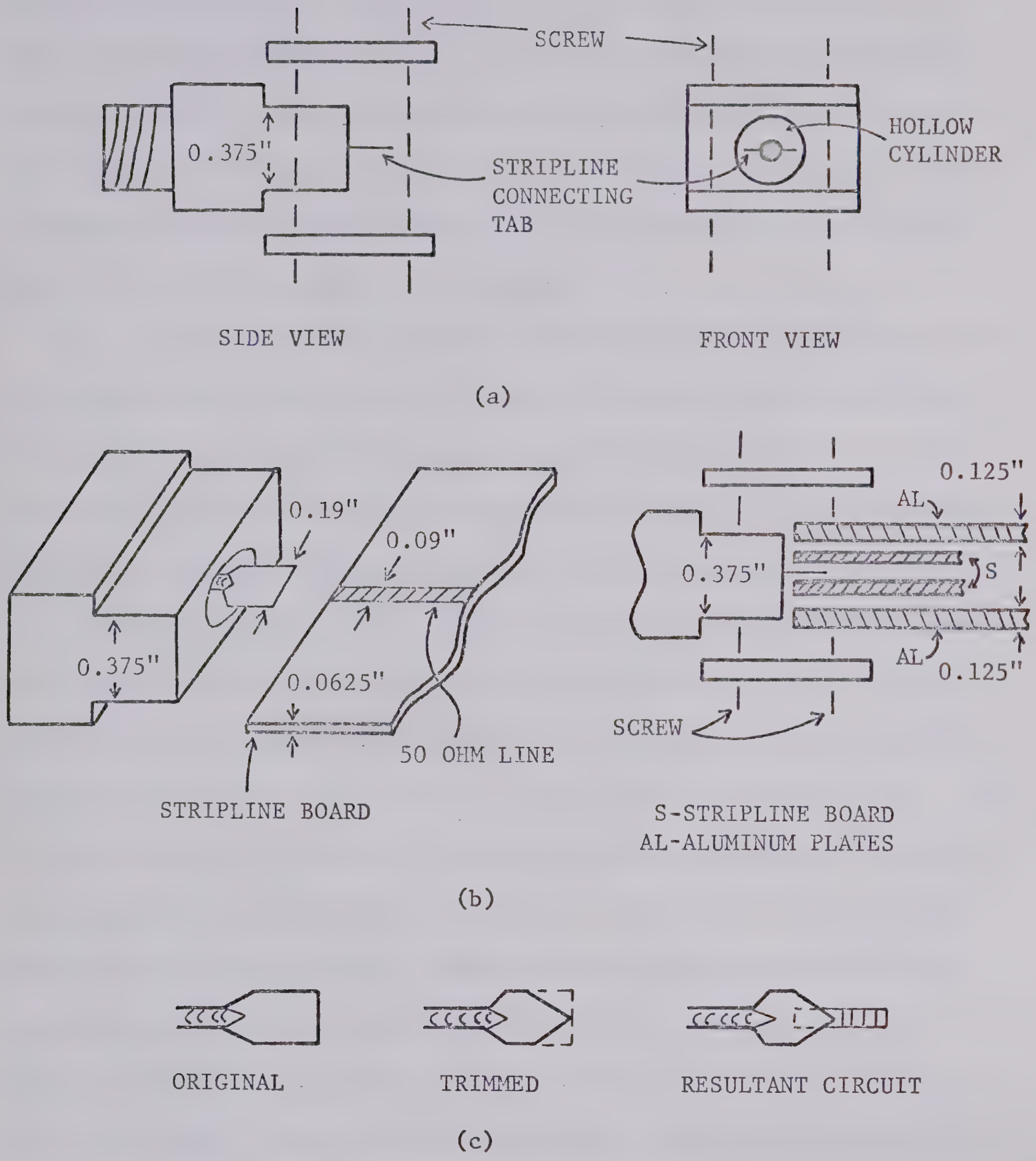

FIGURE B.1 STRIPLINE CONNECTORS AND CIRCUIT CONSTRUCTION
(a) COAX-STRIPLINE CONNECTOR
(b) STRIPLINE CIRCUIT CONSTRUCTION
(c) ADJUSTMENT OF CONNECTOR CENTER TAB

at the other port were taken. These measurements indicated that the test circuit had a VSWR of less than 1.06 over a frequency range of 1.0 to 2.0 GHz. The results of the test circuit measurements and of the initial few circuits constructed were favourable enough to preclude the ordering of new coax-stripline connectors and/or stripline board of the correct physical dimensions.

As the work progressed it became necessary to use the stripline board from a new order lot. Both of the order lots were from the same company and for the same type of stripline board. It was found that the circuits constructed from the second order lot produced significantly high VSWR's at all ports, with respect to those of the first order lot. The exact reason for the lower circuit quality was not determined but in conjunction with the use of the new stripline board (from the second order lot), it was observed that the modified coax-stripline connectors underwent some deterioration with age. The combined effect of the newer stripline board and the older connectors was such that the VSWR characteristics of the two-port test circuit were noticably deteriorated. Measurements on the same test circuit used previously, along with a similar circuit arrangement, gave measured VSWR's ranging from 1.01 at 1.0 GHz, to 1.05 at 1.5 GHz, to 1.2 at 2.0 GHz. Hence, the characteristics of the stripline circuit could be masked at frequencies greater than 1.5 GHz and for frequencies greater than 2.0 GHz, VSWR measurements will probably not be very meaningful. Therefore, for any experimental results to be satisfactory over the frequency range of 1.0 to 2.0 GHz, some form of calibration will be necessary.

B.2 Single Section Quarter-Wave Impedance Transformer Model

The calibration will be more accurate if it is carried out on the actual circuit that will be used for the experiment. Therefore, the three-port hybrid shown in Figure 3.7, along with a single 100 ohm resistor were used as a calibration circuit. During the testing of this circuit it was observed that the insertion of the resistor into the circuit resulted in a center frequency of 1.9 GHz for the characteristics of all the ports. The design center frequency was 1.7 GHz. This shift in the center frequency is due to the reactance added to the circuit by the construction techniques used to form the resistor. Since the resistor construction was limited to the method shown in Figure B.2 (a), the shift in center frequency would be used to determine that portion of the measured VSWR that could be attributed to the impedance mismatch between the connectors and the stripline circuit.

The VSWR of port 1 is theoretically independent of the resistor used, and the isolation between ports 2 and 3 is relatively insensitive to VSWR's of less than 1.5. This leaves the VSWR of ports 2 and 3 as the only characteristic that requires calibration. Since the VSWR at ports 2 and 3 depends upon both the even and the odd modes, both of these modes will have to be calibrated. The calibration procedure was arrived at by noting that the VSWR for port 1 depends only upon the even mode and the isolation between ports 2 and 3 depends upon both the even and the odd modes. Hence, these two characteristics can be used to calibrate both modes of operation. From this calibration a theoretical characteristic can be computed for the VSWR of ports 2 and 3, then the difference between the

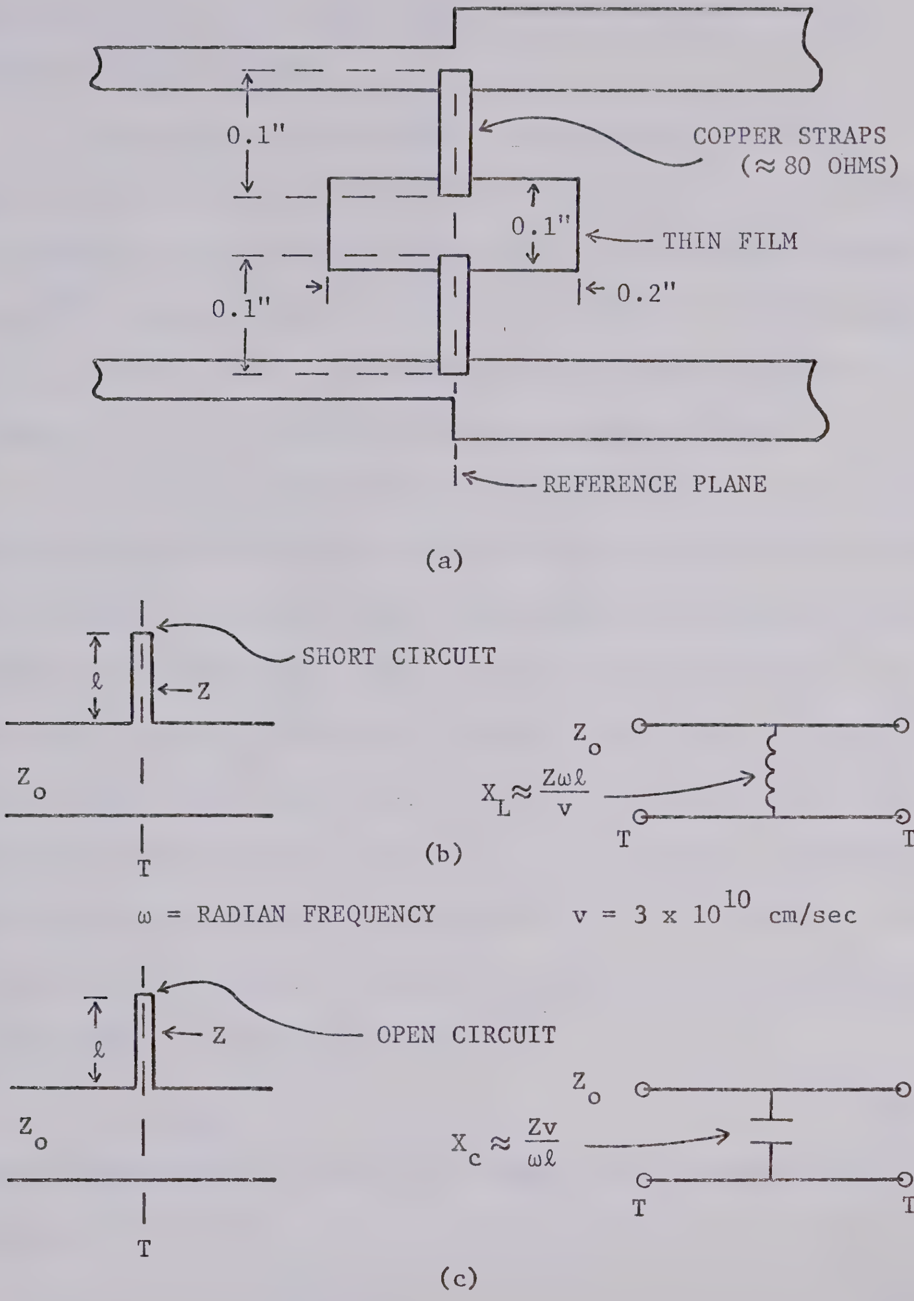

FIGURE B.2 THIN FILM RESISTOR CONSTRUCTION AND EQUIVALENT CIRCUITS
(a) PHYSICAL CONSTRUCTION (PLAN VIEW)
(b) EQUIVALENT CIRCUIT FOR ODD MODE
(c) EQUIVALENT CIRCUIT FOR EVEN MODE

measured values and this theoretical characteristic will be the required correction factor.

The method of construction of the resistor is shown in Figure B.2 (a). Since the line of symmetry is a short circuit for the odd mode and an open circuit for the even mode, the equivalent circuits(22) shown in Figure B.2 (b) and (c) apply. In this manner the same portion of the resistor behaves as a capacitance and as an inductance for the even and odd modes, respectively.

To calibrate the even mode, the VSWR of port 1 was measured, first without the resistor in the circuit and then with the resistor in the circuit. This measurement was carried out with ports 2 and 3 terminated in 50 ohm loads. The experimentally observed shift in the center frequency of operation, could be duplicated in theory by adding a capacitance of 0.3 pf (pico-farads) in shunt, at the reference plane of the resistor. Since only the even mode is involved in the measurement of the port 1 characteristics, the equivalent circuit of Figure B.2 (c) applies; thus the capacitive susceptance (Y_c) of the applicable portion of the resistor is

$$Y_c \simeq \frac{\omega \ell}{Zv} \tag{B.1}$$

where the parameters are defined in Figure B.2. Therefore the capacitance (c) is

$$C = \frac{Y_c}{\omega} \simeq \frac{10^3 \ \ell}{30 \ Z} \text{ pf} \tag{B.2}$$

Using the dimensions given in Figure B.2 (a), the value of capacitance calculated is about 0.3 pf, in good agreement with the theory.

Calibration of the odd mode was carried out in a similar manner to that used for the even mode. For the odd mode, the measurement of the isolation between ports 2 and 3, with port 1 terminated

in a 50 ohm load and with the resistor in the circuit, was used for calibration purposes. The experimentally observed shift in the center frequency of operation could be duplicated in theory by adding an inductance of 0.75 nh, in shunt, at the reference plane of the resistor. This inductance was added to the odd mode only, as the even mode already had a capacitance added to it. For the odd mode, the shunt admittance (Y_G) is no longer only due to a pure resistance but is now

$$Y_G = \frac{1}{\frac{R}{2} + jX_L} \qquad (B.3)$$

where R is the value of the real resistance (100 ohms) and X_L is the reactance of the inductive part of the resistor. Equation (B.3) can be rewritten as

$$Y_G = G - jG^2X_L \qquad (B.4)$$

where G is defined by Equation (2.10) as

$$G = \frac{2}{R} \qquad (B.5)$$

From the equivalent circuit of Figure B.2 (b)

$$X_L = \omega L \simeq \frac{Z\omega\ell}{v} \qquad (B.6)$$

and hence the inductance (L) is

$$L \simeq Z\frac{\ell}{v} \qquad (B.7)$$

The value of the inductance calculated using the dimensions given in Figure B.2 (a) is about 0.7 nh, again in good agreement with the theory.

Using the values found above, the capacitive and inductive effects associated with the resistor construction, were applied to the even and odd modes respectively and the characteristics of ports 2 and 3 were computed. These characteristics are plotted in Figure B.3. By comparing the experimentally measured isolation curves

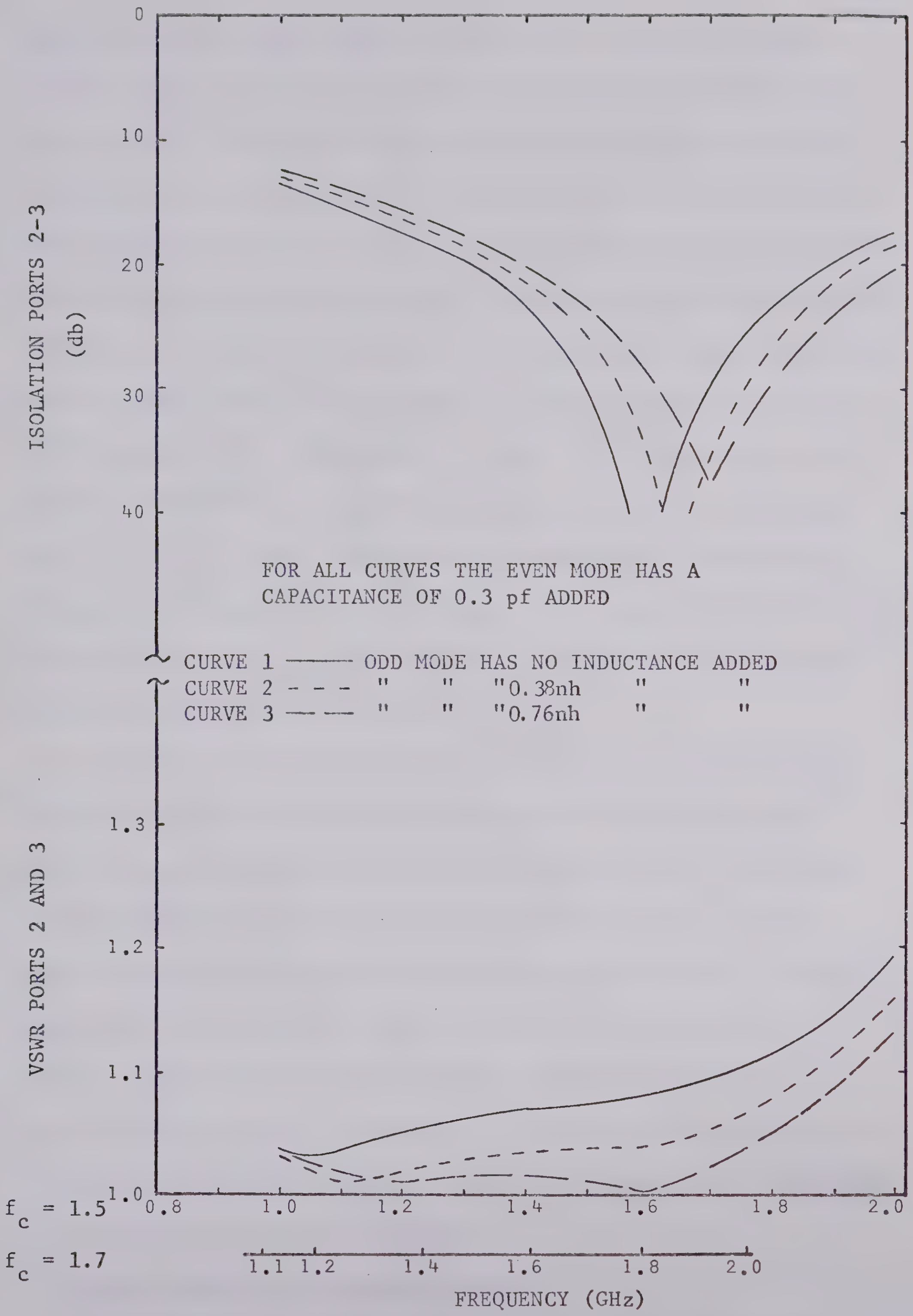

FIGURE B.3 EFFECT OF RESISTOR CONSTRUCTION ON THE CHARACTERISTICS OF THE THREE-PORT WILKINSON HYBRID

(Figure 3.13) with those shown in Figure B.3, it is evident that the most applicable theoretical curve lies about halfway between curves 2 and 3. Since the effects of the coax-stripline connectors is minimal for frequencies below 1.5 GHz, this part of the measured VSWR characteristics for ports 2 and 3 can be directly compared with the appropriate curves of Figure B.3. This comparison also indicates that the most applicable theoretical characteristic is about half way between curves 2 and 3 in Figure B.3. A theoretical curve for the VSWR of ports 2 and 3 that would lie about half way between curves 2 and 3 in Figure B.3, was plotted in Figure 3.14, for a frequency range of 1.5 to 2.0 GHz. The difference between the experimental curve and this theoretical curve would be the correction factor used to compensate for the impedance mismatch between the coax-stripline connectors and the stripline circuit itself.

The numerous possibilities of stray reactances affecting the experimental results and being unaccounted for in the theory, makes the exact correction factor difficult to obtain. By noting that the VSWR's for ports 2 and 3 in Figures 3.13 and B.3 have nearly the same magnitude, for frequencies below 1.5 GHz, it can be assumed that the correction factor obtained here is accurate to within a few per cent. Therefore the calibration procedure developed should produce sufficiently accurate results and make the experimentally observed VSWR's for ports 2 and 3 much more representative of the circuitry being tested.

B.3 Tapered Impedance Transformer Model

The stripline circuits used in this work that employed tapered impedance transmission lines were built from stripline board

that belonged to a different lot from the board used to construct the circuits of Chapter III. Although it is reasonable to assume that the effects of the coax-stripline connectors will be similar to those found in Section B.2, it was felt that the differences in the quality of the circuits produced by the different order lots of stripline board (Section B.1) warranted another investigation. Since there is little published data on the characteristics of three-port hybrids using tapered impedance transformers, the correction factors for the connectors had to be arrived at in a slightly less-direct manner than that used in Section B.2.

To obtain a reasonably accurate estimate of the necessary correction factors, a test circuit was constructed from the stripline of the second lot and the well-used coax-stripline connectors. This test circuit consisted of a short length of stripline, whose characteristic impedance was 50 ohms, placed between two coax-stripline connectors. Two physical lengths of stripline were used, namely 2 inches and 5 inches, with the VSWR measurements of these circuits being taken with one connector terminated in a 50 ohm load. Over a frequency range of 1.0 to 2.0 GHz these two lengths of stripline will vary from about $\frac{\lambda}{4}$ to $\frac{\lambda}{2}$ for the 2 inch model and from about $\frac{5}{8}\lambda$ to $\frac{5}{4}\lambda$ for the 5 inch model. Assuming that the reflection coefficient (Γ) will, in general, be complex

$$\Gamma = \alpha + j\beta \tag{B.8}$$

the above-noted length variations of the test circuit should provide a good basis from which to interpret the VSWR measurements. Upon examining the VSWR measurements of the test circuit, it was evident that the above-mentioned concept of a complex Γ and length variations

had very little influence upon these results. The measured VSWR steadily increased as the frequency increased for both lengths of stripline used. There was a slow increase from 1.0 to 1.5 GHz and then a more rapid increase from 1.5 to 2.0 GHz. It was concluded that the measured VSWR from the two inch length of stripline would be more representative of the coax-stripline connector, impedance mismatch, with the stripline circuit. Therefore this measured VSWR was converted to a magnitude of reflection coefficient and $\frac{1}{2}$ of this magnitude was taken as the correction factor for one connector.

Since the correction factor found above was arrived at using a circuit other than the one it would be applied to, some modification would probably be necessary before this factor could be used directly. The measured VSWR at port 1 depends upon the even mode only and is essentially the characteristic of the type of tapered transmission line used. Since these taper characteristics are published, a comparison between the measured and theoretical values can be made. Any difference between these compared values will in general consist of two parts, an "offset" factor and the effects of the connectors. The "offset" factor will be due to circuit construction and can be considered to be constant across the frequency band. This factor will raise all measured VSWR's a fixed amount and no attempt will be made to correct for it. The effects of the connectors will generally not be constant across the frequency band and can be considered to be the result of the port 1 connector. The correction factor arrived at from the two port test circuit was applied to the measured VSWR's for port 1 shown in Figure 5.9. The results of this correction were compared with the theoretical VSWR for port 1 shown in Figure 5.3. Then the

correction was modified slightly, so that the corrected VSWR curve would have approximately the same symmetry as the theoretical curve of Figure 5.3. The final corrected version of measured VSWR for port 1 is shown in Figure 5.9 and the difference between this curve and the actual measurement is the desired correction factor. This correction factor will compensate for the coax-stripline connector impedance mismatch with the stripline circuit.

It was observed that this final correction factor closely resembled the correction factor found in Section B.2. The only real difference between these two correction factors was that the final correction factor found in this section, was applied from 1.0 to 2.0 GHz, while the correction factor found in the previous section was only applied from 1.5 to 2.0 GHz. Similar to the results of the previous section, the final correction factor arrived at here will not be an exact correction but will bring the experimental results sufficiently close to the theory so an accurate comparison can be made.

APPENDIX C

ACCURACY OF COMPUTED CALCULATIONS

The results of the computations required in this work were usually expressed as values of VSWR and of isolation. In practice, the measurements of these characteristics are only accurate to the second decimal place. Therefore, a comparison of the theoretical and experimental values only requires a two decimal place accuracy. This required accuracy should be readily attainable as the computations were carried out to 7 or 9 significant figures and were not rounded off until the final readout was taken.

One area of this work where some error may occur is in the calculation of the odd mode when the discretization process is applied to the use of distributed resistances. These computations required that the circuit be divided into small intervals and then the transmission line equations were used to calculate the electrical properties from interval to interval along the transformer sections. To estimate the possible error involved in the use of repeated calculations, using complex numbers, the impedance matching properties of a single, quarter-wavelength section of transmission line were computed. These properties are well documented and therefore provide an excellent reference. The properties were first computed using a single transmission line equation and are shown as the VSWR characteristics of port 1 in Figure 3.3 As there was no difference between this curve in Figure 3.3 and similar curves in other publications, it was assumed that the single transmission line equation computations

possess the required two-decimal place accuracy. Following the establishment of the above-computed reference, the calculation of the port 1 VSWR (in Figure 3.3) was carried out by dividing the circuit into 100 segments and then using the transmission line equations to connect all of the segments. The results of the single and of the multiple calculations were identical to within an accuracy of five decimal places. These "identical" results show that there is no significant error due to the multiplicity of the calculations.

When a tapered impedance transformer is used along with multiple calculations, the gradual, continuous transition of its characteristic impedance has to be simulated by a number of discrete values. The maximum error produced by this situation (in this work) should occur with the use of the Chebyshev taper, as this taper has its characteristic impedance given as an infinite series, which itself, has to be numerically interpreted. The impedance matching characteristics of the Chebyshev taper are published(23) and also correspond to the even mode in the analysis of the three-port hybrid given in Section 5.4. These even mode characteristics were computed by using single and multiple calculation methods. Both methods and their results are shown in Table C.1.

Method 1 produced results that agreed with those published and hence was taken as the reference, with the results of method 2 being compared with it, to produce the difference column in Table C.1. The maximum difference between the methods was a VSWR of 0.006 and this value is too small to normally measure and use for most practical design work. From these results it can be concluded that the numerical

TABLE C.1

CHARACTERISTICS OF THE CHEBYSHEV TAPER

FREQUENCY (GHz)	METHOD 1 (VSWR)	METHOD 2 (VSWR)	DIFFERENCE (ΔVSWR)
1.0	1.105	1.111	+0.006
1.1	1.037	1.041	+0.004
1.2	1.017	1.014	-0.003
1.3	1.059	1.056	-0.003
1.4	1.088	1.088	0.000
1.5	1.103	1.102	-0.001
1.6	1.104	1.104	0.000
1.7	1.094	1.094	0.000
1.8	1.073	1.074	+0.001
1.9	1.047	1.048	+0.001
2.0	1.017	1.019	+0.002

METHOD 1 - utilizes the formula(28)

$$\Gamma_i = \frac{1}{2} e^{-j2\beta L} \ \ln \bar{Z}_L \ \frac{\cos L\sqrt{\beta^2-\beta_o^2}}{\cosh \beta_o L}$$

where $\rho = |\Gamma_i|$ $\text{VSWR} = \frac{1+\rho}{1-\rho}$

METHOD 2 - uses a number of discreet steps and the transmission line formulas to calculate Γ_i in a manner similar to the calculation of the odd mode with G(z) equal to zero for all steps. The size of the discreet step used was $\frac{1}{100}$ of the total taper length.

interpretation of a smooth taper, as a number of discrete steps, produces negligible error. Since method 1 used a single calculation with all real numbers, while method 2 made full use of the complex number subroutines stored in the computer, it can also be concluded that these subroutines contribute negligible error to the calculations. (Reducing the number of segments to 50 produced a saving in computer time but introduced a 3-4% error in the calculations of VSWR and isolation)

It has been shown that neither the multiplicity of the calculations nor the complexities of the programming contribute appreciable error. Therefore, it can be concluded that the computer calculations used in this work are sufficiently accurate for their intended purposes.

BIBLIOGRAPHY

1. P.A. Goud, "Solid State Power Sources", The Journal of Microwave Power, Vol. 2-3, pp. 99-103.

2. T.R.W., "10 Watt Amplifier at S Band", Microwaves, Vol. 8, pp. 56, September, 1969.

3. R.S. Engelbrecht and K. Kurokawa, "A Wide Band Low Noise L-Band Balanced Transistor Amplifier", Proc. I.E.E.E., Vol. 53, pp. 237-247, March, 1965.

4. R.L. Bailey, W.P. Bennet, L.E. Heckman, I.E. Martin, "An All Transistor, 1 Kilowatt, High Gain, UHF Power Amplifier", G-MTT Microwave Symposium Digest, pp. 149-153, 1969.

5. Product Review, "80 Watt Amplifier Covers 225-400 MHz", Electronics, Vol. 41, pp. 115, December 23, 1968.

6. I. Tatsuguchi, "A Frequency Modulated Phase Locked Impatt Power Combiner", I.E.E.E. Solid State Circuits Conference, Digest, University of Pennsylvania, pp. 18-19, February 18-20, 1970.

7. J. Bartnik, "Increasing R.F. power By Summing", Electronics, Vol. 39, pp. 101-107, May 30, 1966.

8. R.C.A., "Power Amplifier Doubler Produces 15 Watts at S Band", Electronics, Vol. 43, pp. 44-45, March 16, 1970.

9. E.J. Wilkinson, "An N-Way Hybrid Power Divider", I.R.E. Transactions, M.T.T. Vol. 8, pp. 116-118, January, 1960.

10. E.M.T. Jones, "Wide Band Stripline Magic T", I.R.E. Transactions, M.T.T. Vol. 8, pp. 160-168, March, 1960.

11. W.A. Tyrell, "Hybrid Circuits for Microwaves", I.R.E. Proceedings, M.T.T. Vol. 35, pp. 1294-1316, November, 1947.

12. S. March, "A Wide Band Stripline Hybrid Ring", I.E.E.E. Transactions, M.T.T. Vol. 16, pp. 361, June, 1968.

13. E.M.T. Jones and J.T. Bolljahn, "Coupled Transmission Line Filters and Directional Couplers", I.R.E. Transactions, M.T.T. Vol. 4, pp. 75-81, April, 1956.

14. S. Mizushina, "2^n Oscillators Combined with 3-DB Directional Couplers", Proc. I.E.E.E., Vol. 55, pp. 2166-2167, December, 1967.

15. W.O. Schlosser and A.L. Stillwell, "A Travelling Wave Approach to the High Power Solid State Oscillator", Proc. I.E.E.E., Vol. 56, pp. 1588, September, 1968.

16. S.B. Cohn, "A Class of Broad Band Three-Port TEM Mode Hybrids", I.E.E.E. Transactions, Vol. M.T.T. 16, pp. 110-116, February, 1968.

17. L.I. Parad and R.L. Moynihan, "Split-Tee Power Divider", I.R.E. Transactions, M.T.T. Vol. 13, pp. 91-95, January, 1965.

18. I. Tatsuguchi, "UHF Strip Transmission Line Hybrid Junction", I.R.E. Transactions, M.T.T. Vol. 9, pp. 3-6, January, 1961.

19. S. David, "A Wide Band Coaxial Line Power Divider", I.E.E.E. Transactions, M.T.T. Vol. 15, pp. 270-271, April, 1967.

20. T.E. MacKenzie, "Some Recent Advances in Coaxial Components for Swept Frequency Instrumentation", Microwave Journal, Vol. 12, pp. 69-77, June, 1969.

21. J. Reed and G.J. Wheeler, "A Method of Analysis of Symmetrical Four-Port Networks", I.R.E. Transactions, M.T.T. Vol. 4, pp. 246-252, October, 1956.

22. Matthai, Young and Jones, "Microwave Filters, Impedance Matching Networks and Coupling Structures", pp. 362-363, New York, McGraw Hill, 1964.

23. Microwave Engineers Handbook and Buyers Guide, Microwave Journal, pp. 18, International Division, 1964.

24. R.E. Collin, "Foundations for Microwave Engineering", pp. 232-233, New York, McGraw Hill, 1964.

25. Ibid., pp. 228-229.

26. Ibid., pp. 237-238.

27. Ibid., pp. 239.

28. Ibid., pp. 248.

29. P.C. Goodman, "A Wideband Stripline Matched Power Divider", G-MTT International Microwave Symposium Digest, Detroit, Michigan, pp. 16-20, May 20-22, 1968.

30. A.A. Oliner, "Equivalent Circuits for Discontinuities in Balanced Strip Transmission Line", I.R.E. Transactions, M.T.T. Vol. 3, pp. 134-143, March, 1955.

31. W.B. Weir and D.K. Adams, "Wideband Multiplexers Using Directional Filters", Microwaves, Vol. 8, pp. 44-50, May, 1969.

BRUCE PEEL SPECIAL COLLECTIONS LIBRARY
UNIVERSITY OF ALBERTA LIBRARY

REQUEST FOR DUPLICATION

I wish a photocopy of the thesis by

____(author)

entitled____

The copy is for the sole purpose of private scholarly or scientific study and research. I will not reproduce, sell or distribute the copy I request, and I will not copy any substantial part of it in my own work without permission of the copyright owner. I understand that the Library performs the service of copying at my request, and I assume all copyright responsibility for the item requested.

B29962